

# DYNAMICS of the SHELL MODEL

- ESNT Summer 2008
- P.F. Bortignon
- Gianluca Colò
- Enrico Viguzzi
- Fabio Crespi

# Lecture I

- 1) Empirical information on the dynamical shell model
- 2) Green functions, Mass operator, Dyson and Nambu-Gor'kov (superfluid nuclei) equations, Bell and Squires proof.

# OUR KEY EQUATION

- We introduce the Mass Operator,
- Non local in space and TIME!!

$$i\hbar \frac{\partial \Psi(\mathbf{r}, t)}{\partial t} = -\frac{\hbar^2}{2m} \nabla^2 \Psi(\mathbf{r}, t) + \int d\mathbf{r}' \int dt' \mathcal{M}(\mathbf{r}, \mathbf{r}'; t - t') \Psi(\mathbf{r}', t')$$



The dependence of  $\mathcal{M}$  upon  $t - t'$  can be transformed into a frequency dependence. Let us indeed consider a stationary state with a well-defined frequency:

$$\Psi(\mathbf{r}, t) = \varphi_{\omega}(\mathbf{r}) e^{-i\omega t}. \quad (2.0.2)$$

Equation (0.1) then becomes

$$\hbar\omega \varphi_{\omega}(\mathbf{r}) = -\frac{\hbar^2}{2m} \nabla^2 \varphi_{\omega}(\mathbf{r}) + \int d\mathbf{r}' \mathcal{M}(\mathbf{r}, \mathbf{r}'; \omega) \varphi_{\omega}(\mathbf{r}') \quad (2.0.3)$$

where  $\mathcal{M}(\mathbf{r}, \mathbf{r}'; \omega)$  is the Fourier transform of  $\mathcal{M}(\mathbf{r}, \mathbf{r}'; t - t')$  over  $t - t'$ . *The nonlocality in time of the mean field therefore amounts to a frequency dependence.*

$$\mathcal{E}^{\text{Sk}} = \int d\mathbf{r} \left[ \frac{\hbar^2}{2n} \tau + \frac{3}{8} t_0 \rho^2 + \frac{1}{16} \rho^3 + \frac{1}{16} (3t_1 + 5t_2) \rho \tau \right. \\ \left. + \frac{1}{64} (9t_1 - 5t_2) (\nabla \rho)^2 + \frac{3}{4} W_0 \rho \nabla \cdot \mathbf{J} + \frac{1}{32} (t_1 - t_2) \mathbf{J}^2 \right]$$

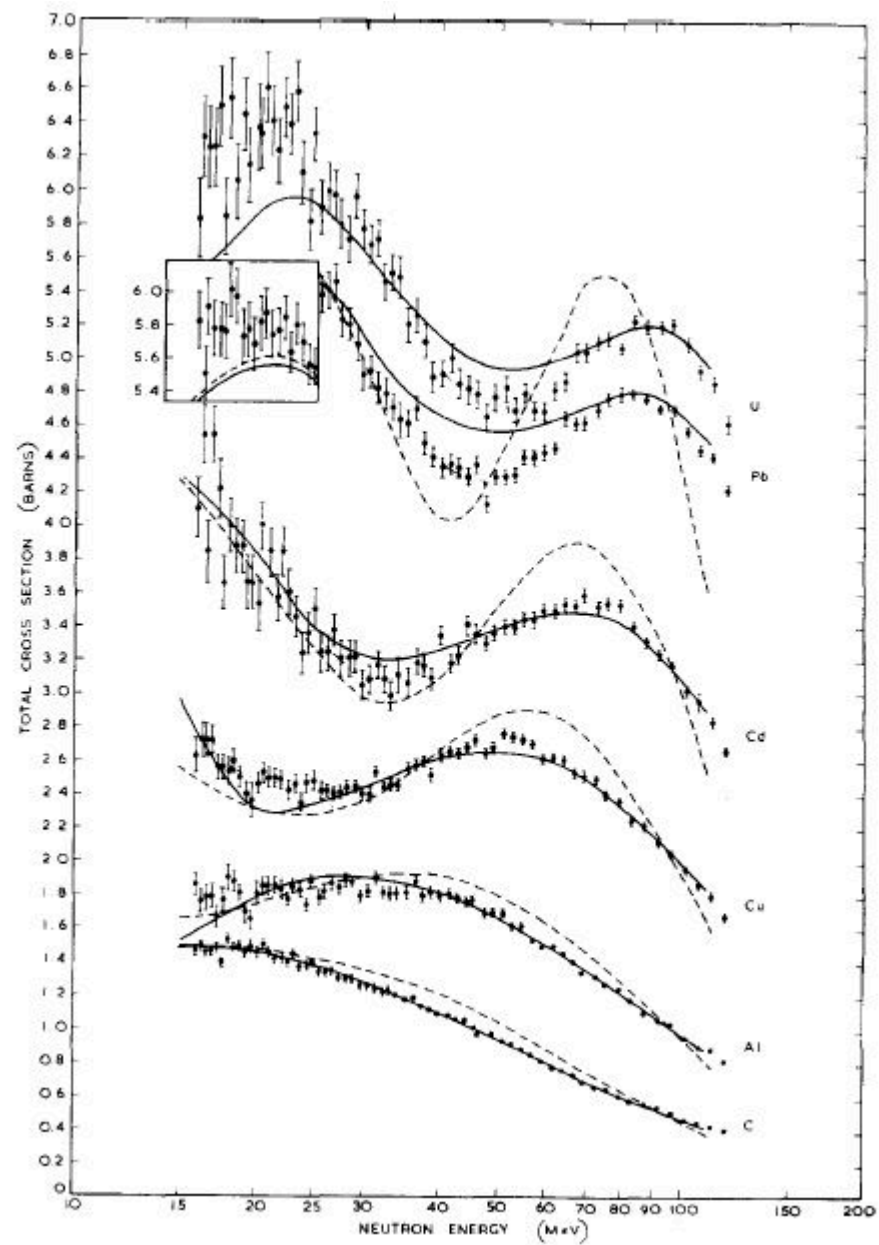


Fig. 2.1. Taken from ref. [11]. The dots show the dependence upon incident energy of the neutron total cross sections of (from bottom to top) carbon, aluminium, copper, cadmium, lead and uranium. The solid and broken lines are calculated from the optical model. As discussed in section 2.4, the broken lines are obtained when the depth of the real part of the potential is not allowed to depend upon energy, while the solid curves correspond to the energy dependence shown in fig. 2.9.

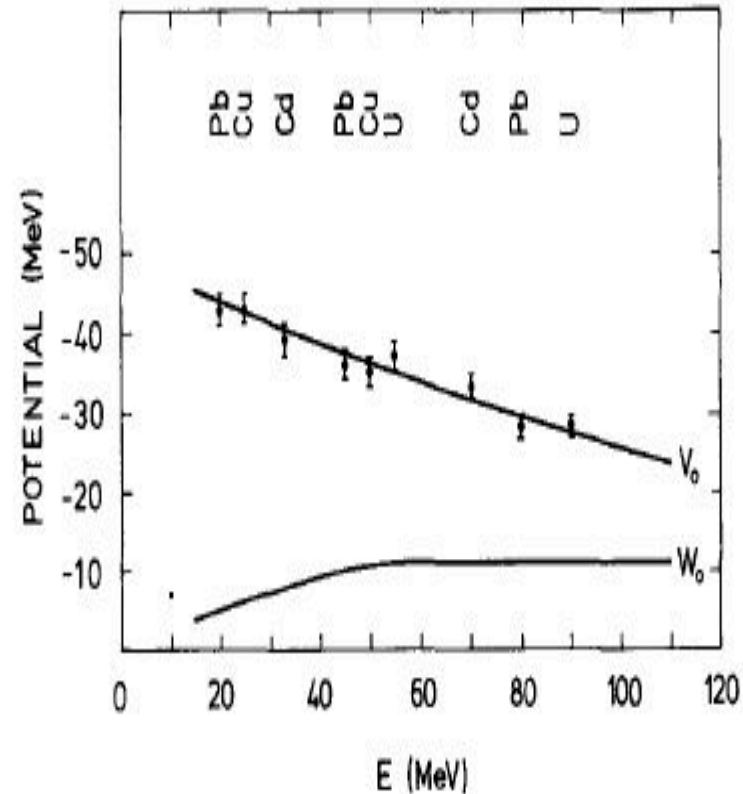


Fig. 2.9. Taken from ref. [11]. Dependence upon incident neutron energy of the depth of the real part and of the imaginary part of the optical-model potential used to generate the solid lines in fig. 2.1. Each empirical point is labelled by the data which led to its determination, i.e. (from left to right) the location of the second maximum of the total cross section in Pb, the location of the first minimum of the total cross section in Cu, etc. The real part and the imaginary parts have been assumed to have the same Woods-Saxon radial shape. The fits below 50 MeV are improved if one allows the shape of the imaginary part to change from a Woods-Saxon to a surface peaked function as the energy decreases.

# Energy Dependence

- For positive energy, the depth of the empirical (WS type) average potential depends upon the energy according to the law:
- $V_0(E) = V^0 + 0.3 E$

$$iW(r)=4iW_D\frac{df}{dx}-iW_Vf(x), \quad (8)$$

with  $r_0=1.295$  fm,  $a=0.59$  fm,

$$\left. \begin{aligned} W_D &= 4.28 + 0.4E - \frac{N-Z}{A} 12.8 \text{ MeV} \\ W_V &= 0 \end{aligned} \right\} E < 15 \text{ MeV}$$

$$\left. \begin{aligned} W_D &= 14.0 - 0.39E - 10.4 \frac{N-Z}{A} \text{ MeV} \\ W_V &= -4.3 + 0.38E \end{aligned} \right\} E > 15 \text{ MeV},$$

# W and LDA

Very often  $W$  is obtained from NM calculations, via LDA.

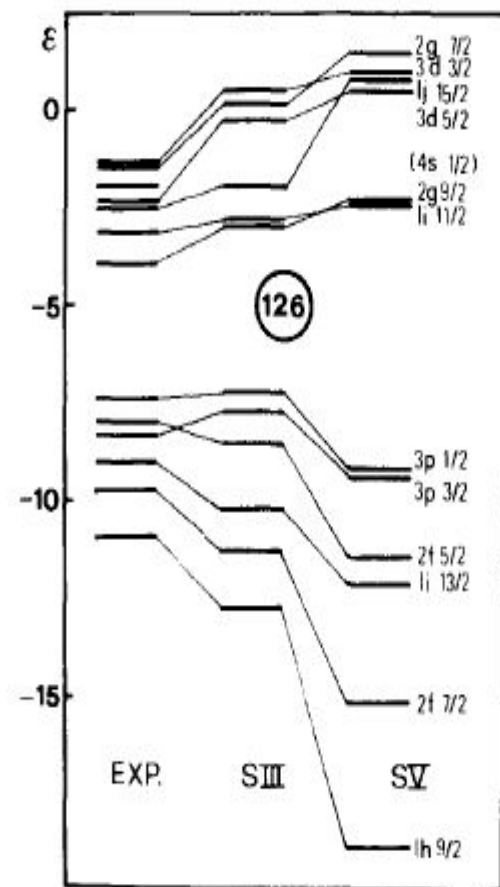
The agreement between the empirical optical potential and the theory based on infinite NM should not be taken too seriously, because there is no justification for treating the surface as low-density NM.

Valerie, may you tell us the true!

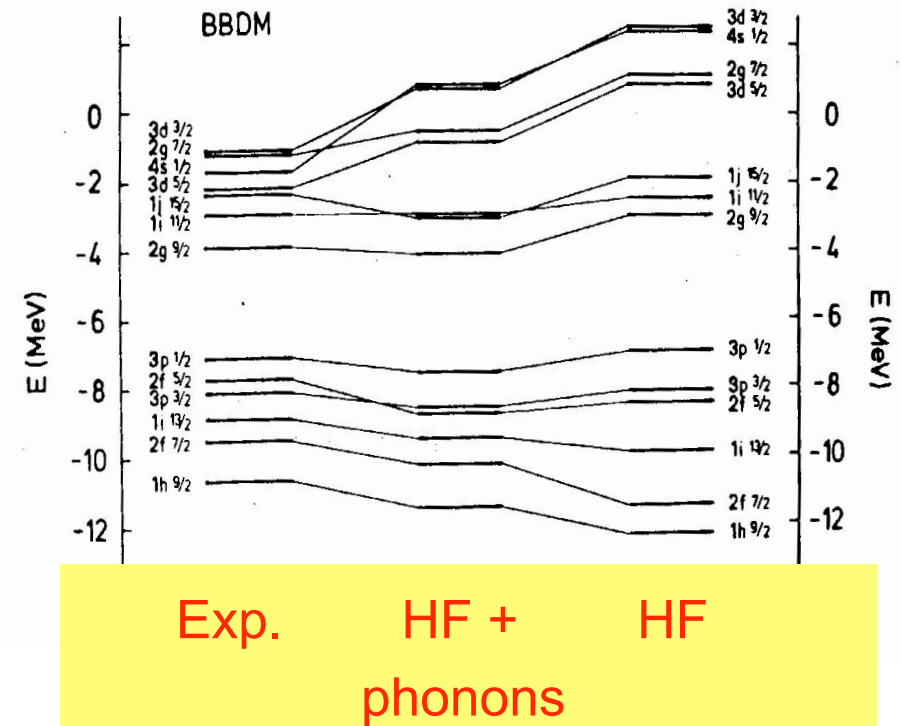
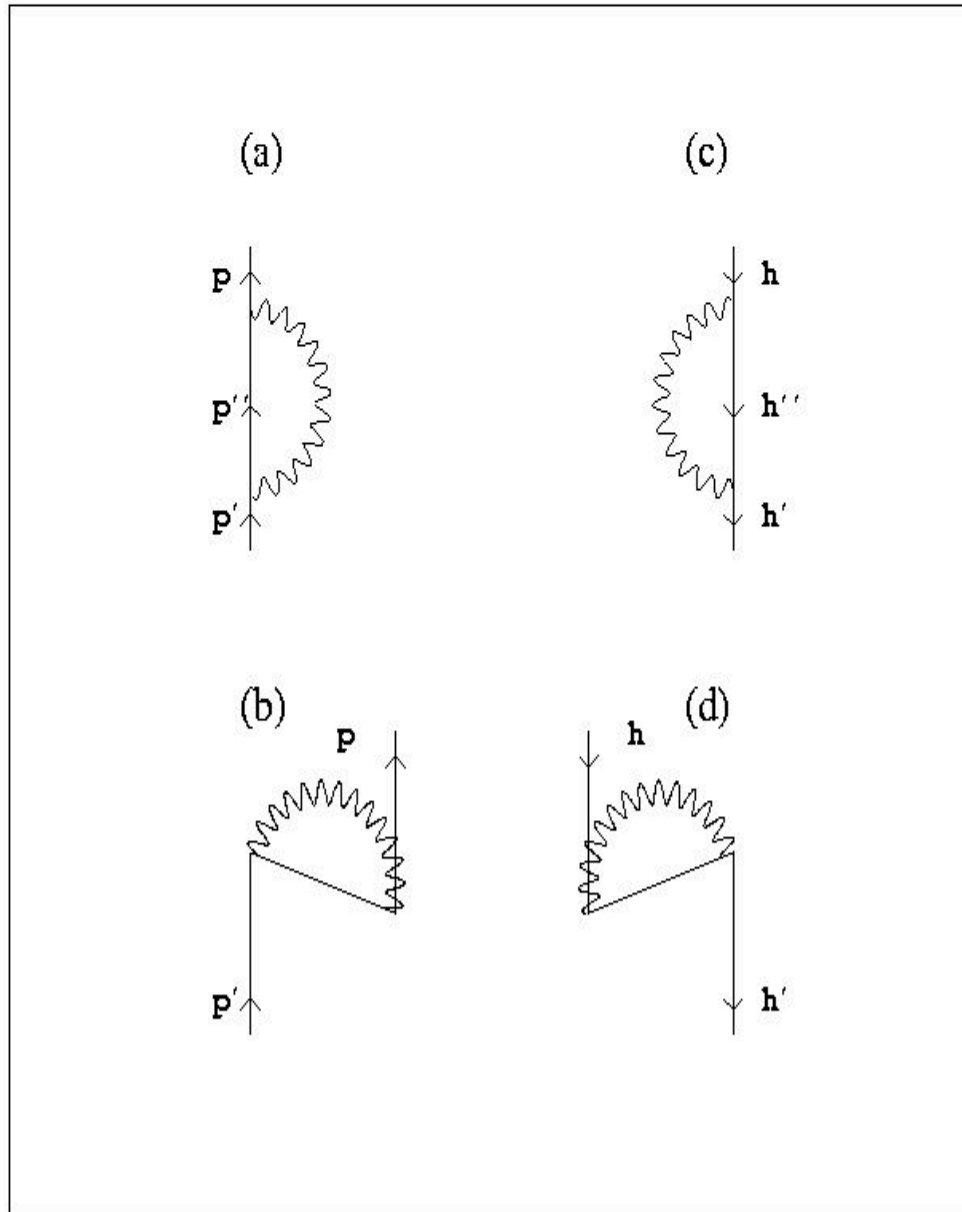


# Now Bound States

- No more Woods-Saxon empirical s.p. potential
- HF with effective forces, like Skyrme, Gogny....



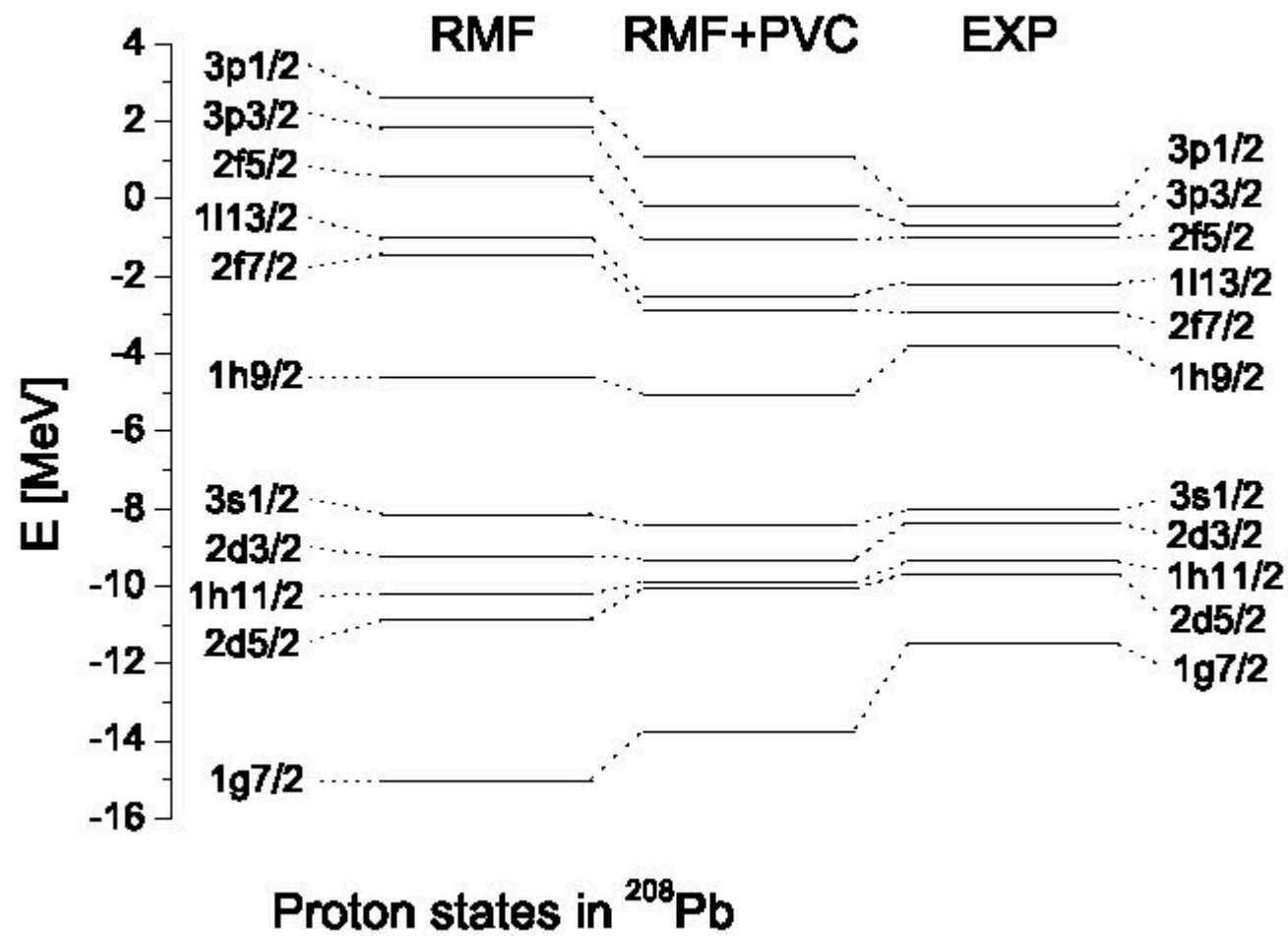
The phonon coupling has been known for many years to be important for the understanding of s.p. states around the  $^{208}\text{Pb}$  core.



C.Mahaux et al., Phys. Rep., 1985  $\Rightarrow$  PV coupling increases  $m^*$

# E. Litvinova and P. Ring

- Covariant theory of particle-vibration coupling and its effect on the single-particle spectrum
- PRC C73, 044328 (2006)



# EFFECTIVE MASS

- $m^*(E)/m = 1 - dV_0(E)/dE$

The origin of the expression “effective mass” will be explained in sections 2.6.3 and 2.8. When the energy dependence of the potential depth is linear, the effective mass is constant. In general, however,  $m^*$  is a function of the energy  $E$ .

### 2.6.2. Empirical energy dependence of the effective mass

The empirical data surveyed in sections 2.3–2.5 indicate that the effective mass depends upon the single-particle energy. Indeed, they yield  $m^*/m \approx 0.65$  for either positive energies or for large negative energies and  $m^*/m \approx 1$  for small negative energies.

Let us be somewhat more quantitative. We define the *Fermi energy*  $\varepsilon_F$  as the average between the energy  $\varepsilon_F^-$  of the last occupied orbit and the energy  $\varepsilon_F^+$  of the first unoccupied orbit

$$\varepsilon_F = (\varepsilon_F^+ + \varepsilon_F^-)/2. \quad (2.6.2)$$

In the case of neutrons in  $^{208}\text{Pb}$  for example, one has  $\varepsilon_F = -5.6$  MeV (see fig. 2.6). With this definition we can summarize as follows the empirical evidence:

$$m^*/m \approx 0.7 \quad \text{for } |E - \varepsilon_F| > 20 \text{ MeV}, \quad (2.6.3)$$

$$m^*/m \approx 1 \quad \text{for } |E - \varepsilon_F| < 10 \text{ MeV}. \quad (2.6.4)$$

The property that *the effective mass presents a narrow enhancement near the Fermi energy* was first pointed out by Brown, Gunn and Gould [1]. We shall devote much attention to its theoretical

$$m^*(r; E)/m = 1 - \partial V(r; E)/\partial E.$$

Let us assume a linear energy dependence for the potential depth, i.e.

$$V(r; E) = \frac{V^0 + (1 - m_0^*/m)E}{1 + \exp\{(r - R_v)/a_v\}}$$

where the index on  $m_0^*$  indicates the effective mass for  $r = 0$ . One has then

$$1 - \frac{m^*(r)}{m} = \frac{1 - m_0^*/m}{1 + \exp\{(r - R_v)/a_v\}}.$$



Note that the effective mass  $m^*$  does not depend on  $E$  because of the linear energy dependence which has been assumed for the potential. The single-particle equation

$$\frac{\hbar^2}{2m} \left[ \frac{d^2}{dr^2} - \frac{l(l+1)}{r^2} \right] \Psi_{nl}(r) + [\varepsilon_{nl} - V(r; \varepsilon_{nl})] \Psi_{nl}(r) = 0 \quad (2.7.20)$$

then has exactly the same bound and scattering eigenstates as the equation

$$\frac{\hbar^2}{2m^*(r)} \left[ \frac{d^2}{dr^2} - \frac{l(l+1)}{r^2} \right] \Psi_{nl}(r) + [\varepsilon_{nl} - \bar{V}(r)] \Psi_{nl}(r) = 0 \quad (2.7.21)$$

with the *energy-independent potential*

$$\bar{V}(r) = \frac{m V^0 / m^*(r)}{1 + \exp\{(r - R_v)/a_v\}}. \quad (2.7.22)$$

# On Self-Energy, Effective Masses, Level Density

$$\Delta E_{\beta}(\omega)=\sum_{\alpha}\frac{V_{pv}^2(\alpha,\beta;L)}{\omega-(\epsilon_{\alpha}+\hbar\omega_L)}$$

$$\frac{d\epsilon}{dk}=\frac{\hbar^2k}{m^{\star}}$$

$$\frac{m^{\star}}{m}=\frac{m_k}{m}\frac{m_{\omega}}{m}$$

$$m_k=m(1+\frac{m}{\hbar^2}\frac{\partial U_{HF}}{\partial k})^{-1}$$

$$m_{\omega}=m(1-\frac{\partial \Delta E}{\partial \omega})$$

$$(\frac{\partial \Delta E}{\partial \omega})_{\omega=0}\approx -N(0)\int_0^{\infty}\frac{V_{pv}^2d\epsilon}{(\epsilon+\hbar\omega_L)^2}=-N(0)\frac{V_{pv}^2}{\hbar\omega_L}$$

We obtain also the quasi-particle strength (spectroscopic factor)

$$Z_{\omega} = (M_{\omega}/m)^{-1}$$

In the Fermi gas model, the level density reads

$$\rho(A, E^*) \propto \exp(2\sqrt{aE^*})$$

being

$$a \propto A/\epsilon_F \propto m^*$$

## Green, Wick, Dyson, Lehmann

1) Green's function:

$$L\psi(x, t) = f(x, t)$$

$$LG(x - x', t - t') = \delta(x - x')\delta(t - t')$$

2) Propagator (or Green's funct. again), retarded  $t_2 > t_1$

$$iG^+(k_2, k_1, t_2 - t_1) =$$

=probability amplitude that if at time  $t_1$  a particle in  $\phi_{k_1}(\vec{r})$  is added to the interacting system in its ground state, then at time  $t_2$  the system will be in its ground state with an added particle in  $\phi_{k_2}(\vec{r})$ .

3) For a free particle

$$L = \frac{\nabla^2}{2m} + \frac{i\partial}{\partial t}$$

and 1) and 2) give the same result

$$G = G_0^+(k, t - t') = -i \exp[-i\epsilon_k(t - t')]$$

The Fourier transform is

$$G_0^+(k, \omega) = \frac{1}{\omega - \epsilon_k + i\delta}$$

Then, the (general) conclusion:

The poles of the Fourier transform of the s.p. propagator occur at values  $\omega$  equal to the energies of the excited states of the interacting (N+1)-particle system minus the g.s. energy of the interacting N-particle system.

Interacting system?

$$G^+(\vec{k}, t - t') = G_0^+(\vec{k}, t - t') + \int_{-\infty}^{+\infty} dt'' G_0^+(\vec{k}, t - t'') V(\vec{k}) G^+(\vec{k}, t'' - t)$$

Note that if  $\hat{H} = \hat{H}_0 + \hat{V}$ , then

$$\begin{aligned}\frac{1}{\omega - \hat{H}} &= \frac{1}{\omega - \hat{H}_0} [\omega - \hat{H}_0] \frac{1}{\omega - \hat{H}} = \frac{1}{\omega - \hat{H}_0} [\omega - \hat{H} + \hat{V}] \frac{1}{\omega - \hat{H}} \\ &= \frac{1}{\omega - \hat{H}_0} \left[ 1 + \hat{V} \frac{1}{\omega - \hat{H}} \right] \\ &= \frac{1}{\omega - \hat{H}_0} + \frac{1}{\omega - \hat{H}_0} \hat{V} \frac{1}{\omega - \hat{H}}.\end{aligned}$$

4) Other definition:

$$G(k_2, k_1, t_2 - t_1) = -i \langle \psi_0 | T \{ c_{k_2}(t_2) c_{k_1}^\dagger(t_1) | \psi_0 \rangle$$

where  $\psi_0$  is the exact w.f. of the g.s. of the interacting system and

$$c_{k_1}(t) = \exp[+iHt] c_{k_1} \exp[-iHt]$$

$T$  is the Wick time-ordering operator. For the free particle, we obtain (again!)

$$G_0^+(k, t) = -i \theta_{(\epsilon - \epsilon_F)} \theta_t \exp[-i\epsilon t]$$

For a boson (phonon), we write

$$D_0(k, \omega) = -i[\theta_t \exp[-i\omega_0 t] + \theta_{-t} \exp[+i\omega_0 t]]$$

5) Wick's theorem:

$$\langle 0 | T \{ ABC \dots XYZ \} | 0 \rangle =$$

=sum over all possible fully "contracted products",  $|0\rangle$  being the Fermi vacuum, and a "contracted product"

$$A^\square B = \langle 0 | T \{ AB \} | 0 \rangle$$

The contraction of the  $c$  operators above is just  $i$  x the unperturbed propagator.

### Lehmann Representation

$$G_{\alpha\alpha} = \sum_h \frac{S_{h\alpha}}{\omega - \omega_h - i\delta} + \sum_p \frac{S_{p\alpha}}{\omega - \omega_p + i\delta}$$

being





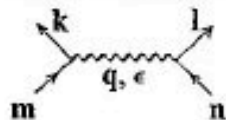

$$S_{h\alpha} = | \langle \psi^{(A-1)} | a_\alpha | \psi_0^{(A)} \rangle |^2$$

and

$$S_{p\alpha} = | \langle \psi_0^{(A)} | a_\alpha | \psi_p^{(A+1)} \rangle |^2$$

that is the spectroscopic factors, that is the residues  $Z_\omega$  above!!

Table 9.1 *Diagram dictionary for interacting many-fermion system with no external potential (Feynman method)*

Diagram element	Factor
$\mathbf{k}, \omega$  or $\mathbf{k}, \omega$ 	$iG(\mathbf{k}, \omega)$
$\mathbf{k}, \omega$  or $\mathbf{k}, \omega$ 	$iG_0(\mathbf{k}, \omega) = \frac{i}{\omega - \epsilon_{\mathbf{k}} + i\delta_{\mathbf{k}}}, \quad \begin{aligned} \delta_{\mathbf{k} > \mathbf{k}_F} &= +\delta \\ \delta_{\mathbf{k} < \mathbf{k}_F} &= -\delta \end{aligned}$ <p>with:</p> $\int \frac{d\omega}{2\pi} [iG_0(\mathbf{k}, \omega)] = -\theta_{k_F - k}$ $= -1, \quad k < k_F$ $= 0, \quad k > k_F$
	$-iV_{klmn}$ or $-iV_q$ (use $V_{klmn}(\epsilon)$ or $V_q(\epsilon)$ for time-dependent interaction)
Each fermion loop	Example:  $(-1)$
Each <u>intermediate energy</u> parameter $\omega$	$\int \frac{d\omega}{2\pi}$
Each <u>intermediate momentum</u> , $\mathbf{k}$	$\sum_{\mathbf{k}}$ or $\int \frac{d^3\mathbf{k}}{(2\pi)^3}$ (for $\Omega = 1$ ) (include sum over spins)



$$\begin{aligned}
& \text{Diagram 1} = \text{Diagram 2} + \text{Diagram 3} + \text{Diagram 4} + \text{Diagram 5} + \text{Diagram 6} + \dots \\
& \quad + \text{Diagram 7} + \text{Diagram 8} + \text{Diagram 9} + \text{Diagram 10} + \dots \\
& \quad + \text{Diagram 11} + \text{Diagram 12} + \dots + \text{Diagram 13} + \dots \\
& \quad + \text{Diagram 14} + \text{Diagram 15} + \dots
\end{aligned}
\tag{9.40}$$

The diagrams represent various Feynman-like graphs with external lines and internal loops. The first row shows the initial expansion. The second row continues the series with more complex topologies. The third and fourth rows show further terms, including diagrams with multiple loops and vertices, all separated by plus signs and followed by ellipses to indicate an infinite series.

(4) Evaluate graphs by means of the dictionary in Table 9.1, on p. 146.

where  $\Sigma$  is the sum of all proper (irreducible) self-energy parts or '*irreducible self-energy*':

$$\Sigma = \text{[diagram 1]} + \text{[diagram 2]} + \text{[diagram 3]} + \text{[diagram 4]} + \text{[diagram 5]} + \text{[diagram 6]} + \text{[diagram 7]} + \dots \quad (10.8)$$

Translated into functions with the aid of Table 9.1 this becomes:

$$G(\mathbf{k}, \omega) = \frac{1}{\omega - \epsilon_{\mathbf{k}} - \Sigma(\mathbf{k}, \omega) + i\delta_{\mathbf{k}}} \quad (10.9)$$

where

$$-i\Sigma(\mathbf{k}, \omega) \equiv \text{[diagram 8]} \quad (10.10)$$

For non-interacting systems,  $\Sigma(\mathbf{k}, \omega) = 0$ . Note that in all of these summations, (10.3)  $\rightarrow$  (10.6), it was necessary to restrict the sum to just repeated *proper* parts. If we had summed over repeated *improper* parts as well, diagrams would have been counted twice, since as seen in diagrams 3, 5 of (10.1), the improper parts themselves contain repetitions.

Equation (10.7) or (10.9) is called Dyson's equation and is the basic equation from which most propagator calculations start. It is exact since all the diagrams in (9.40) are composed of either proper parts or repetitions of proper parts, and we have summed over them all. That is, the summation here is complete rather than just partial. But don't be fooled into thinking that because it is exact (10.7) is the answer to our problem! All that has been done is to sum over repeated proper parts; the sum (10.8) over the proper parts themselves is still left to do, and has the unfortunate quality of being in general impossible. It can, however, be evaluated to various degrees of approximation. For example, the Hartree-Fock is the lowest-order approxi-

mation for  $\Sigma$ :

$$\Sigma \approx \text{[diagram 9]} + \text{[diagram 10]} \quad (10.11)$$

It is easy to see the physical interpretation of  $\Sigma(\mathbf{k}, \omega)$  by comparing the exact (10.7) with the Hartree approximation in (10.3), or the Hartree-Fock in (10.4). By analogy with the argument around (4.73),  $\Sigma(\mathbf{k}, \omega)$  is a generalized

'effective field' or 'effective potential' which the particle in state  $\mathbf{k}$  sees because of its interaction with all the other particles of the system. This field is of course considerably more complicated than the Hartree-Fock field because of its  $\omega$ -dependence, which describes the motion of the quasi-particle cloud (see second paragraph after (4.95)).

It is important to note that the form of the Dyson equation in (10.7) is only valid in the special case (with which we shall be mainly concerned) of a system with no external potential and with diagrams calculated in  $(\mathbf{k}, \omega)$ -space. There is, however, a more general form of the Dyson equation which holds whenever expansion (9.40) holds; the general form is

$$\text{[diagram 11]} = \text{[diagram 12]} + \text{[diagram 13]} \quad (10.12)$$

This may be proved by iteration:

$$\begin{aligned} \text{[diagram 14]} &= \text{[diagram 15]} + \text{[diagram 16]} = \text{[diagram 17]} + \text{[diagram 18]} + \text{[diagram 19]} = \text{[diagram 20]} + \text{[diagram 21]} + \text{[diagram 22]} + \dots \\ &= \text{[diagram 23]} + \text{[diagram 24]} + \text{[diagram 25]} + \text{[diagram 26]} + \text{[diagram 27]} + \text{[diagram 28]} + \dots \end{aligned} \quad (10.13)$$

Equation (10.12) boils down to (10.7) in the above special case because the value of each diagram is then the algebraic product of the values of its parts; thus we have

$$\text{[diagram 29]} = \text{[diagram 30]} + \text{[diagram 31]} \times \Sigma \times \text{[diagram 32]}$$

or

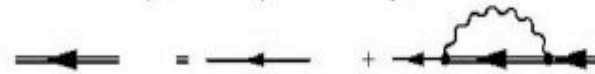
$$G(\mathbf{k}, \omega) = G_0(\mathbf{k}, \omega) + G(\mathbf{k}, \omega) \Sigma(\mathbf{k}, \omega) G_0(\mathbf{k}, \omega), \quad (10.14)$$

## Going beyond the quasi-particle approximation

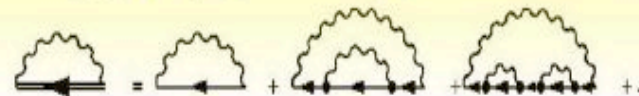
J. Terasaki et al., Nucl.Phys. **A697**(2002)126

by extending the Dyson equation...

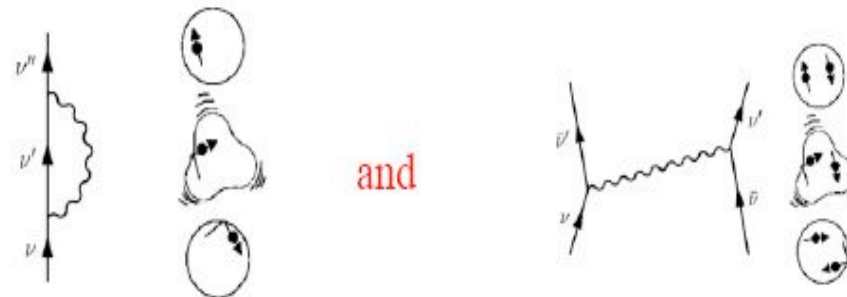
$$G_{\mu}^{-1} = (G_{\mu}^0)^{-1} - \Sigma_{\mu}(\omega)$$



$$\Sigma_{\mu}(\omega) = \int_{-\infty}^{+\infty} \frac{d\omega'}{2\pi} \sum_{\mu'} \frac{1}{\hbar} G_{\mu'}(\omega') \sum_{\alpha} \frac{1}{\hbar} D_{\alpha}^o(\omega - \omega') * V_{\mu\mu',\alpha}^2$$



to the case of superfluid nuclei (Nambu-Gor'kov), it is possible to consider both



# J.S. Bell and E.J. Squires

- Phys. Rev. Lett. 3 (1959) 96

## A FORMAL OPTICAL MODEL:

The propagation of a nucleon in a nucleus is specified by the proper self-energy  $\Sigma$  of the one-particle Green function, which is equivalent to the optical potential.

Denoting by  $|\bar{\alpha}\rangle$  the scattering state and by  $|\bar{0}\rangle$  the target ground state, we define the model wave function as

$$\phi(\vec{r}, t) = \langle \bar{0} | \bar{\psi}(\vec{r}, t) | \bar{\alpha} \rangle, \quad (1)$$

where  $\bar{\psi}$  is the Heisenberg field operator of second quantization. For  $|\bar{\alpha}\rangle$  we take the state

$$|\bar{\alpha}\rangle = \int_{-\infty}^t dt' e^{-iEt'} \bar{\psi}^\dagger(\vec{r}', t') |\bar{0}\rangle, \quad (2)$$

which corresponds to a source of particles of energy  $E$  at the point  $\vec{r}'$ ; if  $r'$  is sufficiently large only a plane wave actually reaches the target. In writing, with  $x \equiv (\vec{r}, t)$ ,

$$\phi(x) = \int_{-\infty}^{+\infty} dt' e^{-iEt'} G(x, x'), \quad (3)$$

$$G = \langle \bar{0} | T(\bar{\psi}(x), \bar{\psi}^\dagger(x')) | \bar{0} \rangle, \quad (4)$$

We construct  $G$  by a perturbation theory where in zero order the real forces are replaced by a fictitious one-body potential, in general nonlocal,

$$\int d\vec{r}d\vec{r}' \bar{\psi}^\dagger(\vec{r}, 0)U(\vec{r}, \vec{r}')\bar{\psi}(\vec{r}', 0).$$

An  $S$  matrix is defined by

$$\frac{\partial}{\partial t}S(t, t') = -iH'(t)S(t, t'),$$

$$S(t', t') = 1, \quad H'(t) = e^{iH_0 t} H' e^{-iH_0 t},$$

where  $H_0$  is the zero-order Hamiltonian and the total Hamiltonian is  $H_0 + H'$ . In terms of interaction representation operators  $\psi$ , the Heisenberg operator  $\bar{\psi}$  can be written

$$\bar{\psi}(x) = S^{-1}(t, 0)\psi(x)S(t, 0),$$

and we have the usual expression

$$G = \frac{\langle 0 | S(\infty, t)\psi(x)S(t, t')\psi^\dagger(x')S(t', -\infty) | 0 \rangle}{\langle 0 | S(\infty, -\infty) | 0 \rangle},$$

$$G(x, x') = G_0(x, x') - iG_0(x, x'')W(x'', x''')G(x''', x'), \quad (6)$$

where repeated arguments are integrated over,  $G_0$  is the zero-order value, and  $-iW$  is the sum of all proper linked diagrams—omitting factors for the terminal lines. Then from (3) with  $t=0$ ,

$$\phi(\vec{r}) = \phi_0(\vec{r}) - iG_0(E, \vec{r}, \vec{r}')W(E, \vec{r}', \vec{r}'')\phi(\vec{r}''), \quad (7)$$

where

$$W(E, \vec{r}, \vec{r}') = \int d(t-t') e^{iE(t-t')} W(x, x'), \quad (8)$$

and likewise for  $G_0$ .

Now if  $u_n$  are a complete set of wave functions for the potential  $U$ , with eigenvalues  $E_0$ ,

$$-iG_0 = \sum_n \frac{\text{unocc. } u_n(\vec{r})u_n^*(\vec{r}')}{E - E_n + i\epsilon} + \sum_n \frac{\text{occ. } u_n(\vec{r})u_n^*(\vec{r}')}{E - E_n - i\epsilon}.$$

Since all the occupied states are of negative energy, for positive  $E$  the sign of the infinitesimal  $i\epsilon$  is unimportant in the last term. Thus

$$\phi(\vec{r}) = \phi_0(\vec{r}) + \sum_n \frac{u_n(\vec{r})u_n^*(\vec{r}')}{E - E_n + i\epsilon} W(E, \vec{r}', \vec{r}'')\phi(\vec{r}''). \quad (9)$$

This is just the integral equation for scattering by an added potential  $W$ , and therefore

$$V(E, \vec{r}, \vec{r}') = U(\vec{r}, \vec{r}') + W(E, \vec{r}, \vec{r}') \quad (10)$$

is the total optical potential. The scattering amplitude averaged over an interval of energy can be obtained from  $V(E + i\epsilon, \vec{r}, \vec{r}')$  with  $\epsilon$  finite.

# Particle-Vibration Coupling

- After BM approach, we must remember
- the paper by Nicole Vinh-Mau:
- Microscopic derivation of the optical potential
- in “Theory of Nuclear Structure: Trieste
- Lectures 1969”
- IAEA, 1970



# Green's Function Approach to Particle-Vibration Coupling.

M. BALDO

*Istituto di Fisica Teorica dell'Università - Catania, Italia*

*Istituto Nazionale di Fisica Nucleare - Sezione di Catania, Italia*

P. F. BORTIGNON

*Istituto di Fisica dell'Università - Padova, Italia*

*Istituto Nazionale di Fisica Nucleare - Sezione di Padova, Italia*

(ricevuto il 3 Ottobre 1975)

In the last few years many attempts <sup>(1)</sup> have been made to introduce the phonon degree of freedom in the description of both single-particle structure and collective excitations of heavy and mean-heavy nuclei (particle-vibration coupling). The main problem in this type of approach is to separate correctly the particle and the phonon degrees of freedom, *i.e.* to avoid Pauli-principle violation and overcounting of terms. The rules for constructing graphs which include explicitly the phonon lines have been extracted, on the basis of a solvable model, in ref. <sup>(2)</sup>, and shown to produce an exact expansion, in the sense that the complete summation of the graph series reproduces the exact results in the model. The general validity of the rules proposed in ref. <sup>(2)</sup> was worked out in ref. <sup>(3)</sup>.

In this letter we want to show that it is possible to approach the problem on general grounds, using techniques developped by many authors <sup>(4)</sup> in the framework of the so-called « conserving » approximations. For the sake of simplicity let us consider a particle coupled to a core, and define the particle and phonon degrees of freedom respectively by the single-particle and density-density correlation functions

$$(1) \quad G_{kl}(t_1, t_2) = -i \langle \Psi_0 | T \{ \psi_k(t_1) \psi_l^\dagger(t_2) \} | \Psi_0 \rangle \quad \text{particle degrees of freedom,}$$

$$(2) \quad \chi_{kl,mn}(t_1, t_2) = - \langle \Psi_0 | T \{ \rho_{kl}'(t_1) \rho_{mn}'^\dagger(t_2) \} | \Psi_0 \rangle \quad \text{phonon degrees of freedom,}$$

---

<sup>(1)</sup> See, for instance, S. T. BELYAEV: *Sov. Journ. Nucl. Phys.*, **1**, 3 (1965); B. R. MOTTelson: *International Conference on Nuclear Structure*, edited by I. Scharaf (Tokyo, 1967); A. Bohr and B. Mottelson: *Nuclear Structure*, 2nd ed. (New York, 1968).



physics case. The main idea is to express the single-particle self-energy in terms of a functional derivative of the single-particle Green's function with respect to a one-body external potential  $\varphi(t)$ , which depends explicitly on time. This functional derivative has to be taken at  $\varphi = 0$ , so that in the final result  $\varphi$  will not appear.

The Hamiltonian of the system will read

$$(3) \quad H' = H + \varphi(t),$$

where  $H$  is a general nuclear Hamiltonian with a two-body residual interaction

$$(4) \quad H = \sum_k \varepsilon_k \psi_k^\dagger \psi_k + \frac{1}{2} \sum_{klmn} (kl|V|mn) \psi_k^\dagger \psi_l^\dagger \psi_n \psi_m,$$

$\varepsilon_k$  being the single-particle energies and

$$(5) \quad \varphi(t) = \sum_{kl} (k|\varphi(t)|l) \psi_k^\dagger \psi_l,$$

Considering the equation of motion of the single-particle Green's function one gets ( $\hbar = 1$ )

$$(6) \quad i \frac{\partial}{\partial t_1} G_{kl}(t_1, t_2) = \delta_{kl} \delta(t_1 - t_2) - i \langle \Psi_0 | T \{ [\psi_k(t_1), H'(t_1)] \psi_l^\dagger(t_2) \} | \Psi_0 \rangle = \\ = \delta_{kl} \delta(t_1 - t_2) + \sum_m [\varepsilon_m \delta_{mk} + (k|V_H(t_1)|m)] G_{ml}(t_1, t_2) + \sum_m M_{km}(t_1, \bar{t}_3) G_{ml}(\bar{t}_3, t_2),$$

where, as usual,

$$(7) \quad \sum_m M_{km}(t_1, \bar{t}_3) G_{ml}(\bar{t}_3, t_2) = -i \sum_{l'n} (kl'|V|mn) \langle \Psi_0 | T \{ \psi_{l'}^\dagger(t_1) \psi_n(t_1) \psi_m(t_1) \psi_l^\dagger(t_2) \} | \Psi_0 \rangle - \\ - \sum_m (k|V_H(t_1)|m) G_{ml}(t_1, t_2)$$

is the single-particle self-energy and  $(k|V_H(t)|m) = \sum_{l'n} (kl'|V|mn) \langle \Psi_0 | \psi_{l'}^\dagger(t) \psi_n(t) | \Psi_0 \rangle$ . A bar over a time variable means integration. It can be shown that (see eq. (B8) of ref. (5))

physics case. The main idea is to express the single-particle self-energy in terms of a functional derivative of the single-particle Green's function with respect to a one-body external potential  $\varphi(t)$ , which depends explicitly on time. This functional derivative has to be taken at  $\varphi = 0$ , so that in the final result  $\varphi$  will not appear.

The Hamiltonian of the system will read

$$(3) \quad H' = H + \varphi(t),$$

where  $H$  is a general nuclear Hamiltonian with a two-body residual interaction

$$(4) \quad H = \sum_k \varepsilon_k \psi_k^\dagger \psi_k + \frac{1}{2} \sum_{klmn} (kl|V|mn) \psi_k^\dagger \psi_l^\dagger \psi_n \psi_m,$$

$\varepsilon_k$  being the single-particle energies and

$$(5) \quad \varphi(t) = \sum_{kl} (k|\varphi(t)|l) \psi_k^\dagger \psi_l,$$

Considering the equation of motion of the single-particle Green's function one gets ( $\hbar = 1$ )

$$(6) \quad i \frac{\partial}{\partial t_1} G_{kl}(t_1, t_2) = \delta_{kl} \delta(t_1 - t_2) - i \langle \Psi_0 | T \{ [\psi_k(t_1), H'(t_1)] \psi_l^\dagger(t_2) \} | \Psi_0 \rangle = \\ = \delta_{kl} \delta(t_1 - t_2) + \sum_m [\varepsilon_m \delta_{mk} + (k|V_H(t_1)|m)] G_{ml}(t_1, t_2) + \sum_m M_{km}(t_1, \bar{t}_3) G_{ml}(\bar{t}_3, t_2),$$

where, as usual,

$$(7) \quad \sum_m M_{km}(t_1, \bar{t}_3) G_{ml}(\bar{t}_3, t_2) = -i \sum_{l'n} (kl'|V|mn) \langle \Psi_0 | T \{ \psi_{l'}^\dagger(t_1) \psi_n(t_1) \psi_m(t_1) \psi_l^\dagger(t_2) \} | \Psi_0 \rangle - \\ - \sum_m (k|V_H(t_1)|m) G_{ml}(t_1, t_2)$$

is the single-particle self-energy and  $(k|V_H(t)|m) = \sum_{l'n} (kl'|V|mn) \langle \Psi_0 | \psi_{l'}^\dagger(t) \psi_n(t) | \Psi_0 \rangle$ . A bar over a time variable means integration. It can be shown that (see eq. (B8) of ref. (5))



tional derivative of  $U$  with respect to  $\varphi$  is

$$(10) \quad \left( \frac{\delta U_{kl}(t_1)}{\delta \varphi_{pq}(t_2)} \right) = \delta_{kp} \delta_{lq} \delta(t_1 - t_2) - i \sum_{mn} \chi_{pq, nm}(t_2, t_1) [(km|V|ln) - (km|V|nl)],$$

where the second term gives rise to the coupling of the fermion degrees of freedom with the phonons. Using the relationships

$$(11) \quad \begin{cases} \frac{\delta G_{kl}(t_1, t_2)}{\delta \varphi_{mn}(t_3)} = - \sum_{pq} G_{kp}(t_1, \bar{t}_4) \cdot \frac{\delta G_{pq}^{-1}(\bar{t}_4, \bar{t}_5)}{\delta \varphi_{mn}(t_3)} \cdot G_{ql}(\bar{t}_5, t_2), \\ \frac{\delta}{\delta \varphi_{mn}(t_1)} = \sum_{pq} \frac{\delta U_{pq}(\bar{t}_2)}{\delta \varphi_{mn}(t_1)} \cdot \frac{\delta}{\delta U_{pq}(\bar{t}_2)}, \end{cases}$$

one can write eq. (8) in the form

$$(12) \quad M_{kl}(t_1, t_2) = -i \sum_{\substack{l'n \\ p, rs}} (kl'|V|mn) G_{mp}(t_1, \bar{t}_3) \frac{\delta U_{rs}(\bar{t}_4)}{\delta \varphi_{l'n}(t_1)} \times \frac{\delta G_{pl}^{-1}(\bar{t}_3, t_2)}{\delta U_{rs}(\bar{t}_4)} = \\ = -i \sum_{\substack{mp \\ rs}} W_{km, rs}(t_1, \bar{t}_4) G_{mp}(t_1, \bar{t}_3) \Gamma_{pl; rs}(\bar{t}_3, t_2, \bar{t}_4),$$

where

$$(13) \quad \begin{cases} W_{km, rs}(t_1, t_2) = \sum_{ln} (kl|V|mn) \frac{\delta U_{rs}(t_2)}{\delta \varphi_{ln}(t_1)} = (kr|V|ms) \delta(t_1 - t_2) - \\ - i \sum_{lnpq} (kl|V|mn) \chi_{ln; qp}(t_1, t_2) [(rp|V|sq) - (rp|V|qs)], \\ \Gamma_{pl, rs}(t_1, t_2; t_3) = - \frac{\delta G_{pl}^{-1}(t_1, t_2)}{\delta U_{rs}(t_3)}. \end{cases}$$

The physical meaning of the last expression of  $W$  is clear: the effective interaction to be used in the calculation of  $M$  involves both the bare interaction and the exchange of phonons. For the vertex function  $\Gamma$  the following integral equation is obtained:

$$(14) \quad \Gamma_{kl, mn}(t_1, t_2; t_3) = \delta_{km} \delta_{ln} \delta(t_1 - t_3) \delta(t_2 - t_3) + \\ + \sum_{\bar{t}_4, \bar{t}_5} \left[ \frac{\delta M_{kl}(t_1, t_2)}{\delta G_{mn}(\bar{t}_4, \bar{t}_5)} + i(kq|V|pl) \delta(t_1 - \bar{t}_4) \delta(t_2 - \bar{t}_5) \right] G_{pr}(\bar{t}_4, \bar{t}_6) G_{sq}(\bar{t}_7, \bar{t}_5) \Gamma_{rs; mn}(\bar{t}_6, \bar{t}_7; t_3).$$



coupling theory, at least for  $M_{kl}$ . In fact starting from the zeroth-order value for  $\Gamma_{kl;mn}(t_1, t_2; t_3) = \delta_{kn} \delta_{ln} \delta(t_1 - t_2) \delta(t_1 - t_3)$  and iterating these equations, one gets an expansion for the self-energy  $M$  and phonon propagator  $\chi$  which involves only  $W$  and  $G$ .

For instance the first two terms of the expansion for  $M$  read

$$(17a) \quad - \sum_{mp} (kp|V|ml) \langle \Psi_0 | \psi_p^\dagger \psi_m | \Psi_0 \rangle,$$

$$(17b) \quad - \sum_{\substack{m p l' \\ n q p'}} (kl'|V|mn) \chi_{l'n;qp'}(t_1, t_2) [(pp'|V|lq) - (pp'|V|ql)] G_{mp}(t_1, t_2).$$

The term (17a) is the exchange part of the Hartree-Fock field; the term (17b) involves the contribution from the phonon field. It should be noted that the interaction at time  $t_2$  includes both the direct and the exchange terms, while the second interaction at time  $t_1$  includes only the direct one. These two and some higher-order contribution to  $M$  are displayed in fig. 1.

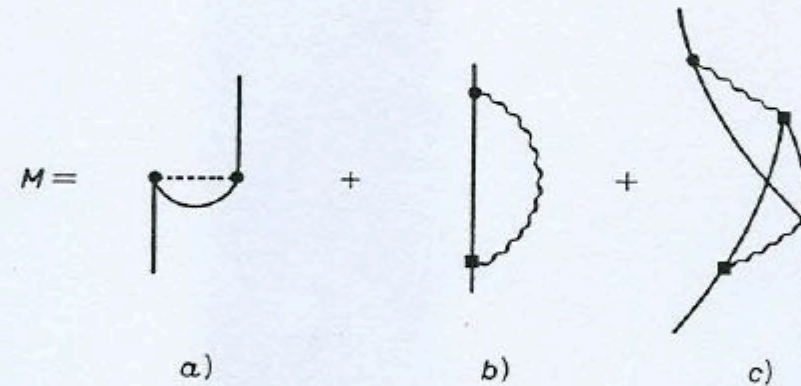


Fig. 1.

In particular the diagram c) corrects for Pauli-principle violation in the intermediate states. In all the drawn diagrams a full dot means only the direct matrix element of  $V$ , while a full square the direct minus the exchange one.

Analogously for  $\chi$  one gets

$$(18) \quad \chi_{kl;mn}(t_2, t_1) = i P_{kl;mn}(t_2, t_1) -$$

$$- i \sum_{pqrstu} \chi_{kl,tu}(t_2, \bar{t}_5) [(ru|V|st) - (ru|V|ts)] G_{mp}(t_1^+, \bar{t}_3) G_{qn}(\bar{t}_4, t_1) \cdot \{ \delta_{pr} \delta_{qs} \delta(\bar{t}_3 - \bar{t}_5) \delta(\bar{t}_4 - \bar{t}_5) -$$



cesses like those depicted in fig. 2c), it follows that the graphs generated by the expansion do not allow any bubble to appear.

We can note that the rules for coupling fermions and phonons we have discussed seem to be quite similar to the rules which have been found in many references by dif-

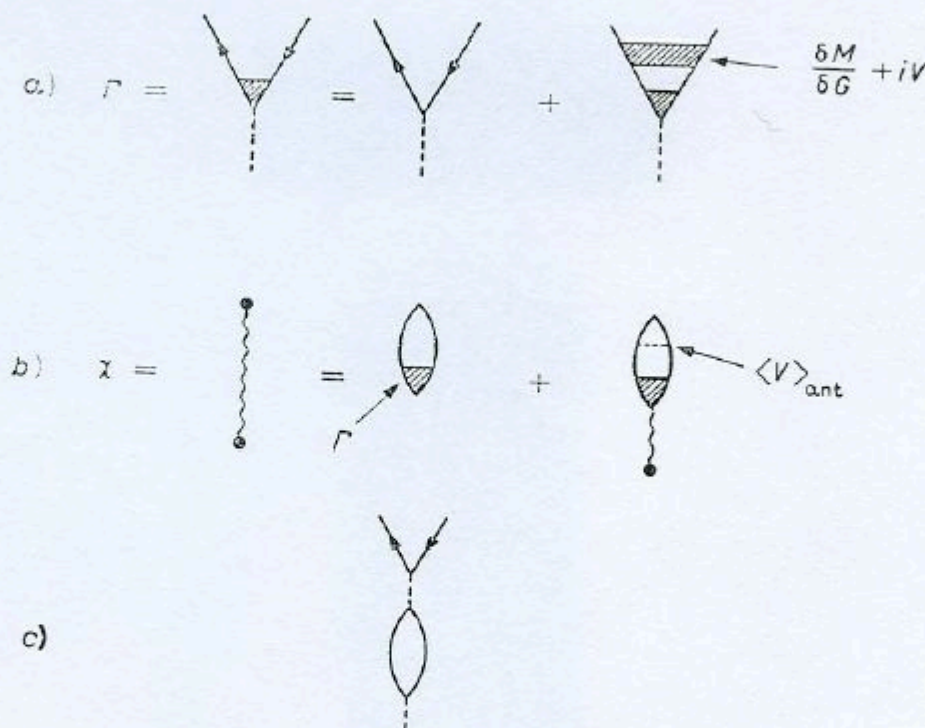


Fig. 2.

ferent and often empirical approaches and for different physical situations <sup>(2,3,6)</sup> (like two phonons or particle plus phonons systems). Then these rules seem to be quite general to handle in a self-consistent way particle-phonon coupling problems avoiding overcounting and Pauli-principle violations.

Finally it should be possible in the formalism to treat also a density-dependent interaction, as shown in ref. (7) for the particle-hole interaction.

\* \* \*

Stimulating discussions with Prof. R. BROGLIA are gratefully acknowledged.

**Role of the surface in the electronic effective mass of metal microclusters**

M. Bernath,<sup>1,2</sup> M. S. Hansen,<sup>3</sup> P. F. Bortignon,<sup>1,2</sup> and R. A. Broglia<sup>1,2,3</sup>

<sup>1</sup>*Dipartimento di Fisica, Università di Milano, Via Celoria 16, 20133, Milan, Italy*

<sup>2</sup>*Istituto Nazionale di Fisica Nucleare, Sezione di Milano, Via Celoria 16, 20133, Milan, Italy*

<sup>3</sup>*The Niels Bohr Institute, University of Copenhagen, DK-2100 Copenhagen, Denmark*

(Received 2 June 1992; revised manuscript received 19 July 1993)

The renormalization of the motion of the valence electrons in metal clusters arising from the coupling to the fluctuations of the cluster surface is calculated. Sizable effects are found, which lead to renormalization coefficients which deviate 30–40 % from unity.

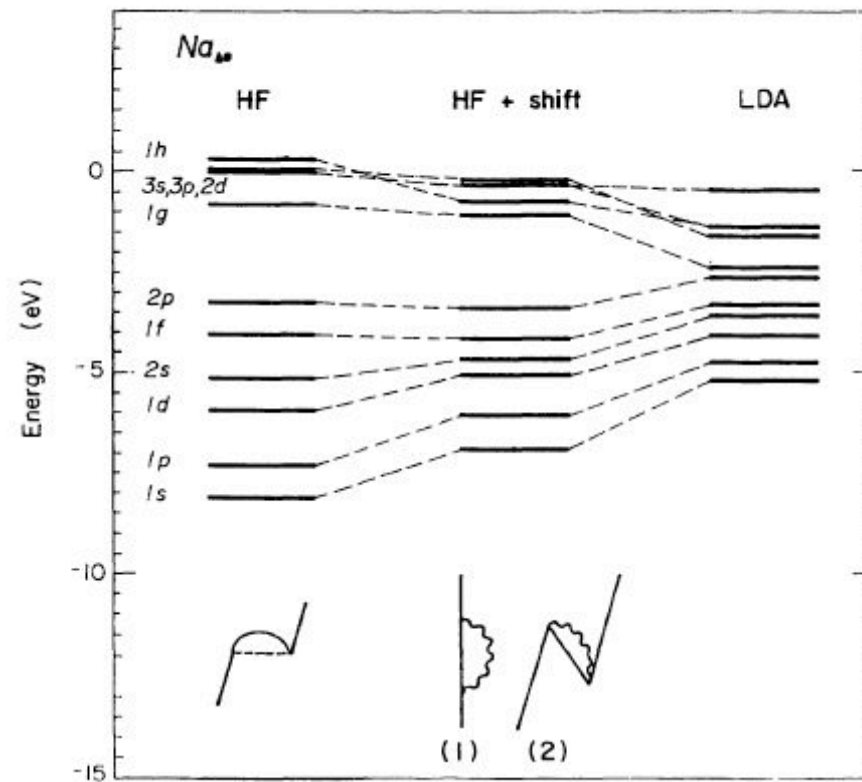


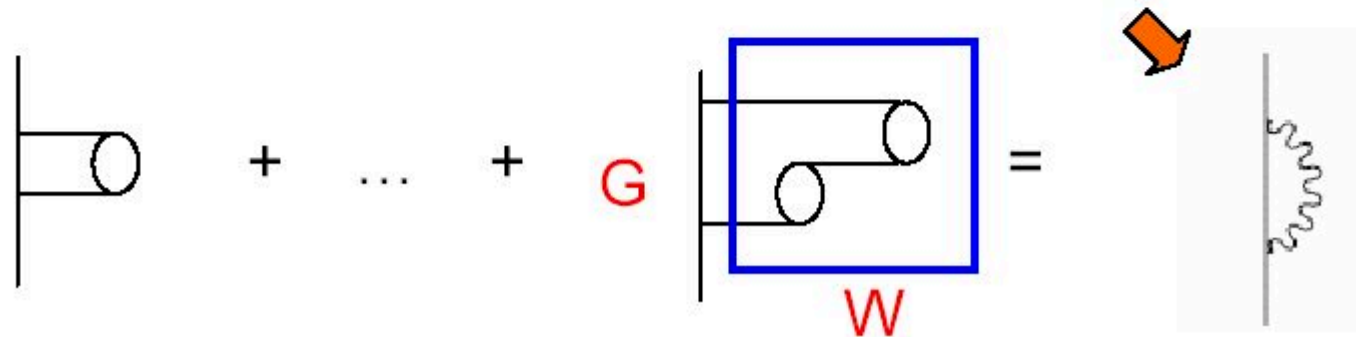
FIG. 1. First and last columns display the energy levels of  $\text{Na}_{40}$  within the Hartree-Fock and LDA, respectively. The middle column shows the Hartree-Fock levels corrected by the self-energy contributions calculated as indicated in the text. In the lowest part of the figure a schematic graphical representation of the exchange (first column) and screening terms (middle column) discussed in the text is shown.



**Table 1** Fundamental band gaps of some materials (eV).

Material	DFT-LDA [6]	GW [6]	Experiment [7]
Si	0.5	1.3	1.2
GaN	2.3	3.5	3.5
Diamond	3.9	5.6	5.5
LiCl	6.0	9.1	9.4

Phys. Stat. Sol. 10, 3365 (2006)



# NUCLEAR FIELD THEORY

NUCLEAR FIELD THEORY AS A METHOD OF TREATING THE PROBLEM  
OF OVERCOMPLETENESS IN DESCRIPTIONS INVOLVING ELEMENTARY  
MODES OF BOTH QUASI-PARTICLES AND COLLECTIVE TYPE \*

D.R. BES \*\*, G.G. DUSSEL \*\*

*Comision Nacional de Energia Atomica, Buenos Aires, Argentina*

R.A. BROGLIA \*

*Physics Department, State University of New York at Stony Brook and  
Niels Bohr Institute, University of Copenhagen, Denmark*

R. LIOTTA

*Niels Bohr Institute, University of Copenhagen, Denmark*

and

B.R. MOTTelson

*NORDITA, Copenhagen, Denmark*

Received 29 August 1974

It is shown that the graphical perturbation treatment of nuclear fields (particle-vibration theory) converges to the exact solution, at least in the case of schematic many-body problems. The corresponding rules as well as all the interaction vertices required to obtain this convergence are here presented.

The elementary modes of excitations of atomic nuclei are found to comprise partly collective (boson) excitations associated with pair addition, shape oscillations, etc., and partly quasi-particle modes as described approximately by independent particle motion. The displacement potential associated with the vibrations of the nuclear density gives rise to the particle vibration coupling. The resulting coupled system of particles and bosons constitutes a nuclear field theory that is extensively employed in the study of the mutual interweaving of these elementary excitations in the physical states of nuclei. However, both types of excitations are ultimately based on the degrees of freedom of the neutrons and protons of the nucleus and thus are not strictly independent. One is thus faced with the problem of exploring the consequences of the antisymmetry (Pauli principle) associated with the identity of the nucleons

that appear in the collective modes and in the particle degrees of freedom as well as the features resulting from the non-orthogonality of the elementary modes. In some cases, it has been shown that the nuclear field theory correctly treats these effects in lowest order of perturbation theory [1]. But the formal basis for this treatment as well as the systematic demonstration of its consistency has not been adequately discussed. In the present note we report on the study of a simplified model which permits comparison of results of an exact solution with those obtained from the perturbation expansion based on the particle-vibration coupling. It is found that simple and general rules can be formulated for evaluating the particle-vibration coupling diagrams and that the systematic application of these rules leads to the same results as the exact solution, at least within the model studied.

The problems considered in the present note are generic to a wide variety of many-body systems in which collective modes are a significant feature; however, the problems are encountered in an especially acute form in the nuclear physics applications due to the relatively

\* Research supported in part by AEC grant No. AG (11-1)-3001.

\*\* Fellow of the Consejo Nacional de Investigaciones Cientificas y Tecnicas.

few particles involved in the nuclear collective degrees of freedom <sup>+1</sup>.

The model considered consists of two single-particle levels, each with degeneracy  $2\Omega$  and with an effective "monopole" twoparticle force coupling particles in the two levels,

$$H = H_{sp} + H_{int} \quad (1)$$

where

$$H_{sp} = \frac{1}{2} \epsilon N_0,$$

$$N_0 = \sum_{\substack{\sigma=\pm 1 \\ m=\pm 1, \pm 2, \dots}} \sigma a_{m\sigma}^+ a_{m\sigma}, \quad (2)$$

and

$$H_{int} = -V\Omega (A_1^+ A_1 + A_1 A_1^+),$$

$$A_1^+ = \frac{1}{\sqrt{2\Omega}} \sum_m a_{m,1}^+ a_{m,-1}. \quad (3)$$

The index  $\sigma$  labels the two levels while  $m$  labels the degenerate states within each level. The strength of the monopole coupling is denoted by  $V$  and the energy difference between the two different one-particle levels is  $\epsilon$ . The symmetrized form of the interaction leads to a slight complication of the formula to be obtained below, but has been employed in (3) in order to exhibit the manner in which the Hartree contributions of the interaction are to be included in the definition of the elementary modes that are employed in the nuclear field theory. The possibility of obtaining an exact solution [2] of the systems described by (1) hinges on the fact that the basic operators of the model,  $N_0$ ,  $A_1$  and  $A_1^+$  obey the commutation relations of the infinitesimal generators of the group  $SU(2)$ .

We now develop an exact solution of the problem (1) based on the concept of particle degrees of freedom coupled to collective modes, with the latter defined by means of the random phase approximation. We consider configurations with approximately  $N = 2\Omega$  particles. The ground state (vacuum state for our descrip-

tion) of the system with  $N = 2\Omega$  is given by the Slater determinant in which all the  $\sigma = -1$  states are occupied (we assume  $\epsilon > 2V(\Omega - \frac{1}{2})$  which is necessary to ensure the stability of this normal ground state).

The basic particle and hole states are obtained by adding or removing a single particle from this configuration <sup>+2</sup>

$$|m, 1\rangle = a_{m,1}^+ |0\rangle, \quad E(m, 1) = \frac{1}{2}(\epsilon + V), \quad (4)$$

$$|m, -1\rangle = a_{m,-1} |0\rangle, \quad E(m, -1) = \frac{1}{2}(\epsilon + V).$$

Thus the unperturbed energy for producing a particle-hole excitation with respect to the ground state is

$$\epsilon' = E(m, 1) + E(m, -1) = \epsilon + V. \quad (5)$$

With this particle-hole energy, the random phase approximation yields for the collective modes

$$\omega_1 = \epsilon' - 2V\Omega, \quad \omega_i = \epsilon', \quad (i = 2, 3, \dots, 2\Omega), \quad (6)$$

corresponding to the normal modes

$$|n_i = 1\rangle = A_1^+ |0\rangle, \quad (7)$$

with  $A_1^+$  given by (3) and the  $\Omega - 1$  other normal modes  $i = 2, \dots, 2\Omega$ , forming an orthogonal basis in the remaining space of particle-hole excitations  $|m, 1; m, -1\rangle$ .

The particle-vibration coupling represents the matrix element of the Hamiltonian linking the normal modes with a single particle-hole state

$$\langle n_i = 1 | H_{int} | m, 1; m', -1 \rangle = -V\sqrt{2\Omega} \delta(m, m') \delta(i, 1), \quad (8)$$

and is represented by the vertex of fig. 1(a). In the diagrammatic rules to be given below we shall also need to include effects resulting from the four-point vertex of fig. 1(b), which has the value

$$\begin{aligned} \langle m, 1; m', -1 | H_{int} | m'', 1; m''', -1 \rangle \\ = -V\delta(m, m') \delta(m'', m'''). \end{aligned} \quad (9)$$

We have found that the results of the exact solution of the Hamiltonian can be reproduced if we take as the basic degrees of freedom both the collective modes (7)

<sup>+1</sup> The ubiquitous appearance of these questions in nuclear physics problems has stimulated a great variety of theoretical approaches and approximations; see, for example the references quoted in the review paper of R.M. Dreizler in Proceedings of the Summer School on Problems in Nuclear and Solid State Physics, Roumania (1973), to appear, and the references quoted in this article.

<sup>+2</sup> Note that the energies are measured from the energy of the vacuum state.

<sup>+3</sup> In the present model this is in fact the Tamm-Dancoff approximation since the Hamiltonian (1) does not contain any interactions that create two-particle, two-hole configurations.

and the particle states (4) coupled through the interactions (8) and (9). The fact that a significant part of the original interaction has already been included in generating the collective mode (7), implies that the rules for evaluating the couplings (8) and (9) involve a number of restrictions as compared with the rules that are employed when evaluating the original interaction (3):

(I) In initial and final states, proper diagrams involve collective modes and particle modes, but not any particle configuration that can be replaced by a combination of collective modes. This restriction permits an initial state comprising the configuration  $|m, 1; n_1=1\rangle$  but excludes  $|m, 1; m, -1\rangle$ .

(II) The couplings are allowed to act in all orders to generate the different diagrams of perturbation lines of these diagrams.

(III) The internal lines of diagrams are, however, restricted by the exclusion of diagrams in which a particle-hole pair is created and subsequently annihilated without having participated in subsequent interactions. As an illustration of this rule, fig. 2(a) shows an excluded diagram, while fig. 2(b) is permitted.

(IV) The energies of the uncoupled particle and phonon fields are given by (5) and (6) and the contributions of all allowed diagrams are evaluated by the usual rules of perturbation theory.

We shall now illustrate the application of the above rules in the evaluation of the different properties of the system and shall confirm that the results of the exact solutions are recovered when the resulting perturbation series is summed.

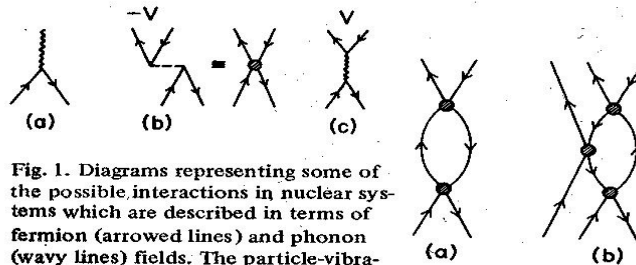


Fig. 1. Diagrams representing some of the possible interactions in nuclear systems which are described in terms of fermion (arrowed lines) and phonon (wavy lines) fields. The particle-vibration coupling and the exchange of one collective phonon are displayed in (a) and (c), while (b) represents a particle-hole scattering through the two-body bare interaction of the model.

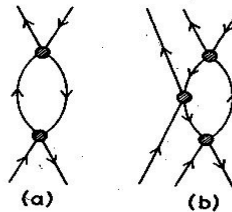


Fig. 2. Illustration of rule III. The diagram (a) is eliminated by rule III but (b) is allowed.

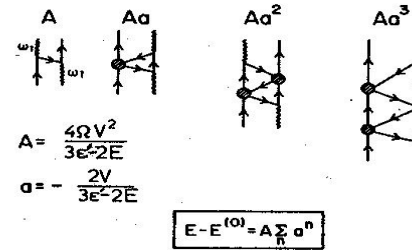


Fig. 3. Graphs describing the interaction between a fermion and a collective boson  $\omega_1$ . The secular equation is given in terms of the quantities  $A$  and  $a$ .

i) States comprising one particle, one hole, or a single particle-hole pair do not suffer interaction effects and therefore their energies are those of the uncoupled configuration. Note that the particle-hole configuration  $|m, 1; m, -1\rangle$  does enter into interactions according to (8) and (9) but this configuration is excluded as an external line according to the rule I. Similarly a configuration of a single collective mode  $|n_1=1\rangle$  does not suffer any interaction effect since any diagram involving only such a configuration in initial and final state is excluded by rule III.

ii) The energy of the state comprising a single particle plus one phonon of the type  $i=1$  is in zeroth order (cf. (4) and (6))

$$E^{(0)}(m, 1; n_1=1) = \frac{1}{2}\epsilon' + \omega_1. \quad (11)$$

The lowest order correction to this energy is given by the graph  $A$  in fig. 3 and the resulting contribution is the expression given in the figure with the energy in the denominator  $E = E^{(0)}$ . The summation of the iterates of this graph to all orders yields the same expression with the energy  $E$  representing the final eigenvalue. The interaction (9) appears first in the graph  $Aa$  of fig. 3 and the iteration of these interactions can be summed as indicated in the figure to give

$$E(m, 1; n_1=1) - E^{(0)}(m, 1; n_1=1) = \frac{4\Omega V^2}{3\epsilon' - 2E(m, 1; n_1=1) + 2V}, \quad (12)$$

which yields the two solutions

$$E = \left\{ \begin{array}{l} \frac{3}{2}\epsilon' \\ E^{(0)}(m, 1; n_1=1) + V \end{array} \right. \quad (13)$$



### On the Small parameter...

The random phase approximation yields for the collective mode

$$\omega = \epsilon' - 2V\Omega.$$

Therefore, it is

$$V\Omega \sim O(1),$$

the bare interaction

$$V \sim O\left(\frac{1}{\Omega}\right)$$

and the particle-vibration coupling

$$V\sqrt{2\Omega} \sim O\left(\frac{1}{\sqrt{\Omega}}\right).$$

"Realistic calculations", also for  $^{209}\text{Bi}$ , in

P.F. Bortignon, R.A. Broglia, D.R. Bes, R. Liotta, Phys. Rep. 30 (1977), 305.

P.F. Bortignon, R.A. Broglia, D.R. Bes, Phys. Lett. B 76 (1978) 153.

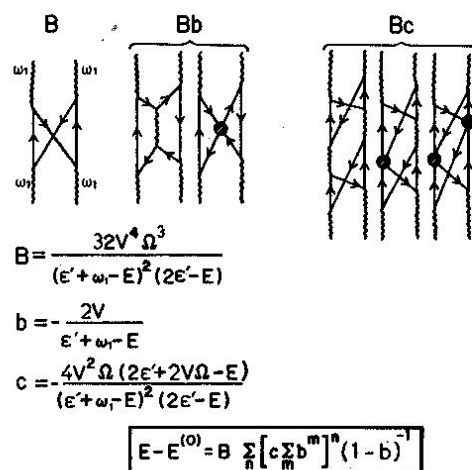


Fig. 4. Graphs describing the interaction between two collective phonons  $\omega_1$ . The secular equation is given in terms of the quantities  $B$ ,  $b$  and  $c$ .

Only the second solution goes to  $E^{(0)}$  for vanishing coupling and thus represents the value that would have been obtained from a more straightforward term by term summation of the perturbation series. The result obtained can be expressed by saying that the non-linearity of the problem in the elementary modes of the system give rise to an effective particle-phonon interaction of magnitude  $V$ . The magnitude of this correction agrees with that obtained from the exact solution. It is characteristic that these correction terms are of order  $\Omega^{-1}$  compared with the collective shift,  $2V\Omega$ , of the phonon with respect to the unperturbed particle-hole energy.

iii) The energy of the two phonon state  $n_1 = 2$  involves summing three series of graphs (see fig. 4); the resulting equation yields three different eigenvalues of which only the one

$$E(n_1 = 2) = 2\omega_1 + 2V, \quad (14)$$

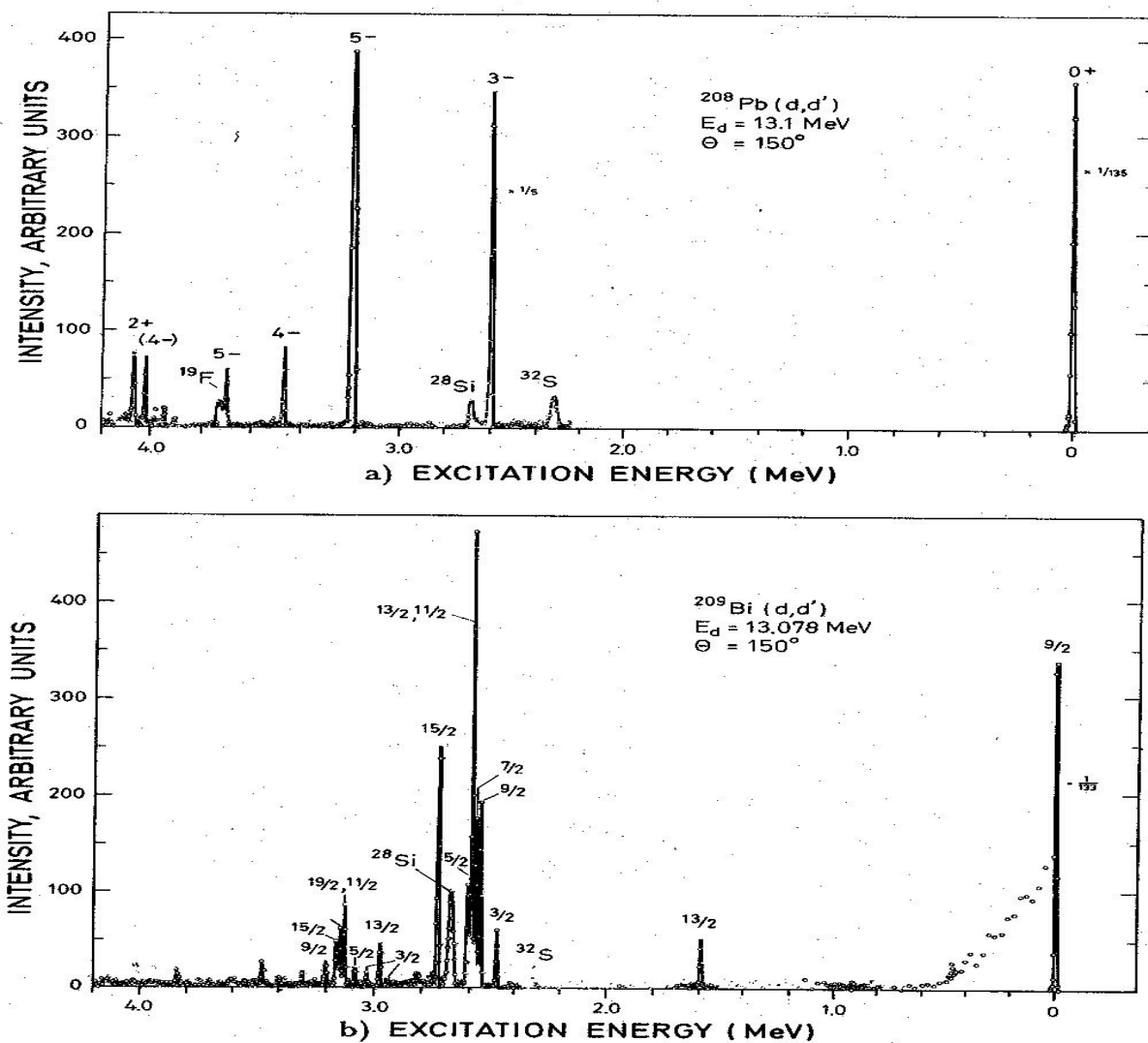
is in the neighbourhood of the unperturbed two-phonon state. Again the eigenvalue obtained from the summation of the particle-vibration diagrams corresponds to that obtained from the exact solution. The expression (14) exhibits an anharmonicity in the collective vibrational motion that can be expressed as a phonon-phonon interaction energy of magnitude  $2V$ .

The examples given above are representative of a rather large variety of properties which we have evaluated and found to be in agreement with the corresponding exact solutions. Based on this empirical evidence, it is our belief that the above rules represent a general prescription for evaluating all the coupling and anharmonicity effects involved when superposing particles and phonons.

Discussions with Aage Bohr are gratefully acknowledged.

## References

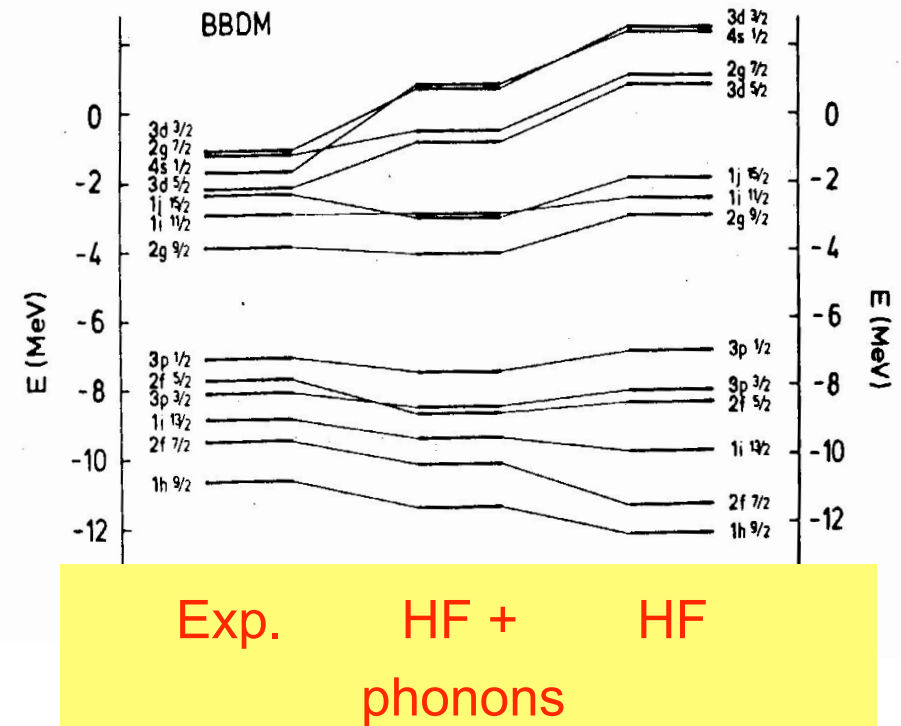
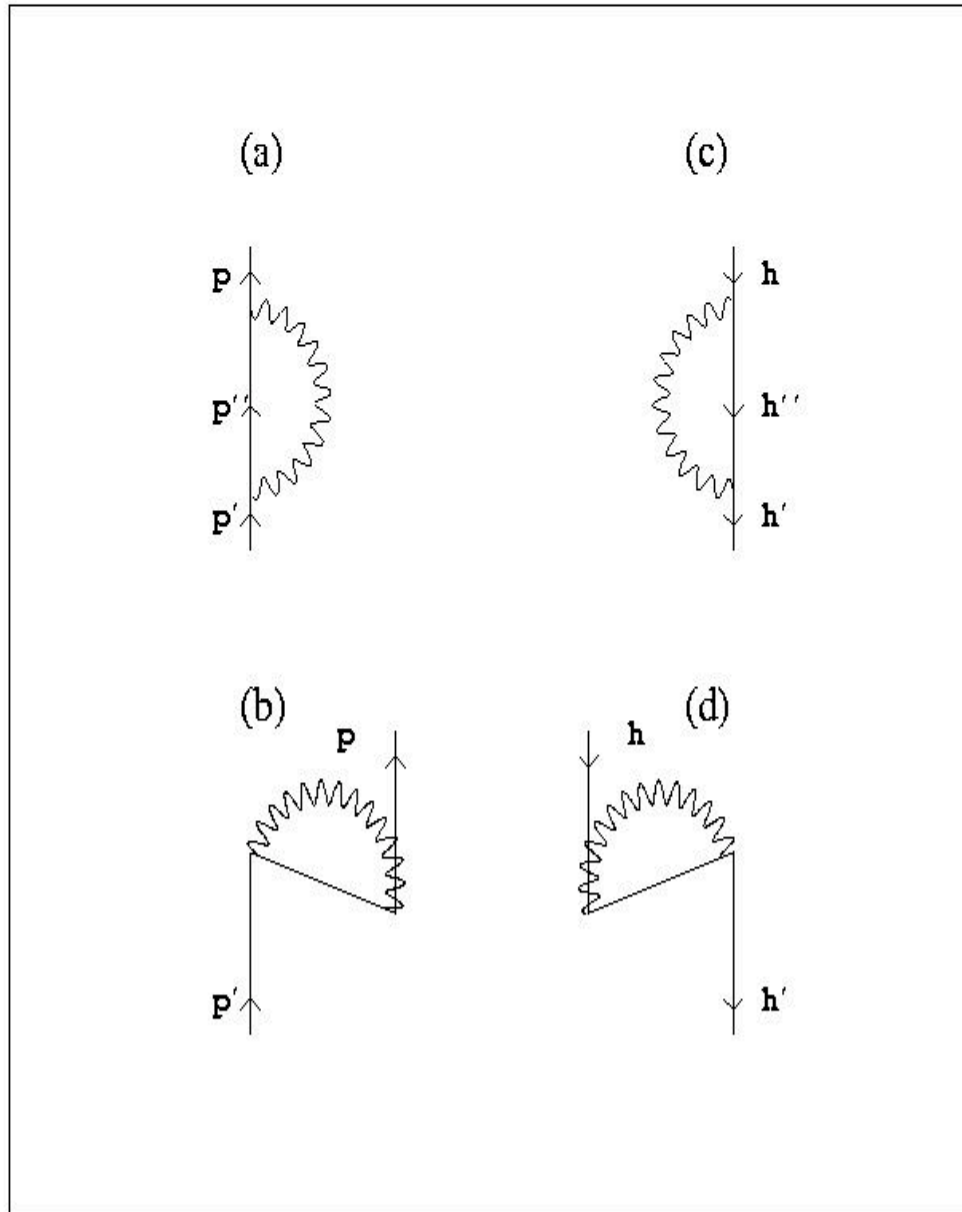
- [1] B.R. Mottelson, J. Phys. Soc. Japan, Suppl. 24 (1968) 87; see also A. Bohr and B. Mottelson, "Nuclear Structure", Vol. II, W.A. (Benjamin Inc.) to appear; D.R. Bes and R.A. Broglia, Phys. Rev. C3 (1971) 2349.
- [2] H.J. Lipkin, N. Meshkov and A.J. Glick, Nucl. Phys. 62 (1965) 188.



**Figure 6-42** Excitation of octupole mode in  $^{208}\text{Pb}$  and  $^{209}\text{Bi}$  by inelastic scattering of deuterons. The figure is based on experimental data by J. Ungrin, R. M. Diamond, P. O. Tjøm, and B. Elbek, *Mat. Fys. Medd. Dan. Vid. Selsk.* **38**, no. 8, 1971.



The phonon coupling has been known for many years to be important for the understanding of s.p. states around the  $^{208}\text{Pb}$  core.



C.Mahaux et al., Phys. Rep., 1985  $\Rightarrow$  PV coupling increases  $m^*$

# On Self-Energy, Effective Masses, Level Density

$$\Delta E_{\beta}(\omega)=\sum_{\alpha}\frac{V_{pv}^2(\alpha,\beta;L)}{\omega-(\epsilon_{\alpha}+\hbar\omega_L)}$$

$$\frac{d\epsilon}{dk}=\frac{\hbar^2k}{m^{\star}}$$

$$\frac{m^{\star}}{m}=\frac{m_k}{m}\frac{m_{\omega}}{m}$$

$$m_k=m(1+\frac{m}{\hbar^2}\frac{\partial U_{HF}}{\partial k})^{-1}$$

$$m_{\omega}=m(1-\frac{\partial \Delta E}{\partial \omega})$$

$$(\frac{\partial \Delta E}{\partial \omega})_{\omega=0}\approx -N(0)\int_0^{\infty}\frac{V_{pv}^2d\epsilon}{(\epsilon+\hbar\omega_L)^2}=-N(0)\frac{V_{pv}^2}{\hbar\omega_L}$$

## Self-energy and effective mass

$$m_{\omega} \approx \left( 1 + \frac{N(0)V^2}{\hbar\omega_{\lambda}} \right) m$$



$$= \frac{V^2}{e_1 - (e_2 + \hbar\omega_{\lambda})} \approx -\frac{V^2}{\hbar\omega_{\lambda}}$$

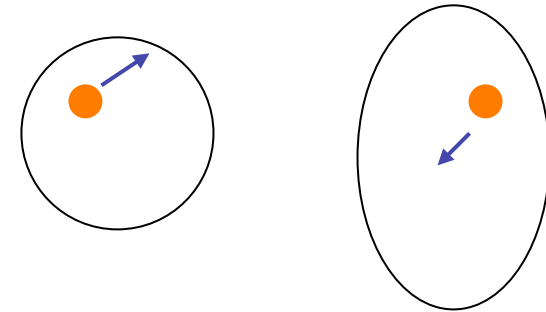
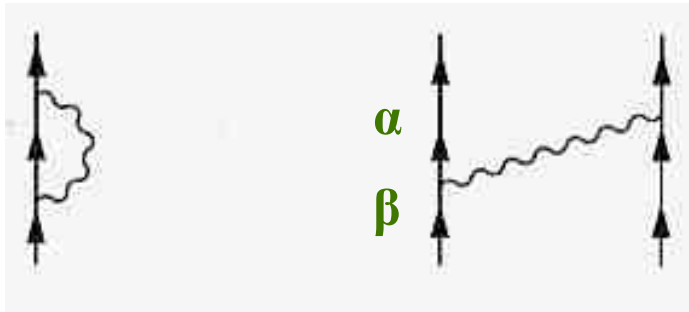
$$m_{\omega} \approx 1.5m$$

$$\hbar\omega_{\lambda} \approx 2\text{MeV}$$

$$N(0) \approx 3\text{ MeV}^{-1}$$



$$V^2 \approx 0.3\text{ MeV}^2$$



Nucleons are coupled to phonons, mainly density vibrations ( $2^+, 3^-$ ). In other words, the nuclear mean field undergoes fluctuations which are felt by the particles.

To deal with these phenomena, a nuclear field theory has been developed by the Copenhagen group. Phenomenological particle-vibration coupling of the type

$$\langle \alpha | V_{PV} | \beta \rangle = \int dr u_\alpha(r) C(dU/dr) u_\beta(r) \times \langle p || Y_L || p' \rangle$$

One can work out the particle-vibration coupling with effective forces and microscopic phonons:

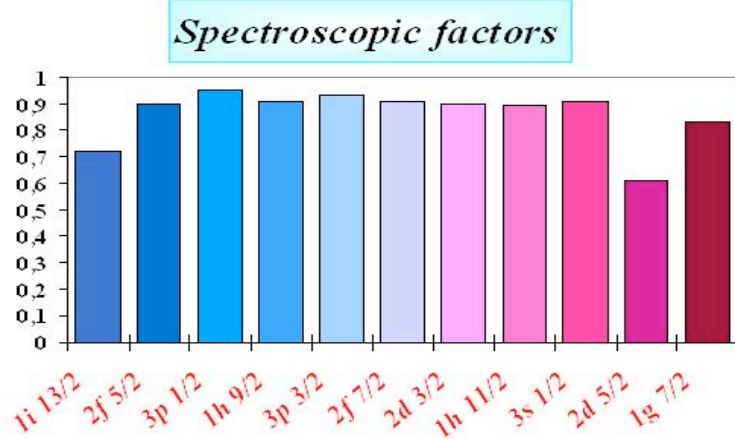
$$\langle \alpha | \varrho_n^{(L)}(r) v(r) Y_{LM}(\hat{r}) | \beta \rangle$$

Removal of simple approximations (assumption of good isospin for vibrations).

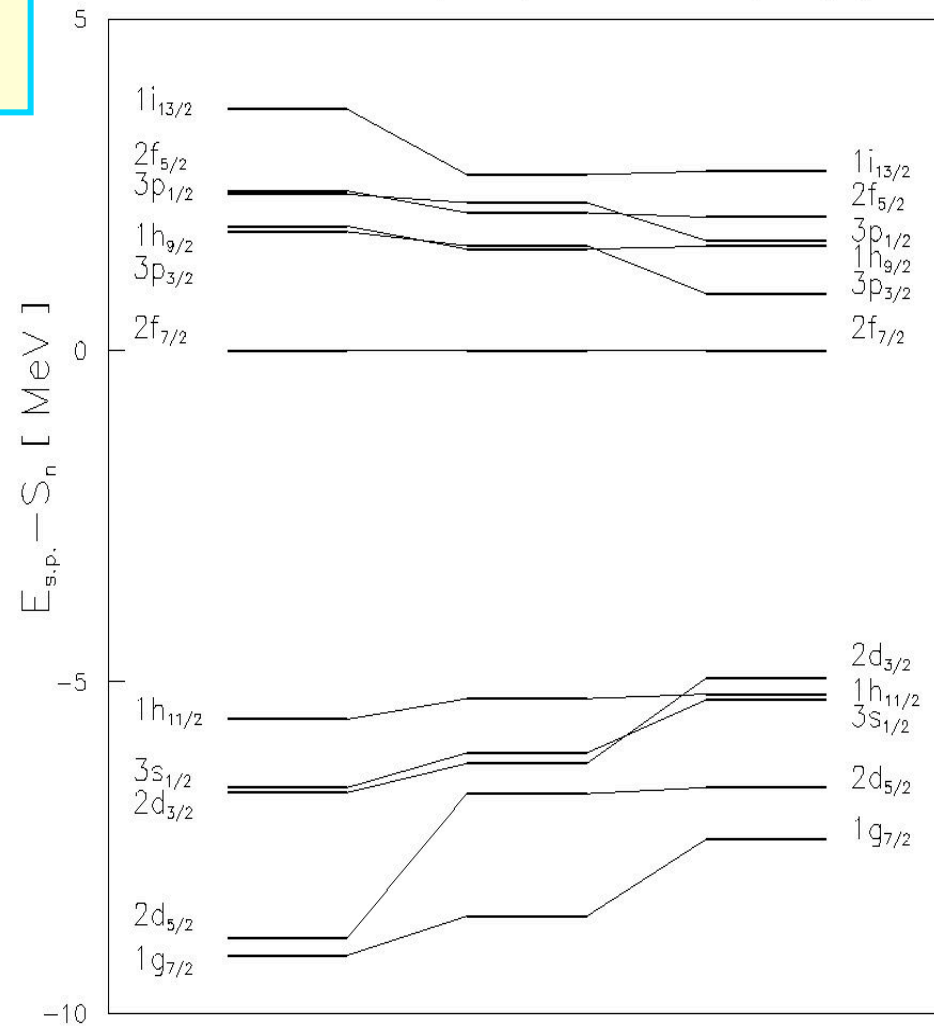
## Spin-orbit splitting

$\Delta E(vh_{9/2}-vh_{11/2})$  [MeV]

	HF	HF+phon.
SLy4	9.44	8.52
SGII	7.44	6.78
Exp. value is	6.75	



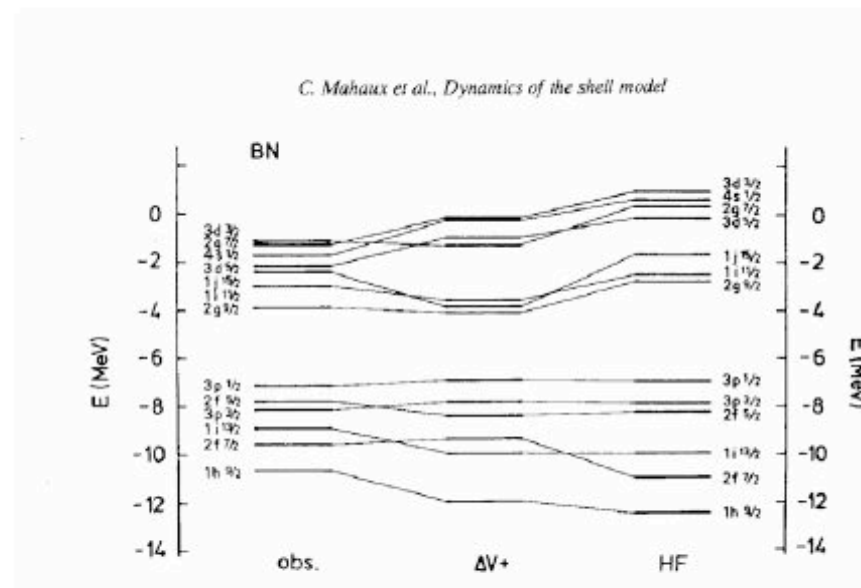
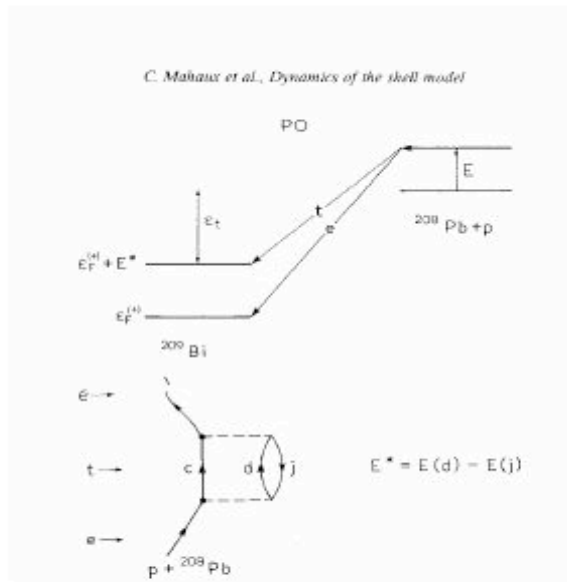
$^{132}\text{Sn}$  – HF plus phonon coupling (SGII)



HF      HF+phon.      Exp.

# CAVEAT

- No  $t_1$  and  $t_2$  terms
- No bubble correction
- Pauli Principle is a correction of  $O(1/\Omega^2)$  ,  
that is there are factors  $1/(2j+1)$  more in  
each term.
- In  $^{208}\text{Pb}$ ,  $\Omega \approx 75!!$



Coupling of vibrations to single-particle motion



Effective mass  $m_\omega$



Increased density at the Fermi energy

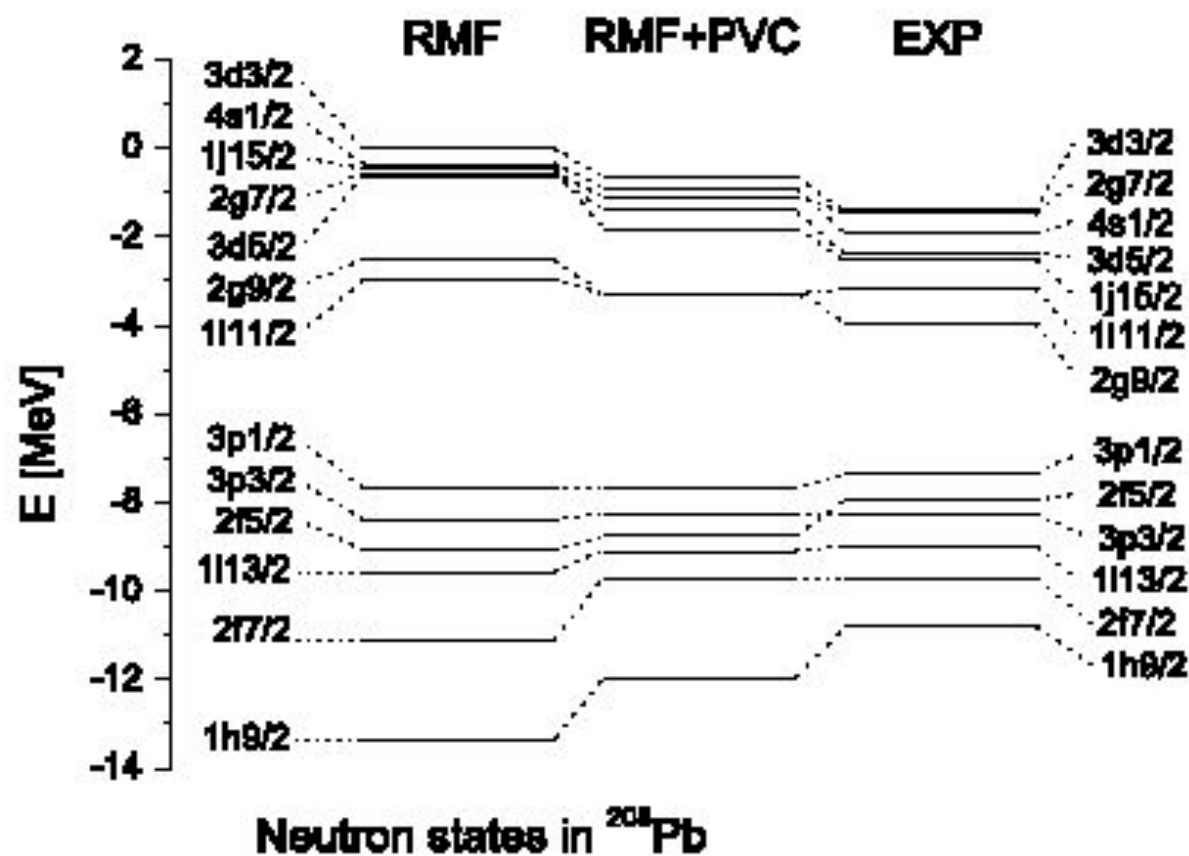


FIG. 7. Neutron single-particle states in  $\text{Pb}^{208}$ : the pure RMF spectrum (left column), the levels computed within RMF with allowance for the particle-vibration coupling (center) and the experimental spectrum (right).



# Average numbers to remember

- 
- $^{208}\text{Pb}$ , average  $\omega$ -mass/m
- Skyrme and similar +PVC:

For neutrons 1.2—1.4

For protons 1.3—1.6

- RMF+PVC 1.26, 1.41

# Tensor term of the Skyrme forces

- Role of the triplet-even and triplet-odd tensor forces on the spin-orbit splitting

$$\begin{aligned}
v_T = & \frac{T}{2} \left\{ \left[ (\boldsymbol{\sigma}_1 \cdot \mathbf{k}') (\boldsymbol{\sigma}_2 \cdot \mathbf{k}') - \frac{1}{3} (\boldsymbol{\sigma}_1 \cdot \boldsymbol{\sigma}_2) \mathbf{k}'^2 \right] \delta(\mathbf{r}_1 - \mathbf{r}_2) \right. \\
& + \delta(\mathbf{r}_1 - \mathbf{r}_2) \left[ (\boldsymbol{\sigma}_1 \cdot \mathbf{k}) (\boldsymbol{\sigma}_2 \cdot \mathbf{k}) - \frac{1}{3} (\boldsymbol{\sigma}_1 \cdot \boldsymbol{\sigma}_2) \mathbf{k}^2 \right] \left. \right\} \\
& + U \left\{ (\boldsymbol{\sigma}_1 \cdot \mathbf{k}') \delta(\mathbf{r}_1 - \mathbf{r}_2) (\boldsymbol{\sigma}_1 \cdot \mathbf{k}) - \frac{1}{3} (\boldsymbol{\sigma}_1 \cdot \boldsymbol{\sigma}_2) \right. \\
& \times \left. \left[ \mathbf{k}' \cdot \delta(\mathbf{r}_1 - \mathbf{r}_2) \mathbf{k} \right] \right\}.
\end{aligned}$$

$$\delta H = \frac{1}{2}\alpha(J_n^2 + J_p^2) + \beta J_n J_p.$$

**In the Skyrme  
framework...**

The contribution of the tensor to the total energy is not very large;

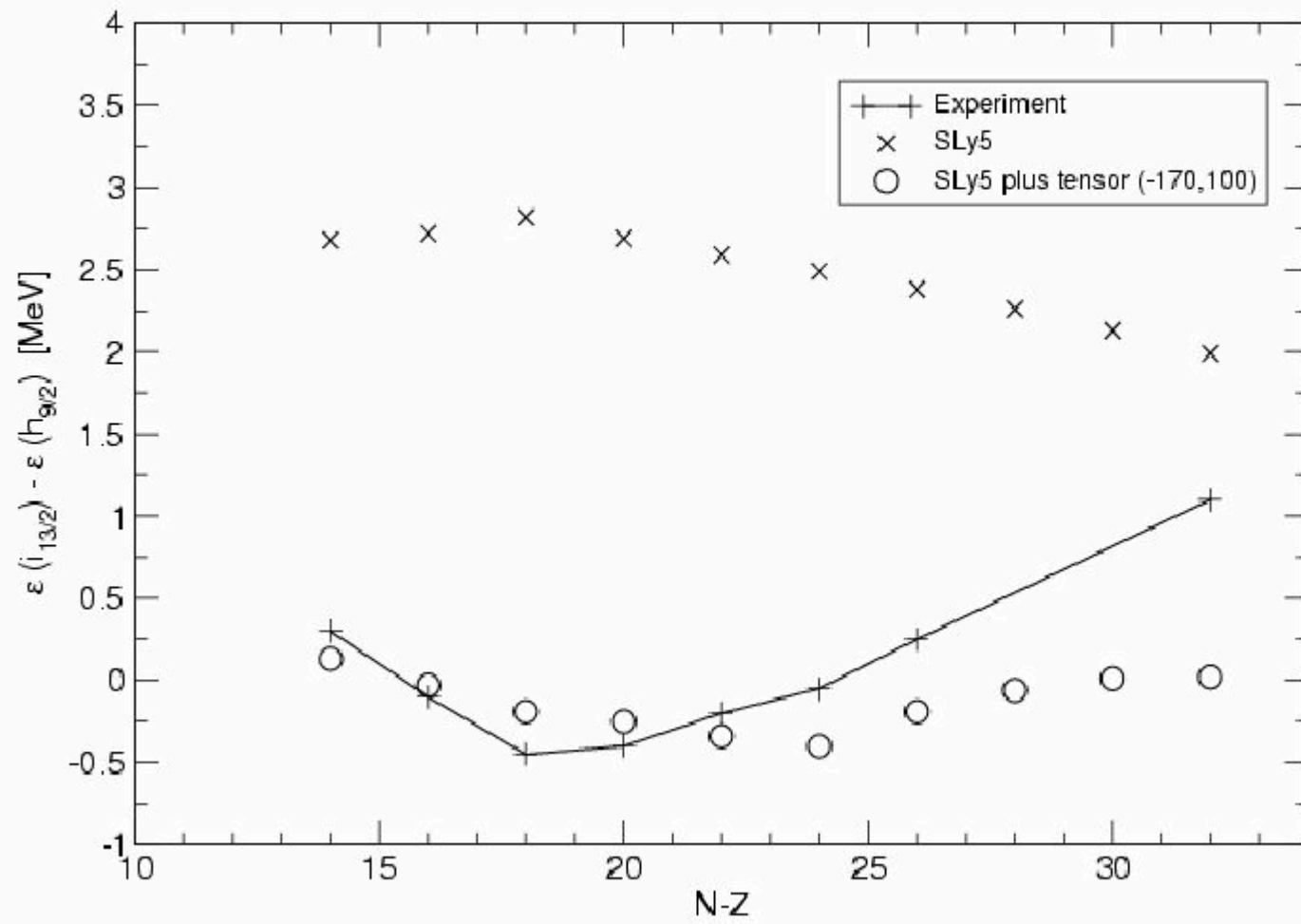
however, it may be relevant for the spin-orbit splittings.

$$U_{s.o.}^{(q)} = \frac{W_0}{2r} \left( 2 \frac{d\rho_q}{dr} + \frac{d\rho_{q'}}{dr} \right) + \left( \alpha \frac{J_q}{r} + \beta \frac{J_{q'}}{r} \right),$$

$$J_q(r) = \frac{1}{4\pi r^3} \sum_i v_i^2 (2j_i + 1) \left[ j_i(j_i + 1) - l_i(l_i + 1) - \frac{3}{4} \right] R_i^2(r).$$

The contribution of the tensor force to the spin-orbit splittings can be seen **ONLY** through isotopic or isotonic dependencies. Not in  $^{40}\text{Ca}$  !!

Neutrons on N=82 core



# Different works

- G. Colo', H. Sagawa, S. Fracasso and P.F. Bortignon, PLB 646 (2007) 227

PHYSICAL REVIEW C 77, 014314 (2008)

## Tensor correlations and evolution of single-particle energies in medium-mass nuclei

Wei Zou,<sup>1,2,3</sup> Gianluca Colò,<sup>1</sup> Zhongyu Ma,<sup>2</sup> Hiroyuki Sagawa,<sup>4</sup> and Pier Francesco Bortignon<sup>1</sup>

<sup>1</sup>*Dipartimento di Fisica, Università degli Studi and INFN, Sezione di Milano, via Celoria 16, I-20133 Milano, Italy*

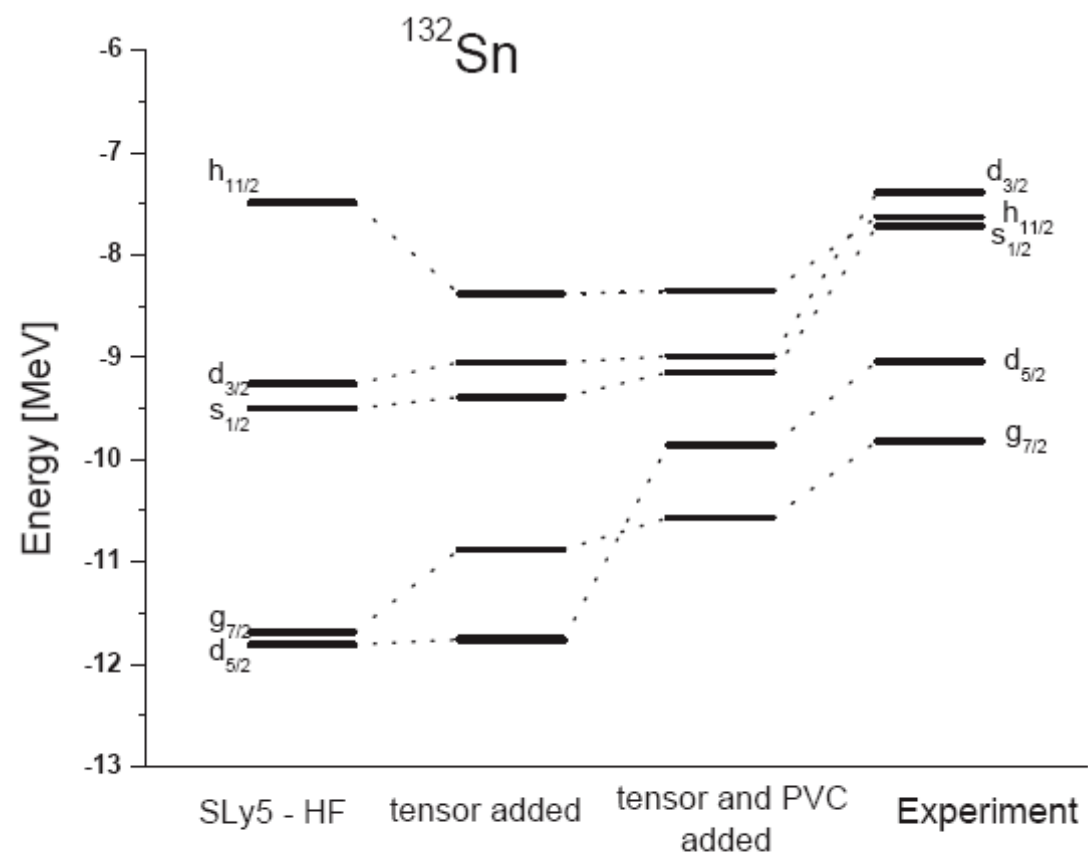
<sup>2</sup>*China Institute of Atomic Energy (CIAE), Beijing 102413, People's Republic of China*

<sup>3</sup>*Physics Department, Jilin University, Changchun 130012, People's Republic of China*

<sup>4</sup>*Center for Mathematical Sciences, University of Aizu, Aizu-Wakamatsu, Fukushima 965-8560, Japan*

(Received 26 September 2007; published 22 January 2008)

We analyze the evolution of the spin-orbit splittings in the Ca isotopes and in the  $N = 28$  isotones. We also focus on the reduction of the spin-orbit splittings associated with  $f$  and  $p$  orbits from  $^{48}\text{Ca}$  to  $^{46}\text{Ar}$ . We conclude that adding the tensor contribution can qualitatively explain in most cases the empirical trends, whereas this is not the case if one simply employs existing Skyrme parametrizations without the tensor force.





but

- Lesinski, Bender, Bennaceur, Duguet, Meyer in PRC 76 (2007) 014312

showed that ....the overall agreement of the s.p. spectra in double-magic nuclei is deteriorated by tensor coupling, if refit is done...

Minimum for  $\beta=0$

( $\beta = 0$ ), but for the parametrizations T12, only the proton-neutron term in  $\mathcal{H}^t$  contributes ( $\alpha = 0$ ). Note that the earlier parametrizations T6 and Z $_{\infty}$  have a pure like-particle  $J^2$  terms as a consequence of the constraint  $x_1 = x_2 = 0$  employed for both (and most other early parametrizations of Skyrme's interaction).

### B. The fit protocol and procedure

The list of observables used to construct the cost function  $\chi^2$  minimized during the fit (see Eq. (4.1) in Ref. [51]) reads as follows: binding energies and charge radii of  $^{40}\text{Ca}$ ,  $^{48}\text{Ca}$ ,  $^{56}\text{Ni}$ ,  $^{90}\text{Zr}$ ,  $^{132}\text{Sn}$ , and  $^{208}\text{Pb}$ ; the binding energy of  $^{100}\text{Sn}$ ; the spin-orbit splitting of the neutron  $3p$  state in  $^{208}\text{Pb}$ ; the empirical energy per particle and density at the saturation point of symmetric nuclear matter; and the equation of state of neutron matter as predicted by Wiringa *et al.* [16].

Furthermore, some properties of infinite nuclear matter are constrained through analytic relations between coupling constants in the same manner as they were in Refs. [51,52]: The incompressibility modulus  $K_{\infty}$  is kept at 230 MeV, and the volume symmetry energy coefficient  $a_v$  is set to 32 MeV. The isovector effective mass, expressed through the Thomas-Reiche-Kuhn sum rule enhancement factor  $\kappa_v$ , is taken such that  $\kappa_v = 0.25$ .

When using a single density-dependent term in the central Skyrme force [Eq. (10)], the isoscalar effective mass  $m_0^*$  cannot be chosen independently from the incompressibility modulus for a given exponent  $\alpha$  of  $\rho_0$ . We follow here the prescription used for the SLy parametrizations [51,52] and use  $\alpha = 1/6$ , which leads to an isoscalar effective mass close to 0.7 in units of the bare nucleon mass for all T1J parametrizations. This value allows for a correct description of dynamical properties, as for example the energy of the giant quadrupole resonance [83]. Using such a protocol we cannot reproduce the isovector effective mass consistent with recent *ab initio* predictions [84]. Regarding the present exploratory study of the tensor terms this is not a critical limitation, in particular as the influence of this quantity on static properties of finite nuclei turns out to be small.

There are three modifications of the fit protocol compared to that of Refs. [51,52]. The obvious one is that the values for  $C_0^t$  and  $C_1^t$  are fixed beforehand as the parameters that will later on label and classify the fits. The second is that we have added the binding energies of  $^{90}\text{Zr}$  and  $^{100}\text{Sn}$  to the set of data. Indeed, we observed that the latter nucleus is usually significantly overbound when not included in the fit. The third is that we have dropped the constraint  $x_2 = -1$  that was imposed on the SLy parametrizations [51,52] to ensure the stability of infinite homogeneous neutron matter against a transition into a ferromagnetic state. This stability criterion

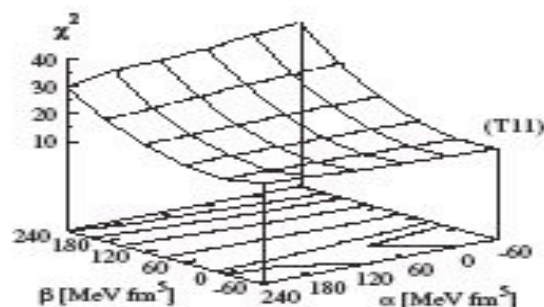


FIG. 2. Values of the cost function  $\chi^2$  as defined in the fit procedure, for the set of parametrizations T1J. The label “T11” indicates the position of this parametrization in the  $(\alpha, \beta)$  plane as obtained from Eqs. (36). Contour lines are drawn at  $\chi^2 = 11, 12, 15, 20, 25$ , and  $30$ . The minimum value is found for T21 ( $\chi^2 = 10.05$ ), and the maximum for T61 ( $\chi^2 = 37.11$ ).

concerning the stability in polarized systems in the presence of a tensor force to future work that will also address finite-size instabilities [84]. It also has to be stressed that the actual stability criterion, as with all properties of the time-odd part of the Skyrme energy functional, depends on the choices made for the interpretation of its coupling constants (i.e., antisymmetrized vertex or density functional [76]).

The properties of the finite nuclei entering the fit are computed by using a Slater determinant without taking pairing into account. The cost function  $\chi^2$  was minimized by using a simulated annealing algorithm. The annealing schedule was an exponential one, with a characteristic time of 200 iterations (also referred to as “simulated quenching”). Thus, assuming a reasonably smooth cost function, we strive to obtain satisfactory convergence to its absolute minimum in a single run, allowing a systematic and straightforward production of a large series of forces. The coupling constants for all 36 parametrizations can be found in the *Physical Review* archive [85].

Figure 2 displays the value of  $\chi^2$  after minimization as a function of the recoupled coupling constants  $\alpha$  and  $\beta$ . The first striking feature is the existence of a “valley” at  $\beta = 0$ , that is, a pure like-particle tensor term  $\sim (J_n^2 + J_p^2)$ . The abrupt rise of  $\chi^2$  around this value can be attributed to the term depending on nuclear binding energies, as sharp variations of energy residuals can be seen between neighboring magic nuclei with functionals of the T6J series ( $\beta = 240$ ). For example,  $^{48}\text{Ca}$  and  $^{90}\text{Zr}$  tend to be significantly overbound in this case. We will return later to a discussion of the implications for the quality of the functionals.

# Pairing renormalization

- Jon lectures!!

## The weak-coupling approximation:

$$\Delta_k = -\frac{1}{2\pi^2} \int_0^\infty dk' \quad k'^2 \frac{V(k, k')}{2E_{k'}} \Delta_{k'}$$

Let us make two approximations for  $k \approx k_F$ :

$$E_k \approx \sqrt{\left(\frac{\hbar^2 k^2}{2m^*} - \epsilon_F\right)^2 + \Delta_{k_F}^2}$$

$$\frac{1}{\sqrt{(x^2 - 1)^2 + \alpha^2}} \approx \ln\left(\frac{8}{\alpha}\right) \delta(x - 1)$$

Then

$$\Delta_{k_F} \approx -\frac{m^* k_F}{2\pi^2 \hbar^2} \ln\left(\frac{8}{\bar{\Delta}_{k_F}}\right) V(k, k_F) \Delta_{k_F}$$

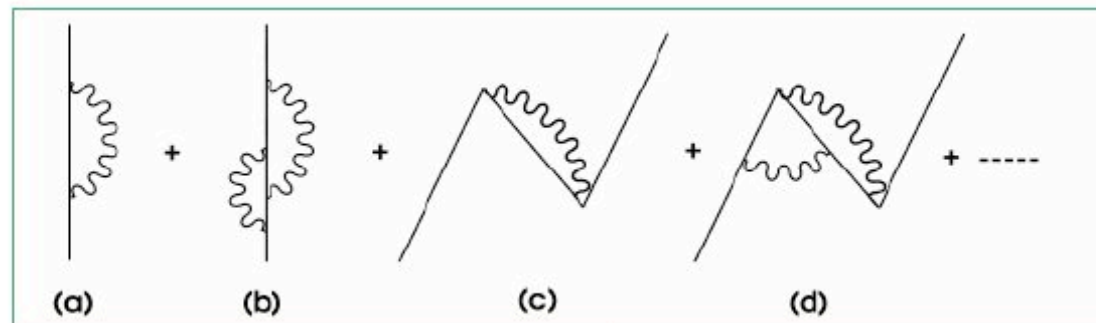
$$\bar{\Delta}_{k_F} = 8 \exp\left(\frac{2\pi^2 \hbar^2}{m^* k_F V(k_F, k_F)}\right) = 8 \exp\left(\frac{1}{N(0) V(k_F, k_F)}\right)$$

with

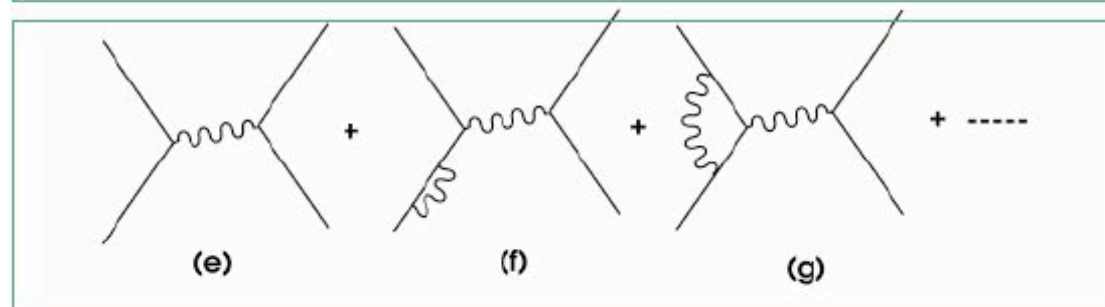
$$\bar{\Delta}_{k_F} \equiv \Delta_{k_F} / \epsilon_F$$

Going beyond mean field: medium polarization effects

Self-energy



Induced interaction  
(screening)

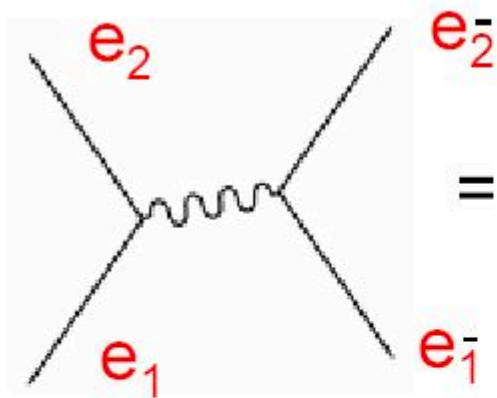


$$V(a, b\lambda) = h(a, b\lambda)(u_a u_b - v_a v_b)$$

$$W(a, b\lambda) = -h(a, b\lambda)(u_a v_b + v_a u_b)$$

## Pairing from exchange of vibrations (induced interaction)

Two time orderings



$$= \frac{V^2}{2e_1 - (e_1 + e_2 + \hbar\omega_\lambda)} = \frac{V^2}{e_1 - (e_2 + \hbar\omega_\lambda)} \approx -\frac{V^2}{\hbar\omega_\lambda}$$

$$V_{ind} = -\frac{2V^2}{\hbar\omega_\lambda} \approx -0.3 \text{ MeV}$$

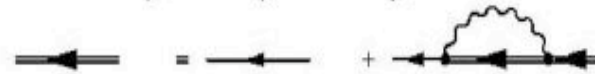


## Going beyond the quasi-particle approximation

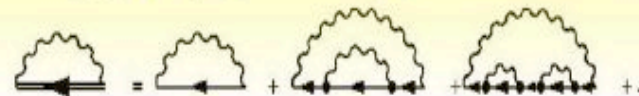
J. Terasaki et al., Nucl.Phys. **A697**(2002)126

by extending the Dyson equation...

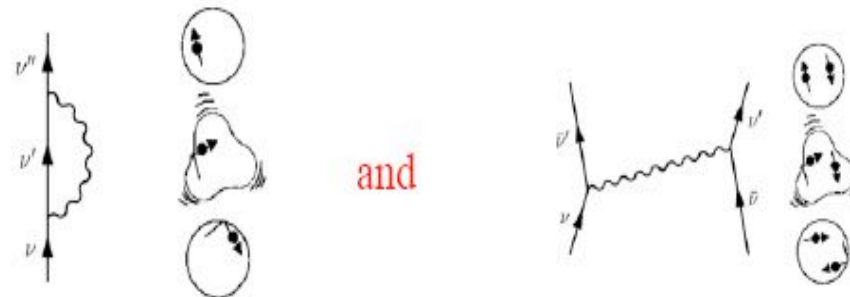
$$G_{\mu}^{-1} = (G_{\mu}^0)^{-1} - \Sigma_{\mu}(\omega)$$



$$\Sigma_{\mu}(\omega) = \int_{-\infty}^{+\infty} \frac{d\omega'}{2\pi} \sum_{\mu'} \frac{1}{\hbar} G_{\mu'}(\omega') \sum_{\alpha} \frac{1}{\hbar} D_{\alpha}^o(\omega - \omega') * V_{\mu\mu',\alpha}^2$$

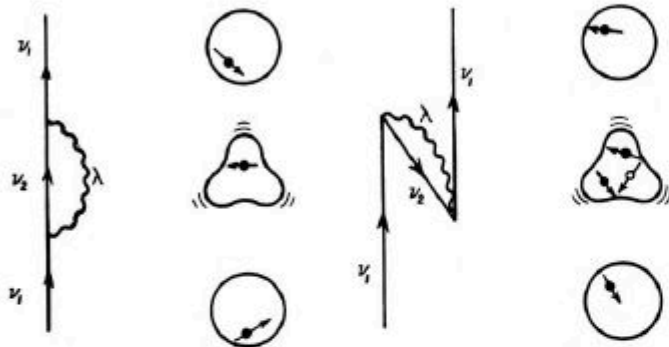


to the case of superfluid nuclei (Nambu-Gor'kov), it is possible to consider both





We first perform a BCS calculation with the bare force, obtaining the quasiparticle amplitudes  $u_a, v_a$ . We then couple the quasiparticle to the 1qp, 1ph states.



$$V(a, b\lambda) = h(a, b\lambda)(u_a u_b - v_a v_b)$$

$$W(a, b\lambda) = -h(a, b\lambda)(u_a v_b + v_a u_b)$$

$$\begin{pmatrix} E_a & V(a, b\lambda) & 0 & W(a, b\lambda) \\ V(a, b\lambda) & (E_b + E_\lambda) & W(a, b\lambda) & 0 \\ 0 & W(a, b\lambda) & -E_a & -V(a, b\lambda) \\ W(a, b\lambda) & 0 & -V(a, b\lambda) & -(E_b + E_\lambda) \end{pmatrix} \begin{pmatrix} x^{ai} \\ C_{b\lambda}^{ai} \\ y^{ai} \\ D_{b\lambda}^{ai} \end{pmatrix} = E_i^a \begin{pmatrix} x^{ai} \\ C_{b\lambda}^{ai} \\ y^{ai} \\ D_{b\lambda}^{ai} \end{pmatrix}$$

$$U^{ai} = x^{ai} u_a - y^{ai} v_a$$

$$V^{ai} = x^{ai} v_a + y^{ai} u_a$$

$$\begin{aligned} (x^{ai})^2 + (y^{ai})^2 &< 1 \\ \sum_i (x^{ai})^2 + (y^{ai})^2 &= 1 \end{aligned}$$

Projecting on the single-particle configuration, we obtain an equation for the normal and abnormal energy-dependent self-energies (Nambu-Gor'kov):

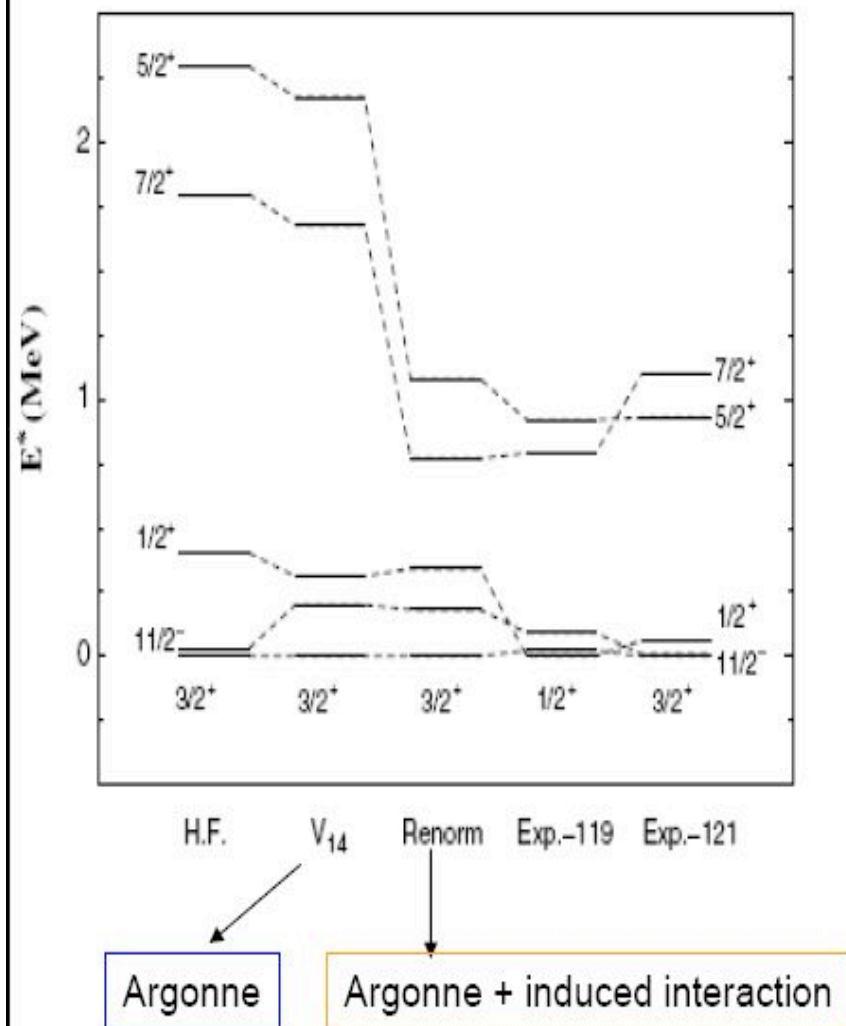
$$\left[ \begin{pmatrix} E_j^0 & 0 \\ 0 & -E_j^0 \end{pmatrix} + \begin{pmatrix} \Sigma_{11}(E_j) & \Sigma_{12}(E_j) \\ \Sigma_{12}(E_j) & \Sigma_{22}(E_j) \end{pmatrix} \right] \begin{pmatrix} x_j \\ y_j \end{pmatrix} = E_j \begin{pmatrix} x_j \\ y_j \end{pmatrix}$$

$$\Sigma_{11}(E_j) = \sum_{j'\lambda'} \left[ \frac{V_{jj'\lambda'}^2}{E_j - (E_{j'} + \hbar\omega'_{\lambda})} + \frac{W_{jj'\lambda'}^2}{E_j + (E_{j'} + \hbar\omega'_{\lambda})} \right] \quad \Sigma_{11}(E_j) = -\Sigma_{22}(-E_j)$$

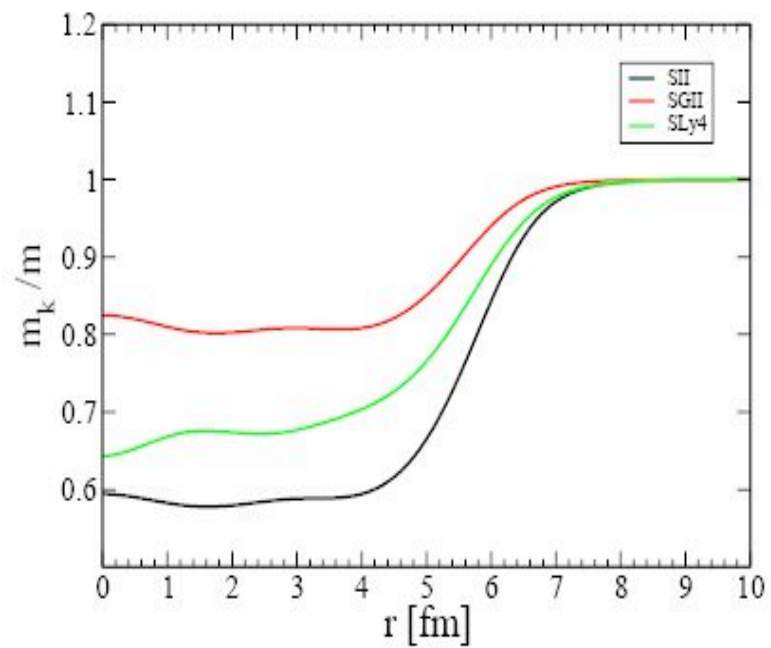
$$\Sigma_{12}(E_j) = - \sum_{j'\lambda'} V_{jj'\lambda'} W_{jj'\lambda'} \left[ \frac{1}{E_j - (E_{j'} + \hbar\omega'_{\lambda})} - \frac{1}{E_j + (E_{j'} + \hbar\omega'_{\lambda})} \right]$$

-

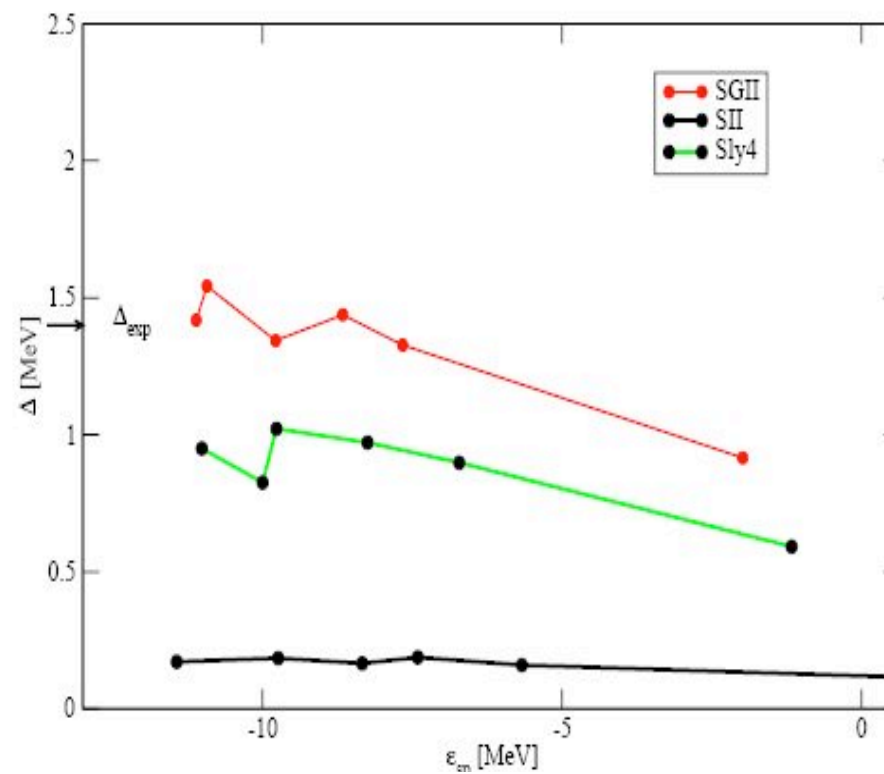
Renormalized pairing gap:  $\Delta_j = 2E_j \frac{u_j v_j}{u_j^2 + v_j^2}$



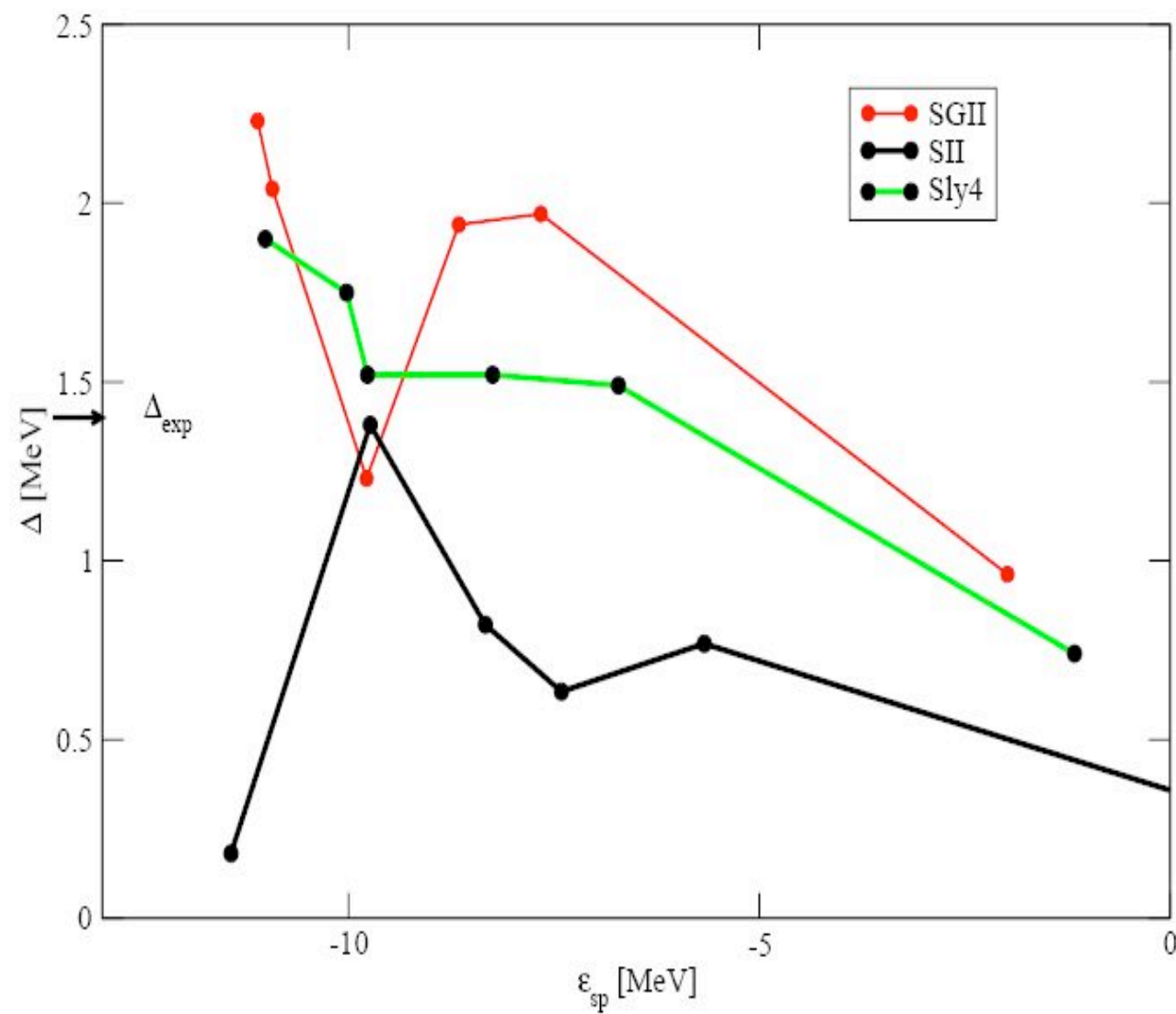
## Effective masses



## Bare gaps



## Renormalization of pairing gaps



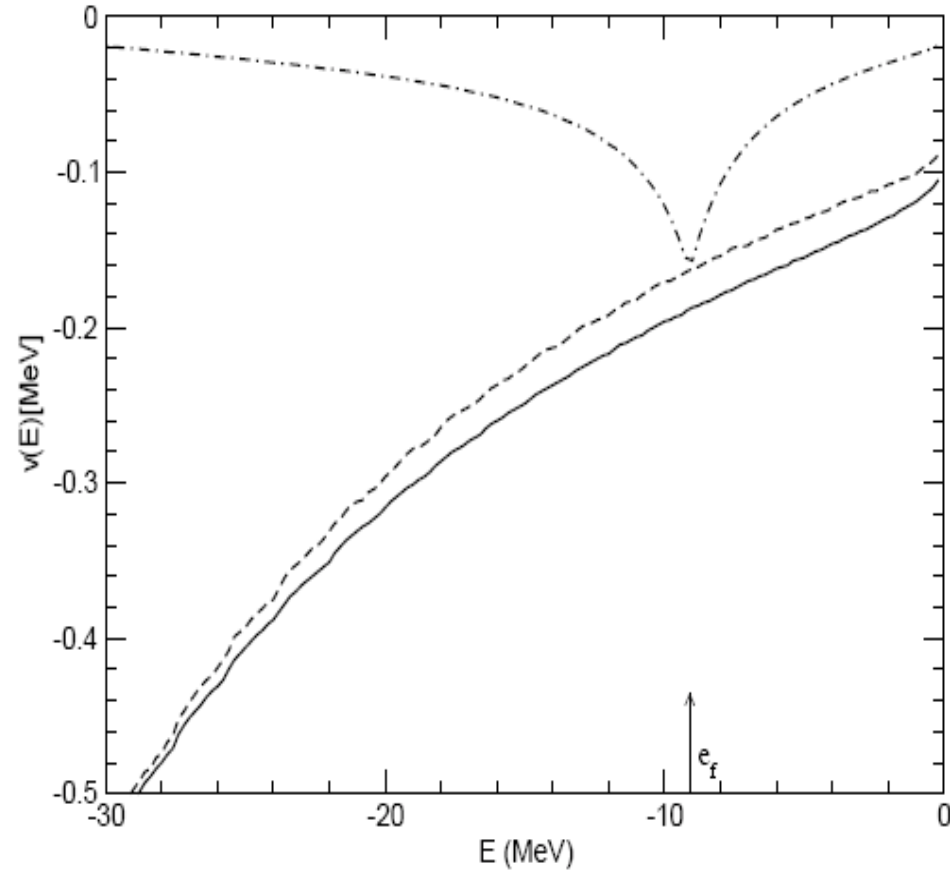


Figure 5: The nucleus  $^{120}\text{Sn}$ . The semiclassical matrix elements of the induced interaction, calculated according to Eq. (9) (dash-dotted curve), are compared with the matrix elements of the Gogny force (solid curve, cf. Fig. 3) and with those of the  $v_{\text{low}-k}$  interaction (dashed curve). Calculations are performed with  $m_k = m$  and with the same Woods-Saxon potential used in Figs. 1 and 3.

$$|\langle n(A+1) | c_{\alpha}^{+} | 0 \rangle|^2 = (U^{ai})^2 \quad |\langle n(A-1) | c_{\alpha} | 0 \rangle|^2 = (V^{ai})^2$$

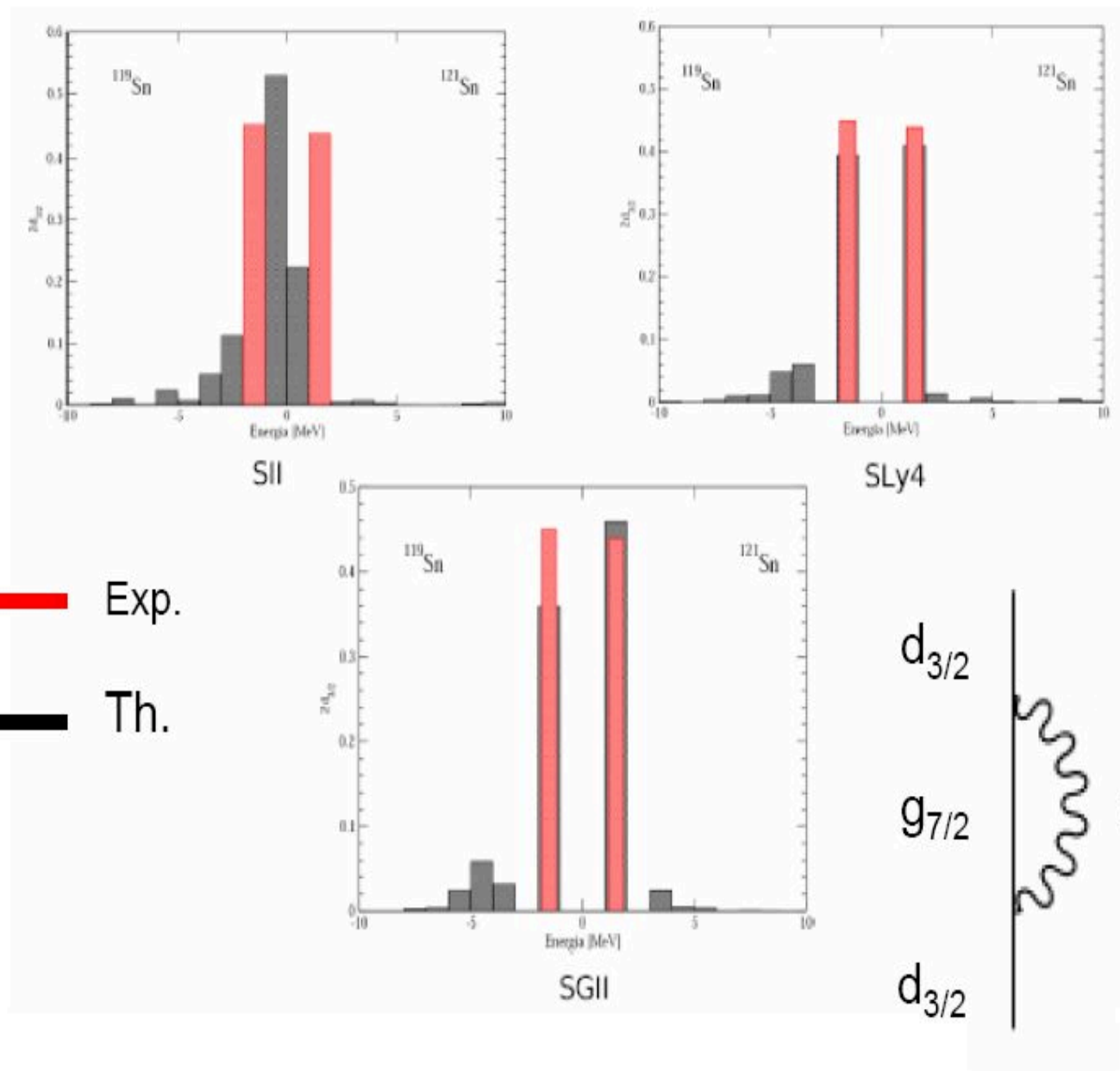
The calculated distribution of quasi particle strength can be compared with spectroscopic factors from transfer reactions like  $^{120}\text{Sn}(d,p)^{121}\text{Sn}$  or  $^{120}\text{Sn}(p,d)^{119}\text{Sn}$ .

Theoretical spectra appear to be too fragmented, but one should also consider that the (rather old) available experimental data have low resolution and cover a small interval in excitation energy.

$^{120}\text{Sn}(d,p)^{121}\text{Sn}$ : M.J. Bechara and O. Diezsch, Phys. Rev. C12 (1975)90

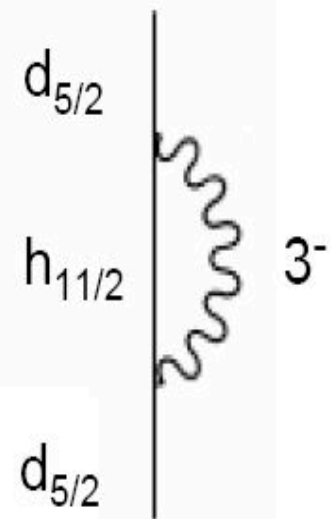
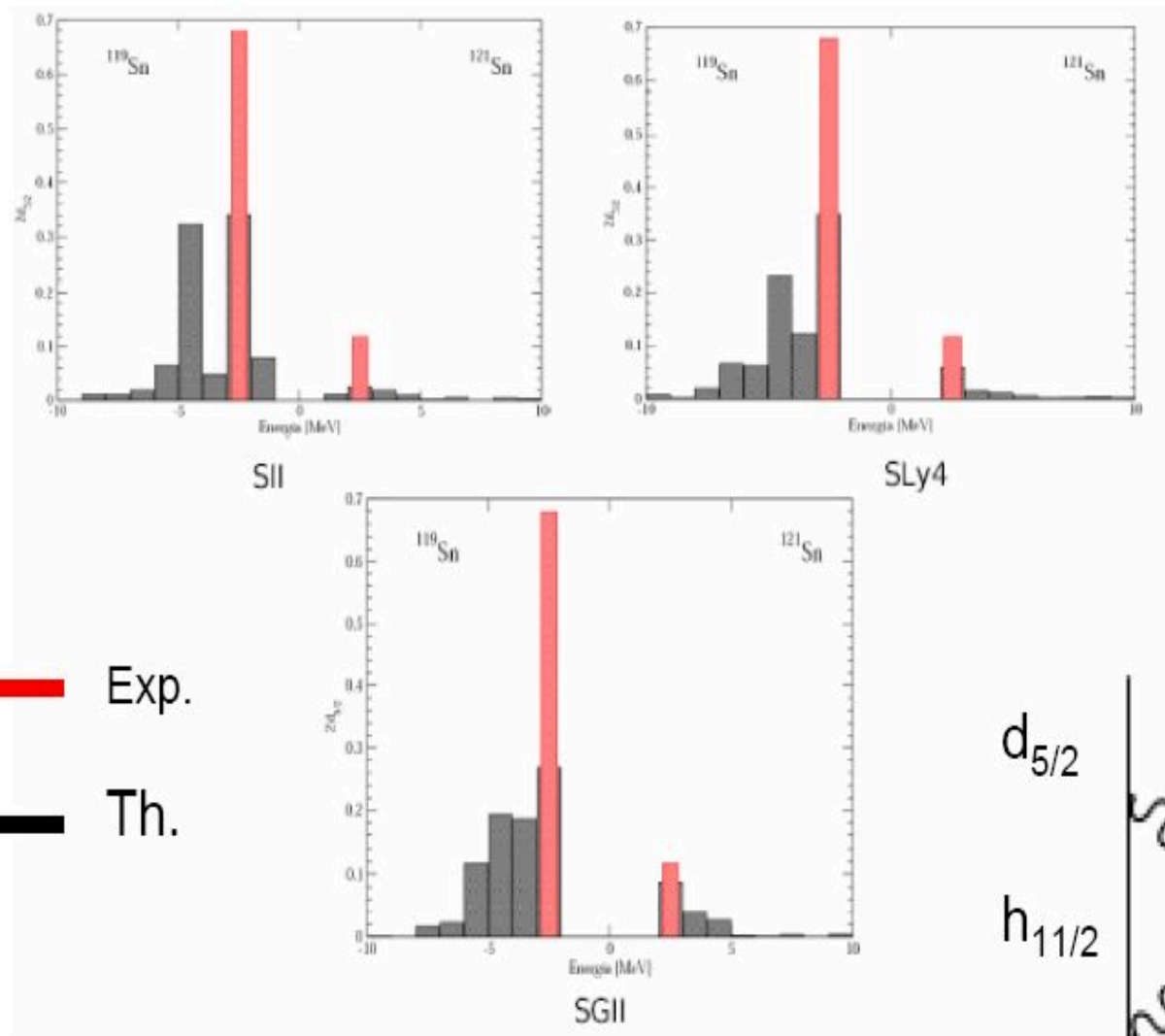
$^{120}\text{Sn}(^3\text{He},\alpha)^{119}\text{Sn}$ : E. Gerlic et al., Phys. Rev. C21(1980)124

$d_{3/2}$





$d_{5/2}$



# Paul Bonche et al.

- Let us emphasize that this study was done at the mean-field (HF) level. However, NO ingredient in our protocol prevents further studies beyond the mean field approximation. If needed be, further correlations can be explored and it is quite legitimate to use these interactions for RPA or configurations mixing (GCM) calculations. This would NOT has been the case if we had included in our protocol detailed information such as s.p. energies of some selected nuclei.

# Dependence of single-particle energies on coupling constants of the nuclear energy density functional

M. Kortelainen,<sup>1</sup> J. Dobaczewski,<sup>1,2</sup> K. Mizuyama,<sup>1</sup> and J. Toivanen<sup>1</sup>

<sup>1</sup>*Department of Physics, P.O. Box 35 (YFL), FI-40014 University of Jyväskylä, Finland*

<sup>2</sup>*Institute of Theoretical Physics, University of Warsaw, ul. Hoża 69, 00-681 Warsaw, Poland.*

(Dated: March 18, 2008)

We show that single-particle energies in doubly magic nuclei depend almost linearly on the coupling constants of the nuclear energy density functional. Therefore, they can be very well characterized by the linear regression coefficients, which we calculate for the coupling constants of the standard Skyrme functional. We then use these regression coefficients to refit the coupling constants to experimental values of single-particle energies. We show that the obtained rms deviations from experimental data are still quite large, of the order of 1.1 MeV. This suggests that the current standard form of the Skyrme functional cannot ensure spectroscopic-quality description of single-particle energies, and that extensions of this form are very much required.

# ABOUT S. P. SPREADING WIDTH

- $\Gamma_j = 2\langle W_j \rangle$  with
- $W_j = \text{Im } \Sigma_j$

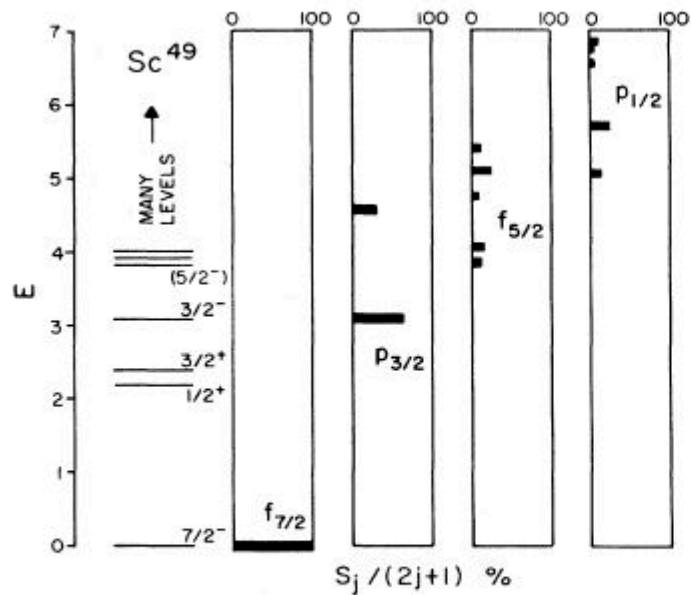


FIG. 1. Spectroscopy of  $^{49}\text{Sc}$  from the  $^{48}\text{Ca}(^3\text{He},d)^{49}\text{Sc}$  reaction, measured by Erskine, Marinov, and Schiffer (1966). The ground state has practically all of the  $f_{7/2}$  strength, while for higher orbits the strength is spread over several states.

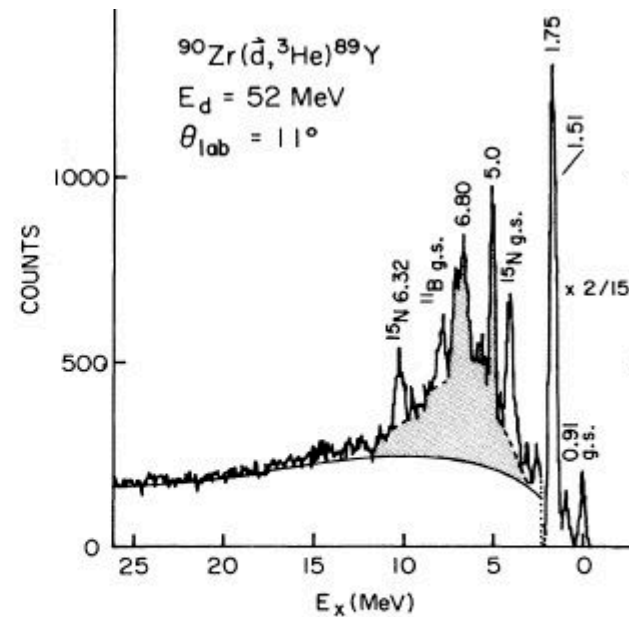


FIG. 2. The energy spectrum of  $^3\text{He}$  in the proton pickup reaction,  $^{90}\text{Zr}(d,^3\text{He})^{89}\text{Y}$ , from Stuirbrink *et al.* (1980). The shaded bump shows an angular dependence and analyzing power characteristic of the  $f_{7/2}$  hole orbit.

$$\text{Gamma(s.p.)} = 0.5 (E - E_F)$$

# How to proceed?

- Add a small imaginary part in the energy denominators:

$$1/(\omega - \varepsilon + i\Delta)$$

# Giant Resonances

- Centroid and strength reproduced by (Q)RPA, as well as escape width.  
What about spreading width?

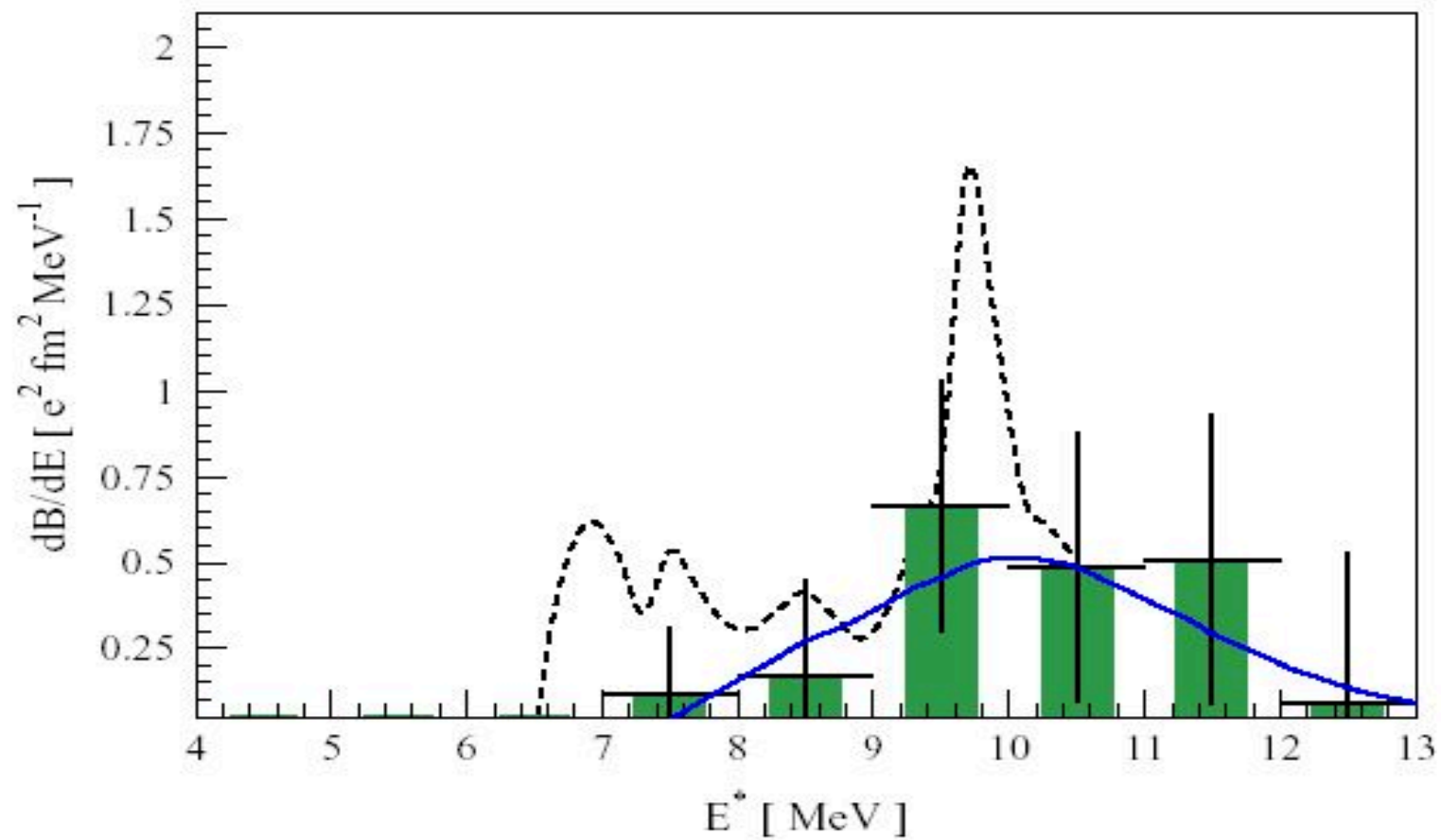
Low-lying dipole strength in  
unstable nuclei



# References:

- 1) N. Ryezayeva et al., Phys. Rev. Lett. 89 (2002) 272502.
  - 2) P. Adrich, A. Kimkiewicz et al., Phys.Rev. Lett. 95 (2005) 132501.
  - 3)
  - 4) D. Sarchi, PFB, G. Colò, Phys. Lett. B 601 (2004) 27.
  - 5) N. Paar, D. Vretenar, E. Khan, G. Colò, nucl-th/0701081, submitted to Reports on Progress in Physics.
- E. Litvinova, P. Ring, D. Vretenar, nucl/th/0701046v1

## $^{132}\text{Sn}$ low-lying GDR strength



**Blue line = theory of 3) (dashed line) convoluted with the dete  
by A. Klimkiewicz to compare with the experiment of 2) (gre**

GSI-LAND  
 PRL 95 (2005)  
 132501

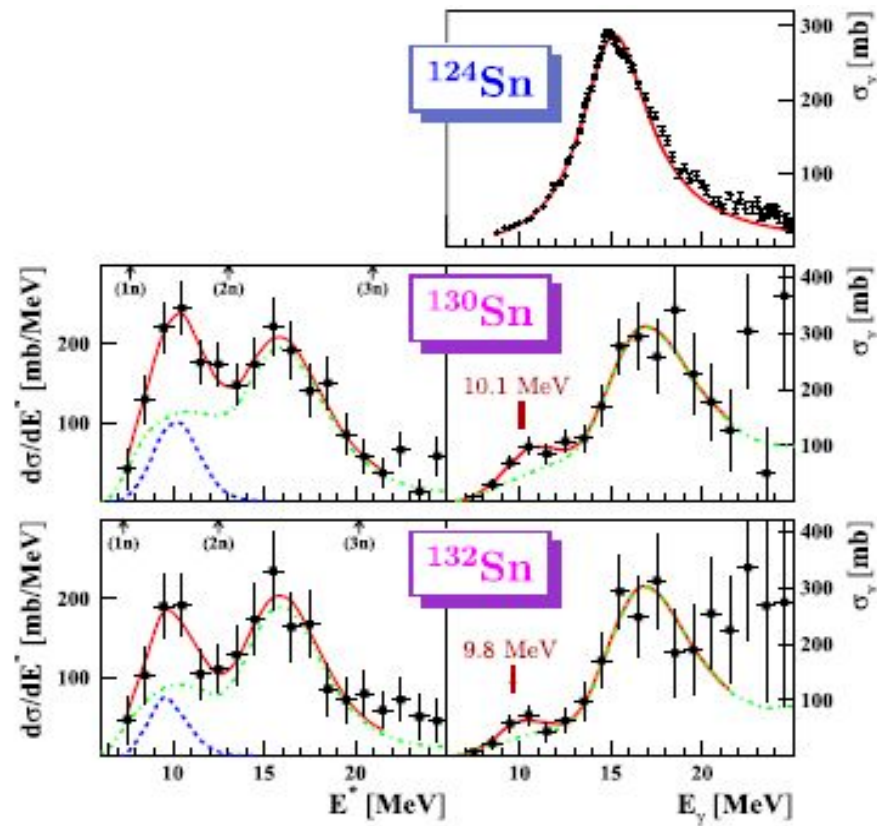


TABLE I. Summary of the parameters deduced for the PDR and GDR peaks. The parameters for  $^{124}\text{Sn}$  are from [18].

	PDR			GDR		
	$E_{\max}$ [MeV]	FWHM [MeV]	$\int \sigma_\gamma$ [mb MeV]	$E_{\max}$ [MeV]	FWHM [MeV]	$\int \sigma_\gamma$ [mb MeV]
$^{124}\text{Sn}$	...	...	...	15.3	4.8	2080
$^{130}\text{Sn}$	10.1(7)	$<3.4$	130(55)	15.9(5)	4.8(1.7)	2680(410)
$^{132}\text{Sn}$	9.8(7)	$<2.5$	75(57)	16.1(7)	4.7(2.1)	2330(590)

**Theory: 15.5 5.8**

# Spreading width in GR

- G.F. Bertsch, P.F. Bortignon, R.A. Broglia, Rev. Mod. Phys. 55
- $\Gamma(\text{GR}) = ? \Gamma(\text{part.}) + \Gamma(\text{hole})$  NO!!!

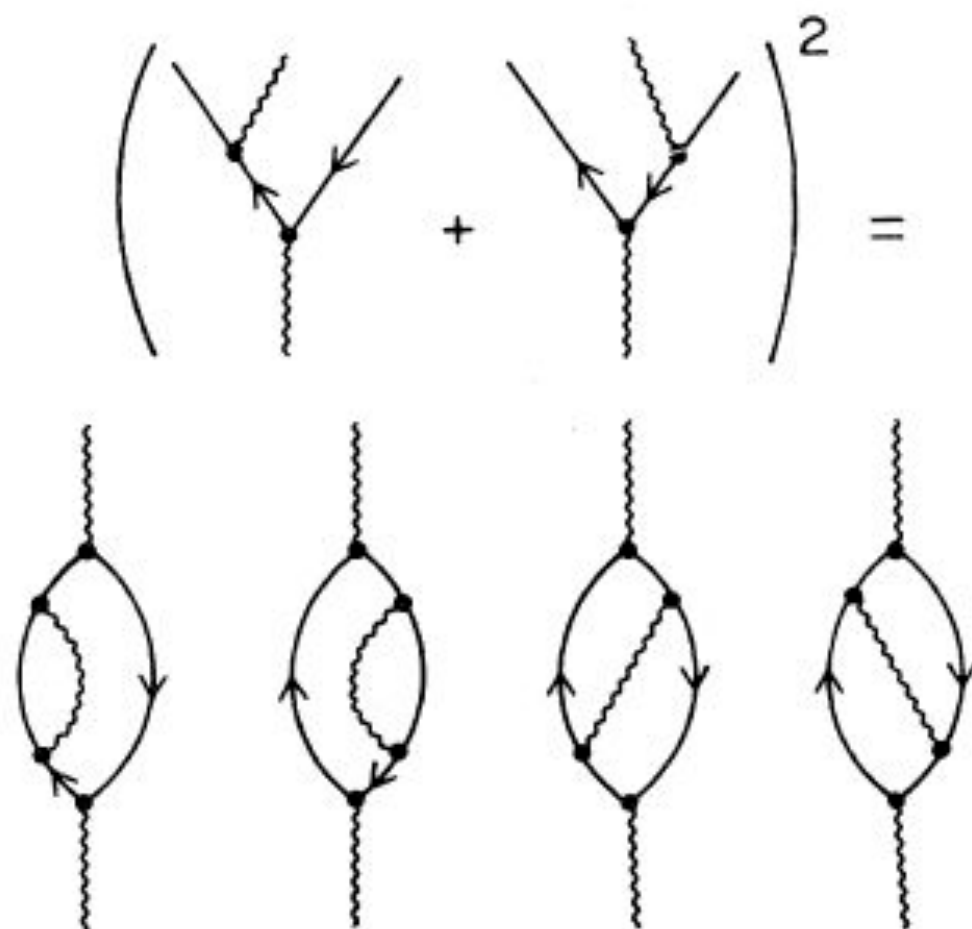


FIG. 22. Perturbation graphs for the damping of a vibration. On the top is shown the coherent sum of amplitudes for doorway coupling via the particle and the hole. They give rise to the four contributions to the imaginary part of the self-energy of the vibration. The two graphs on the left arise from the independent damping of the particle and the hole, and the two remaining graphs give an interference.



cesses like those depicted in fig. 2c), it follows that the graphs generated by the expansion do not allow any bubble to appear.

We can note that the rules for coupling fermions and phonons we have discussed seem to be quite similar to the rules which have been found in many references by dif-

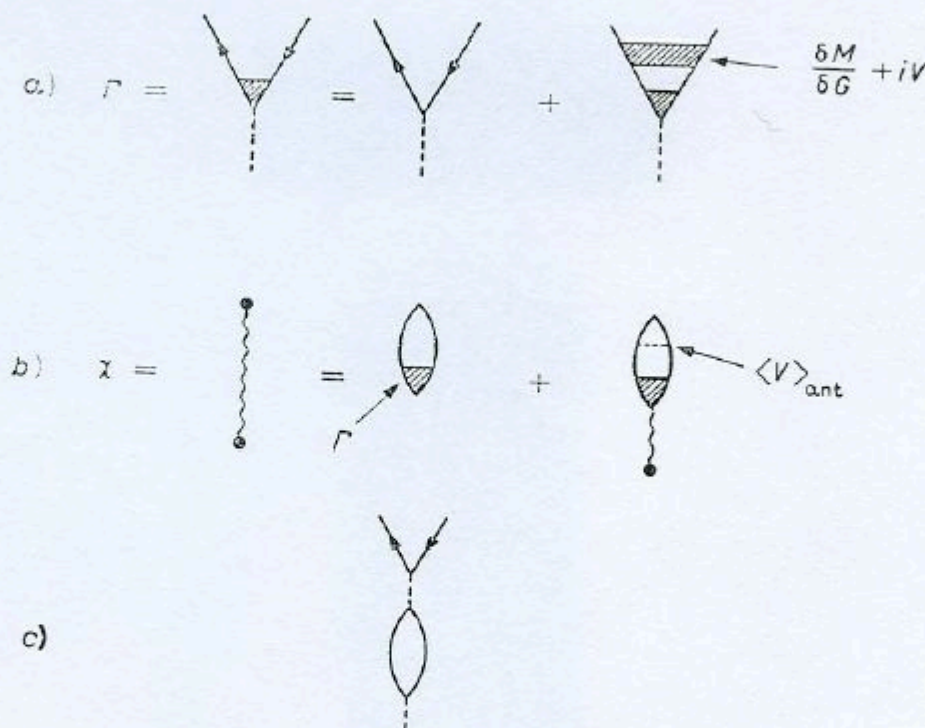


Fig. 2.

ferent and often empirical approaches and for different physical situations <sup>(2,3,6)</sup> (like two phonons or particle plus phonons systems). Then these rules seem to be quite general to handle in a self-consistent way particle-phonon coupling problems avoiding overcounting and Pauli-principle violations.

Finally it should be possible in the formalism to treat also a density-dependent interaction, as shown in ref. (7) for the particle-hole interaction.

\* \* \*

Stimulating discussions with Prof. R. BROGLIA are gratefully acknowledged.



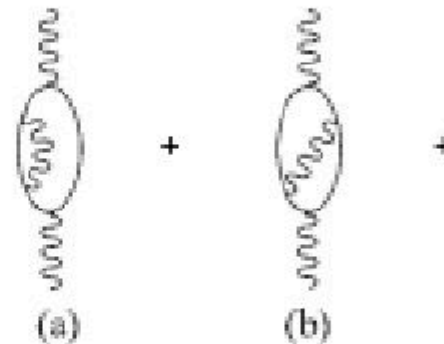
TABLE III. Particle-hole interference in the vibration self-energy. The sign of the quantity Eq. (44) is shown for all possible values of the quantum numbers associated with the initial vibration and with the intermediate doorway vibration. Note that if either vibration is purely scalar, the interference is destructive.

$n_{\tau_0} \ n_{\sigma_0}$	$n_{\tau'} n_{\sigma'}$			
	00	10	01	11
00	-	-	-	-
10	-	+	-	+
01	-	-	+	+
11	-	+	+	-

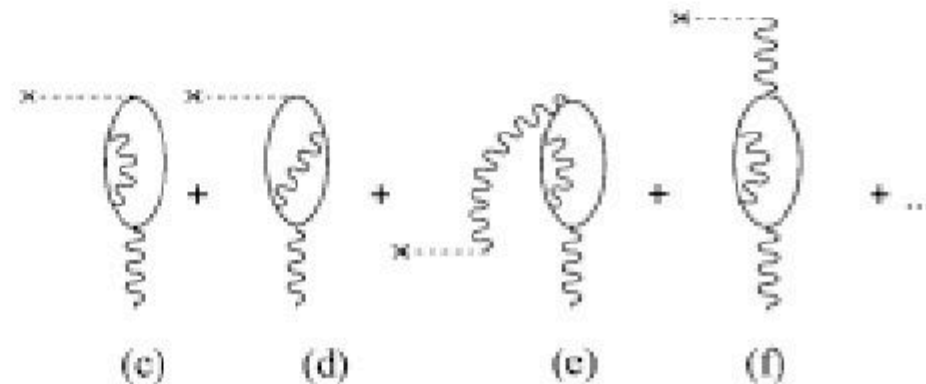
# Renormalization of the properties of $2+$ low-lying state due to mixing with more complex configurations

	$\hbar\omega_{2+}$ (MeV)	$B(E2 \uparrow)$ ( $e^2 \text{ fm}^4$ )
RPA (Gogny)	2.9	660
RPA (Sly4)	1.5	890
RPA + renorm. [23]	0.9	2150
Exp.	1.2	2030

Energy correction



Transition amplitude correction



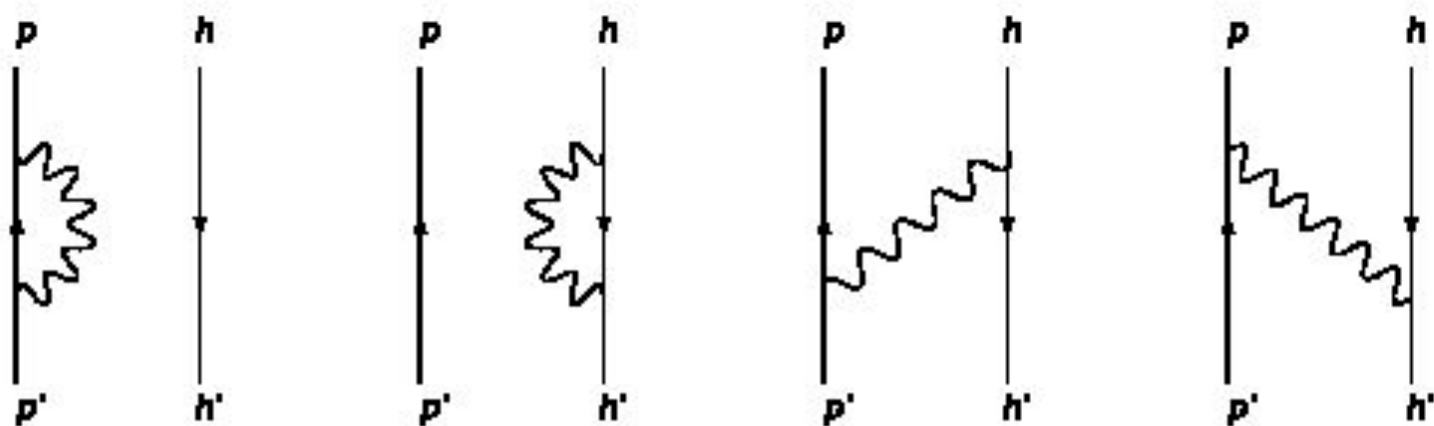


Figure 2. Diagrams which correspond to the coupling of the  $p - h$  components of a giant resonance with phonon states.

In the last decade we have developed, within a Milano-Orsay collaboration, a microscopic model aimed to a detailed description of GR excitation and decay [G. Colò *et al.* Phys. Rev. C50, 1496 (1994)].

The model includes the coupling with 1p-1h plus 1 phonon configurations and with the continuum (allowing the description of particle decay).

The model has been able to reproduce the total width of the GMR, and total and partial decay widths of GTR and IAR in  $^{208}\text{Pb}$ .

Recently, we have extended the model to include pairing correlations (without the continuum coupling).

$$\mathcal{H}(\omega) \equiv Q_1 H Q_1 + W^\dagger(\omega) + W^\downarrow(\omega) = Q_1 H Q_1 + Q_1 H P \frac{1}{\omega - PHP + i\epsilon} P H Q_1 + Q_1 H Q_2 \frac{1}{\omega - Q_2 H Q_2 + i\epsilon} Q_2 H Q_1, \quad (2.2)$$



RPA



continuum  
coupling



1p-1h-1  
phonon  
coupling

This effective Hamiltonian can be diagonalized and from its eigenvalues and eigenvectors one can extract the response function to a given operator  $O$ .

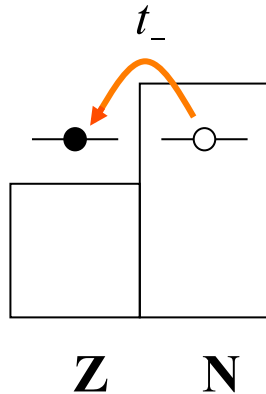
$$R(\omega) = \langle 0 | O^\dagger \frac{1}{\omega - \mathcal{H}(\omega) + i\epsilon} O | 0 \rangle, \quad S(\omega) = -\frac{1}{\pi} \text{Im} R(\omega).$$

$$S(\omega) = -\frac{1}{\pi} \text{Im} \sum_{\nu} \langle 0 | O | \nu \rangle^2 \frac{1}{\omega - \Omega_{\nu} + i \frac{\Gamma_{\nu}}{2}}$$

It is possible to extract at the same time to calculate the branching ratios associated with the decay of the GR to the A-1 nucleus in the channel c (hole state).

$$B_c(\omega) \equiv \frac{\sigma_c(\omega)}{\sigma_{\text{exc}}(\omega)} = \frac{\sum_{\nu, \nu'} S_{\nu' \nu} \gamma_{\nu' \nu, c} (\omega - \Omega_{\nu} - i \frac{\Gamma_{\nu}}{2})^{-1} (\omega - \Omega_{\nu'} + i \frac{\Gamma_{\nu'}}{2})^{-1}}{-2 \text{Im} \sum_{\nu, \nu'} S_{\nu' \nu} (F^* F^T)_{\nu \nu'} (\omega - \Omega_{\nu'} - i \frac{\Gamma_{\nu'}}{2})^{-1}}$$

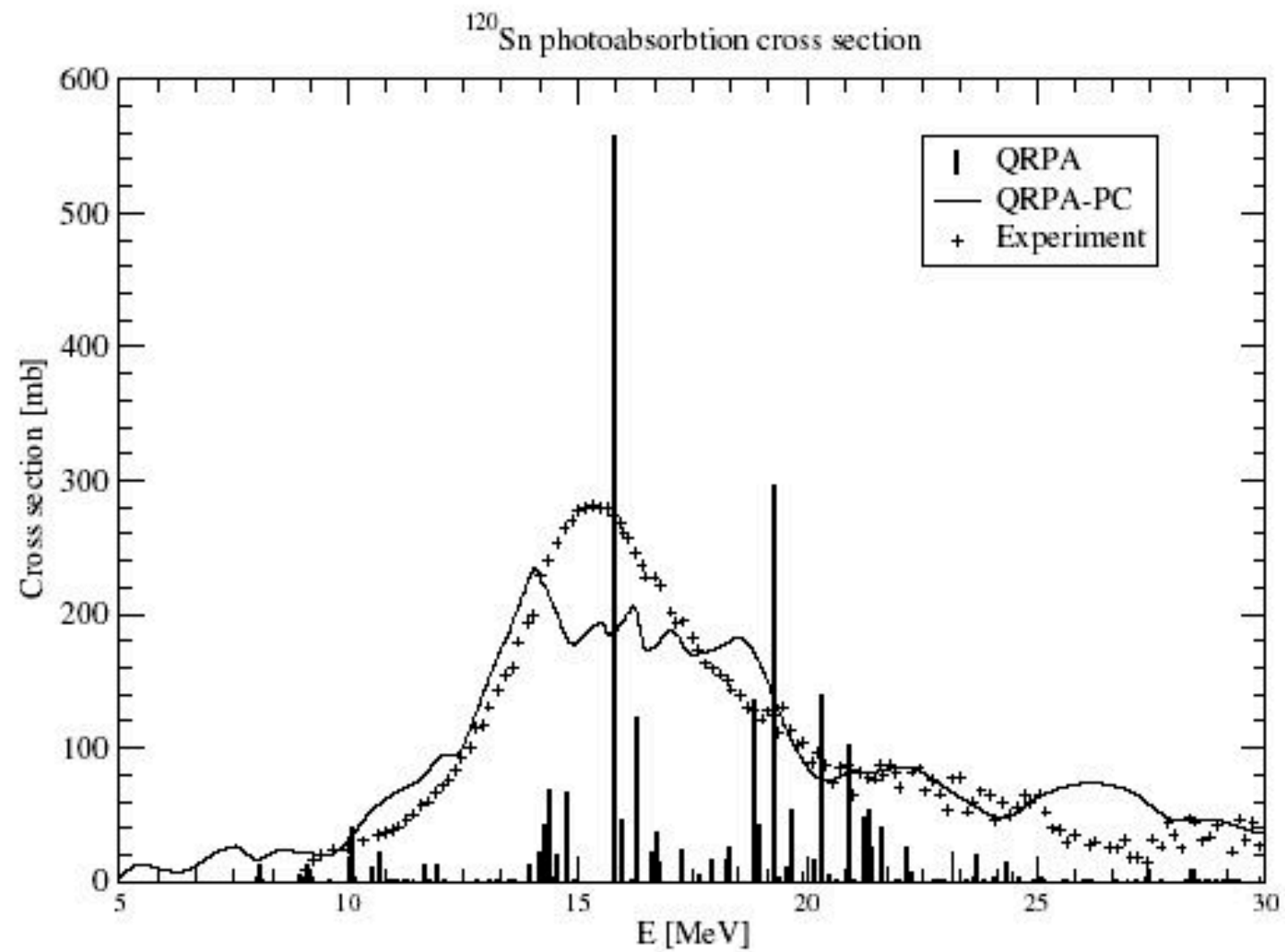
## The IAS: a stringent test

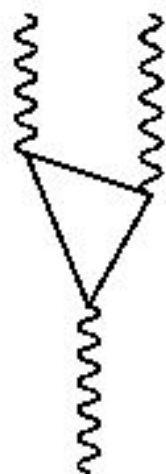


	(a) Discrete TDA		(b) RPA + $\pi^\pm$			(c) RPA + $\pi^\pm + \pi^\pm$			
	$E_{\text{IAR}}$	% of $m_0$	$E_{\text{IAR}}$	$\Gamma^\dagger$	% of $m_0$	$E_{\text{IAR}}$	$\Gamma_{\text{tot}}$	$\Gamma^\dagger$	% of $m_0$
I	0.268	99.9	-	-	-	0.267	24	24	99.7
II	18.50	85	18.50	124	97	18.36	194	70	97
	18.28	16							
III	18.64	80	18.65	128	96	18.54	228	100	96
	18.39	11							

The measured total width ( $\Gamma_{\text{exp}}=230$  keV) is well reproduced. The accuracy of the symmetry restoration (if  $V_{\text{Coul}}=0$ ) can be established.

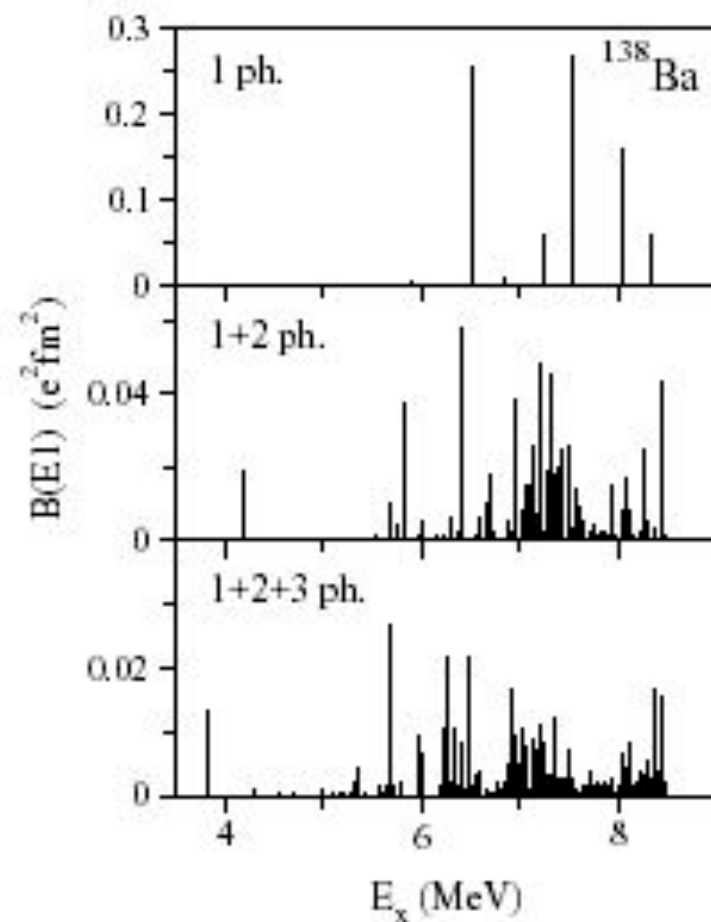
Decay channel	Theory				Experiment [4]
	Only $W^\uparrow$	$W^\uparrow + W^\downarrow$			
		(a)	(b)	(c)	
$p_{1/2}$	0.472	0.346	0.253	0.237	$0.22 \pm 0.02$
$p_{3/2}$	0.396	0.287	0.238	0.196	$0.34 \pm 0.04$
$i_{13/2}$	0.015	0.011	0.008	0.010	-
$f_{5/2}$	0.117	0.086	0.065	0.061	included in $p_{3/2}$ $0.015 \pm 0.007$
$f_{7/2}$	$< 10^{-3}$	$< 10^{-3}$	$< 10^{-3}$	$< 10^{-3}$	
$h_{9/2}$	$< 10^{-3}$	$< 10^{-3}$	$< 10^{-3}$	$< 10^{-3}$	-
$\sum_c B_c$	1.0	0.730	0.564	0.504	$0.575 \pm 0.07$





**Figure 4.** Basic diagram which gives rise to the spreading width of one-phonon states in the QPM.





**Figure 6.** Fragmentation of the low-lying electric dipole strength in  $^{138}\text{Ba}$ . Calculations are performed in the one-phonon approximation (top panel), and taking into account the coupling to two-phonon configurations (middle panel), or to two- and three-phonon configurations (bottom panel).

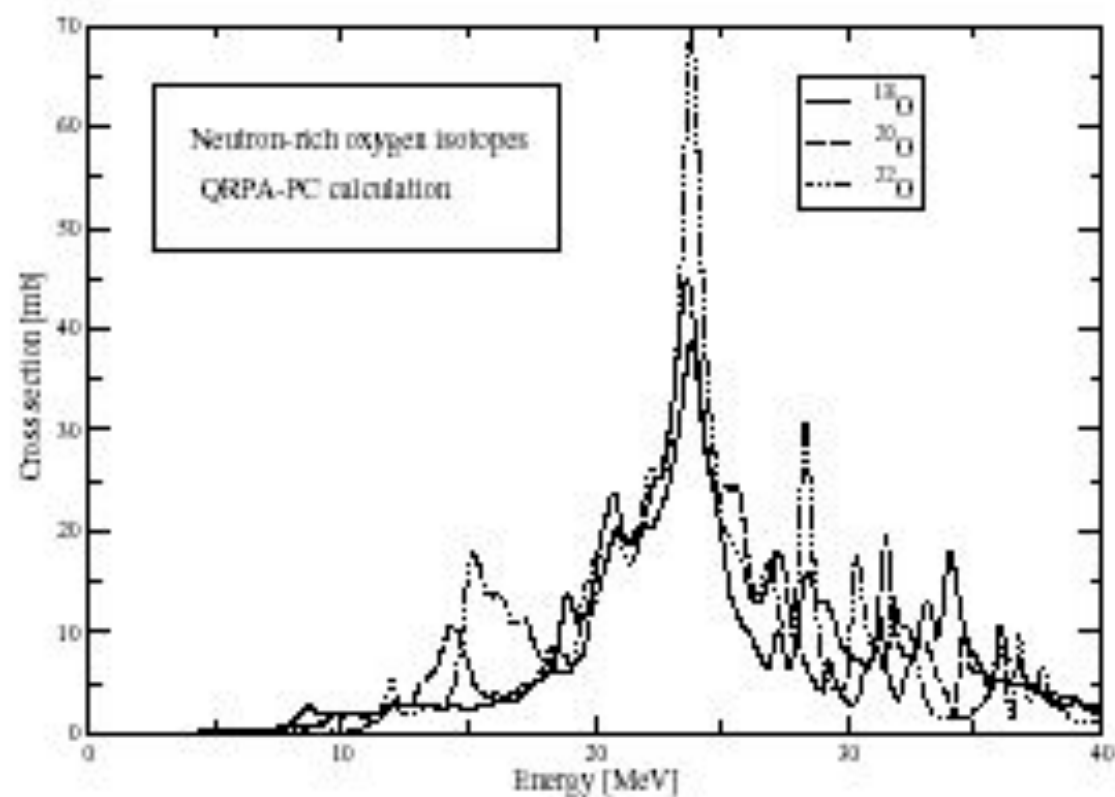


Figure 10. Total photoabsorption cross section for the isotopes  $^{18,20,22}\text{O}$ , calculated using the full QRPA plus phonon coupling [92].

A	18	20	22	24
Shell model [90]	0.06	0.11	0.10	0.09
continuum QRPA [91]	0.07	0.11	0.16	0.21
QRPA-PC [92]	0.07	0.09	0.07	
RHB + RQRPA(DD-ME2)	0.04	0.06	0.15	0.18
Exp. [85]	0.08	0.12	0.07	
Exp. [94]	0.11			

Table 1. Sum of the energy-weighted dipole strength for  $^{18-24}\text{O}$  up to 15 MeV excitation energy, in units of the TRK sum rule.

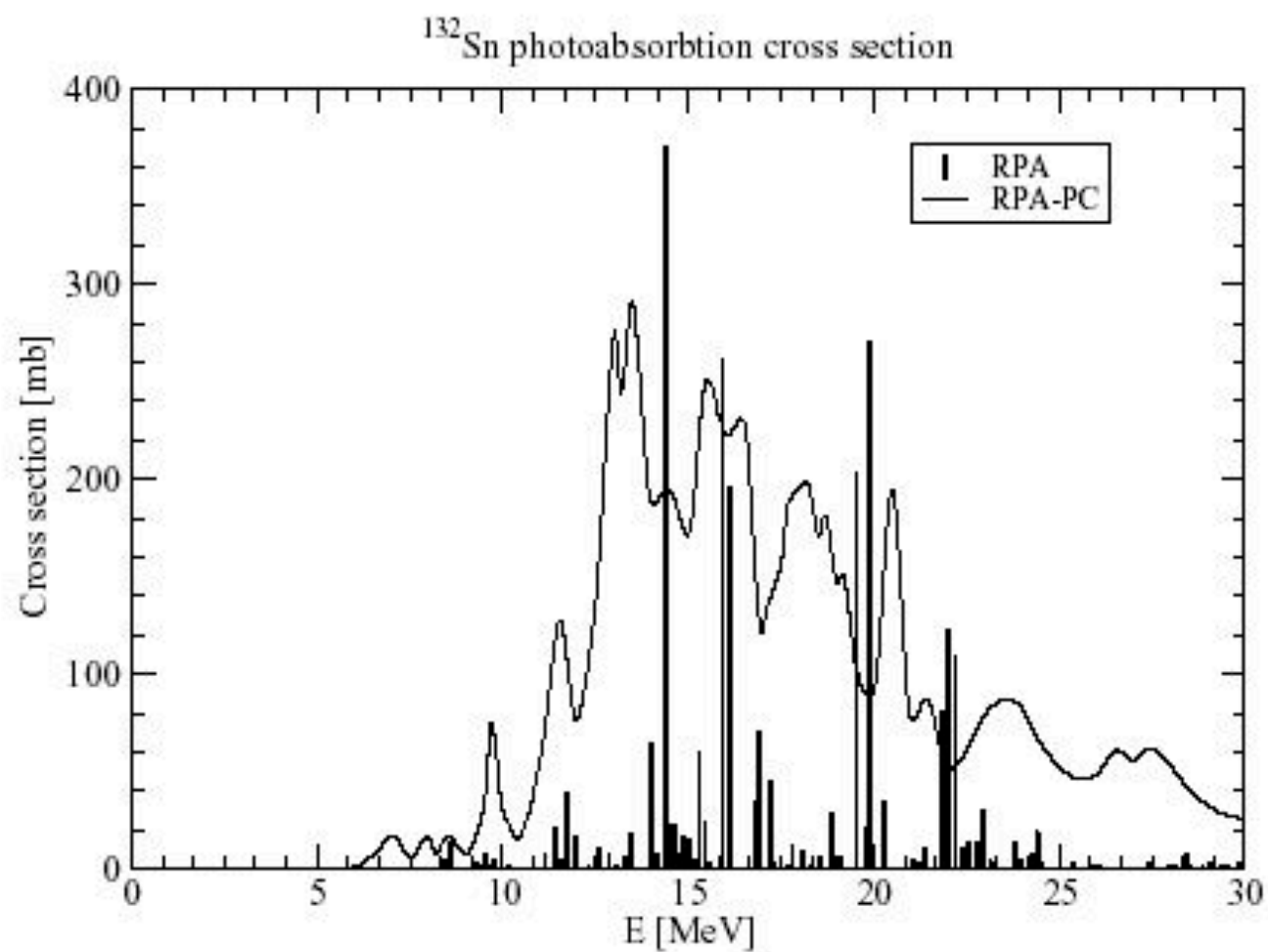
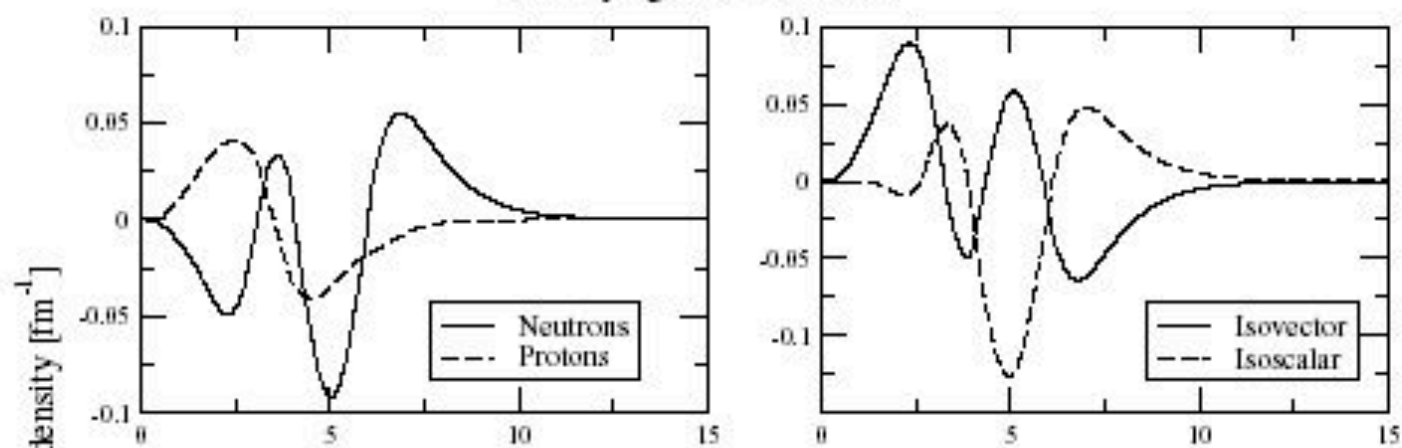
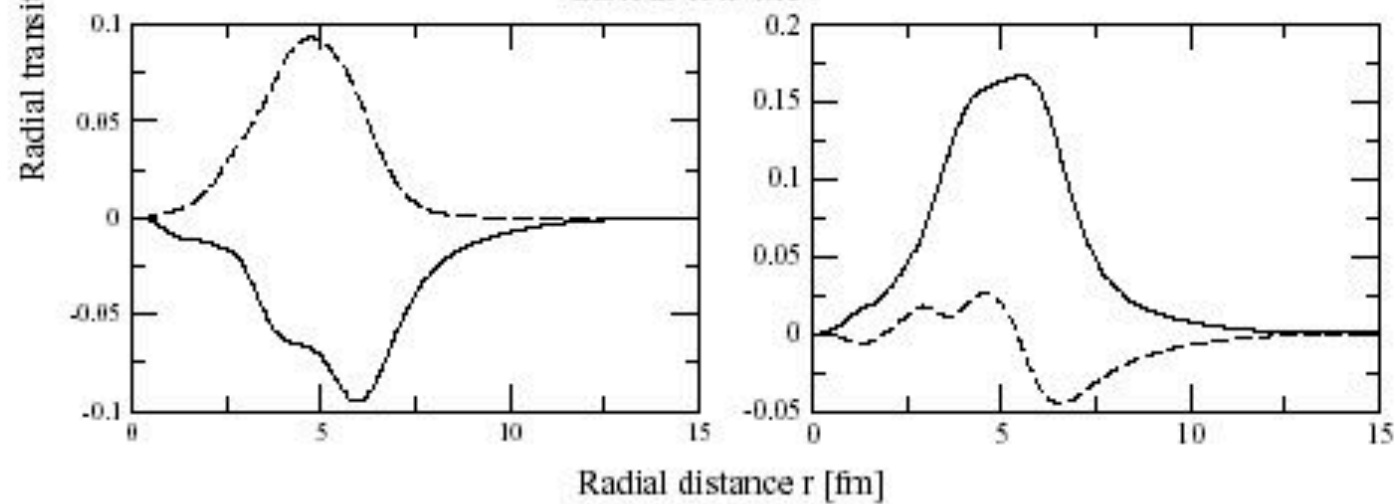


Figure 14. Photoabsorption cross section for  $^{132}\text{Sn}$ , calculated with the RPA and RPA-PC models. The effective interaction is Skyrme SIII.

Low-lying state at 9.7 MeV



GDR at 13.5 MeV



At low energy, there is not a single "collective" pygmy state

8.44 MeV  $3s_{1/2} \rightarrow 3p_{1/2}$  0.2%

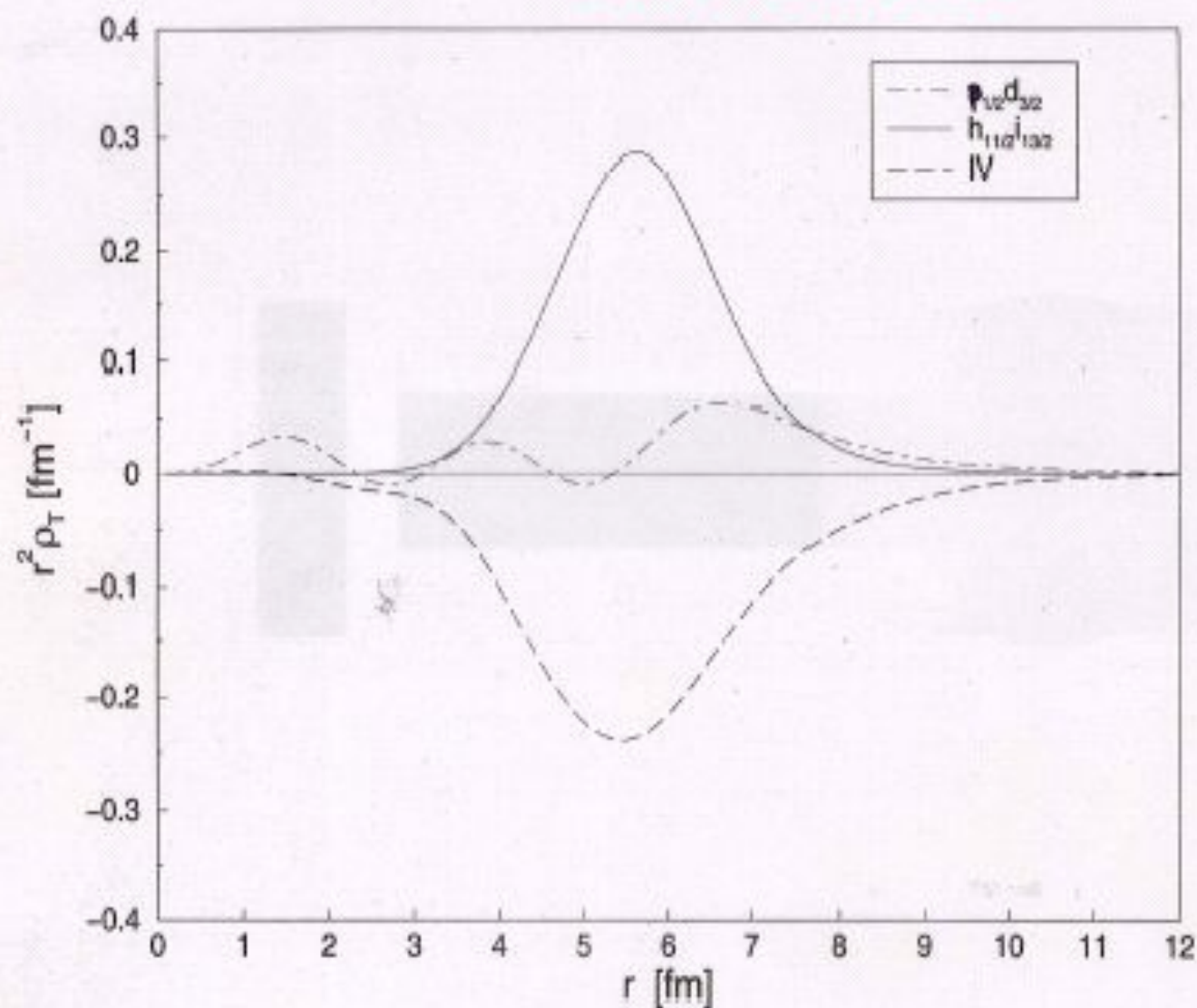
8.61 MeV  $2d_{3/2} \rightarrow 3p_{1/2}, 3s_{1/2} \rightarrow 3p_{1/2}$  0.5%

9.53 MeV 0.3%

Screening bb

See H. Soga et al, H. Feshbach  
NPA 693 (2001) 448

Book of  
George and  
Riccardo Bruglia





**Problem of the  $2d_{3/2} - 1h_{11/2}$  position, wrong in all mean-field**

**Not cured by coupling to vibrations (see below , G. Colò and P**

**But tensor contribution may help: G. Colò et al., PLB 646 (200**  
**However see also T. Lesinski et al., nucl-th7 0704.0731**

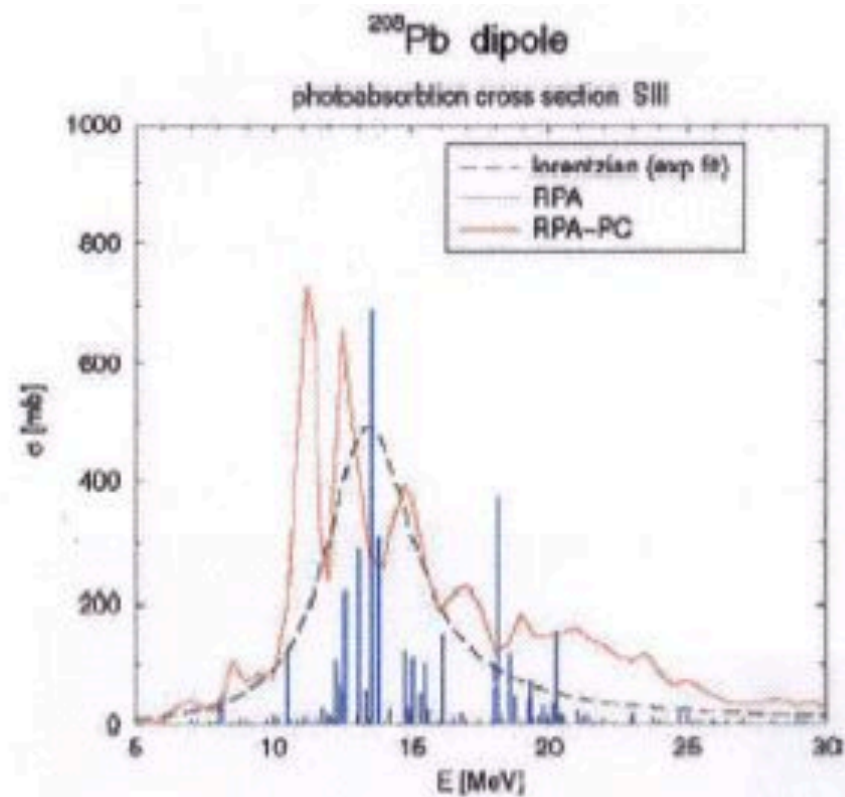


Fig. 2. Photoabsorption cross section for <sup>208</sup>Pb.

$\Sigma B(E1)$  in  $e^2\text{fm}^2$

	< 6 MeV	< 8 MeV
Exp.*	0.53	0.80
Th.	0.52	1.27

\*N. Ryezayeva et al., PRL 89 (2002) 272502

Table 1

Centroid energies  $E_0 = m_1/m_0$  obtained within RPA or QRPA (together with the unperturbed HF or HF-BCS result in parenthesis), compared with the empirical prediction  $80 A^{-1/3}$  ( $41 A^{-1/3}$ )

Nucleus	SIII	SLy4	$80 A^{-1/3}$ ( $41 A^{-1/3}$ )
$^{208}\text{Pb}$	14.9 (9.4)	13.4 (9.8)	13.5 (6.9)
$^{120}\text{Sn}$ (RPA)	17.1 (10.9)	15.0 (11.0)	16.2 (8.3)
$^{120}\text{Sn}$ (QRPA)	17.3 (11.3)	15.1 (11.6)	16.2 (8.3)
$^{132}\text{Sn}$	17.0 (10.7)	15.2 (11.0)	15.7 (8.1)

Table 2

Centroid energies  $E_0 = m_1/m_0$  in MeV, obtained in the (Q)RPA and (Q)RPA-PC calculations. Only in the case of  $^{208}\text{Pb}$  we observe an appreciable shift when the phonon coupling is introduced. In the other two cases the downward shift is smaller than 100 keV

Nucleus	(Q)RPA	(Q)RPA-PC
$^{208}\text{Pb}$	14.9	14.4
$^{120}\text{Sn}$	17.1	17.1
$^{132}\text{Sn}$	17.0	17.0

Table 3

Values of the peak energy (width) in MeV calculated in (Q)RPA-PC (calculated by means of a Lorentzian fit to the cross sections) in comparison with the experimental values

Nucleus	(Q)RPA-PC	Exp.
$^{208}\text{Pb}$	13.1 (3.7)	13.46 (3.9)
$^{120}\text{Sn}$	15.7 (5.3)	15.4 (4.9)
$^{132}\text{Sn}$	15.5 (5.8)	—

← 16.1(4.7)

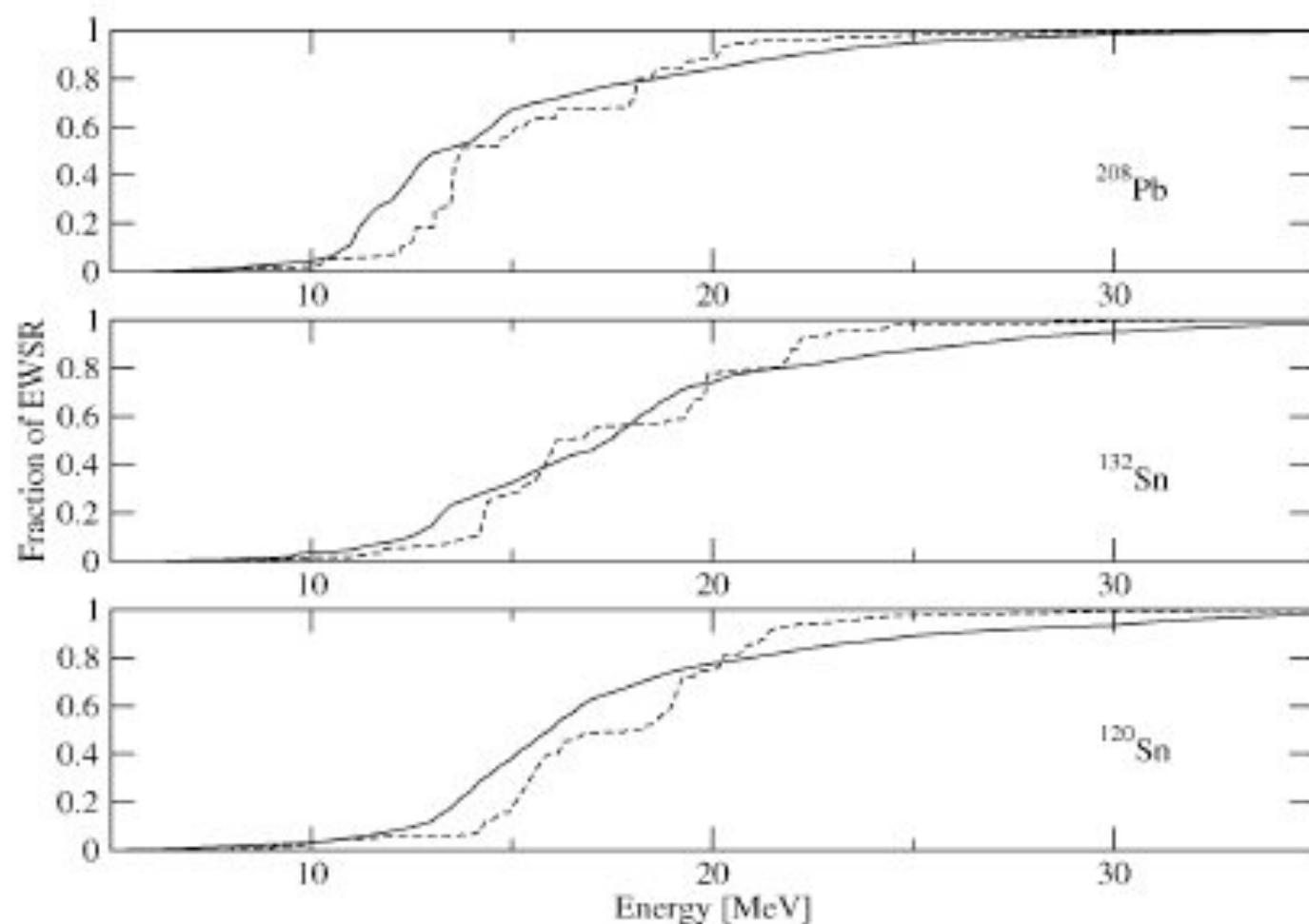


Fig. 1. Exhaustion of the dipole EWSR in the three nuclei considered in the present Letter. The full line refers to the complete (Q)RPA calculation, while the dashed line to the (Q)RPA calculation.

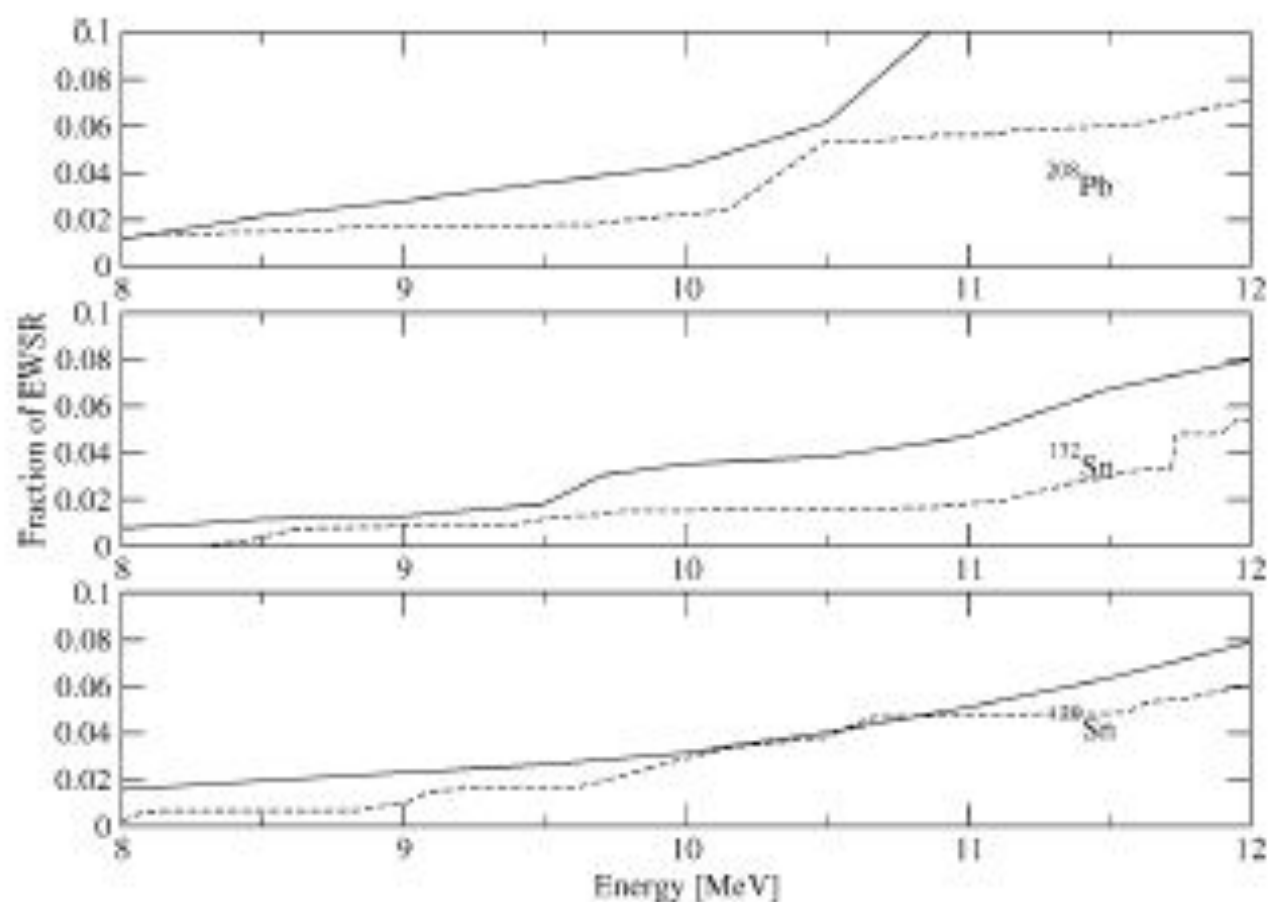


Fig. 5. Low-lying dipole strength in the three isotopes studied. The figure has the same pattern of Fig. 1, but it refers only to the interval 8–12 MeV.

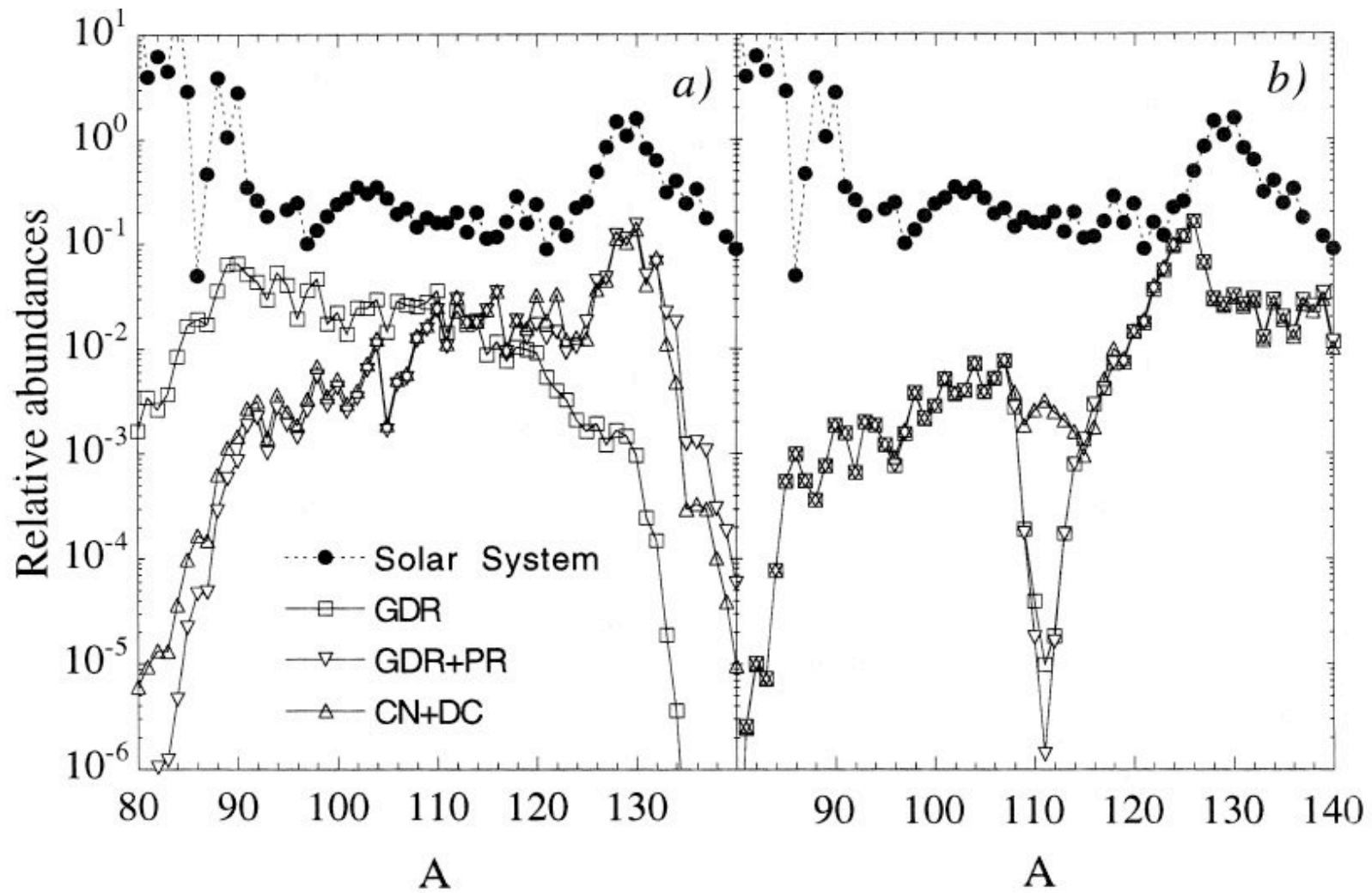


Fig. 6. a)  $r$ -abundance distributions for  $T = 10^9$  K,  $N_v = 10^{20} \text{ cm}^{-3}$  and  $\tau_{\text{irr}} = 2.4$  s with 3 different estimates of the neutron capture rates: the standard GDR component, the GDR + PR strength and the damped statistical (CN) plus DC contribution. The top curve corresponds to the solar  $r$ -abundances arbitrarily normalized. b) same as a) for  $T = 1.5 \times 10^9$  K,  $N_v = 10^{28} \text{ cm}^{-3}$  and  $\tau_{\text{irr}} = 0.3$  s.



# Coulomb excitation of $^{68}\text{Ni}$ at 600 MeV A

## Search for pygmy Dipole Resonance



Dipole strength shifts at low energy.

Collective or non-collective nature of the transitions?

In neutron rich coulomb excited  $^{68}\text{Ni}$  a structure centered at  $\sim 10.5$  MeV has been measured in the  $\gamma$ -ray spectra

Stable nuclei  $\Rightarrow$  photoabsorption

Exotic nuclei



Virtual photon breakup

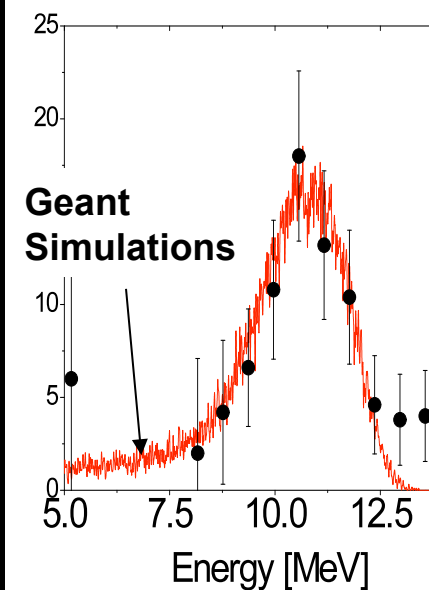
LAND experiment

Aldrich PRL95(2005)132501

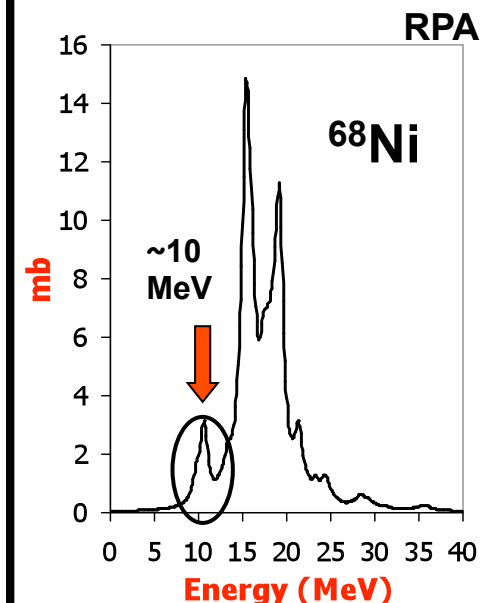
Virtual photon scattering

RISING experiment

Measured  $\gamma$ -ray spectra



Theory



G. Colo private communications



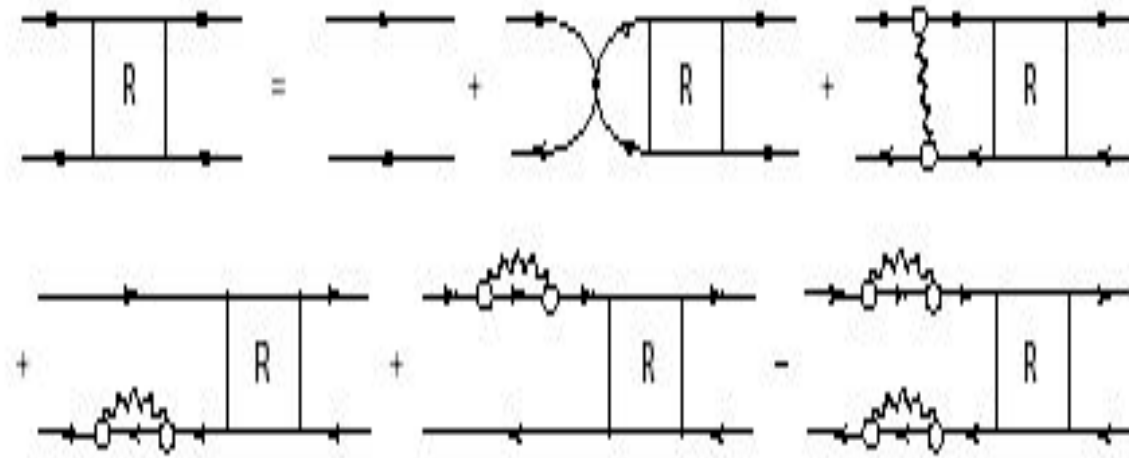


FIG. 1: Bethe-Salpeter equation for the p-h response function in the graphical representation. Solid lines with arrows denote one-body propagators through the particle, hole or antiparticle states, wavy lines denote phonon propagators, empty circles are the particle-phonon coupling amplitudes and the small black circle means the static part of the residual p-h interaction.

. Lit

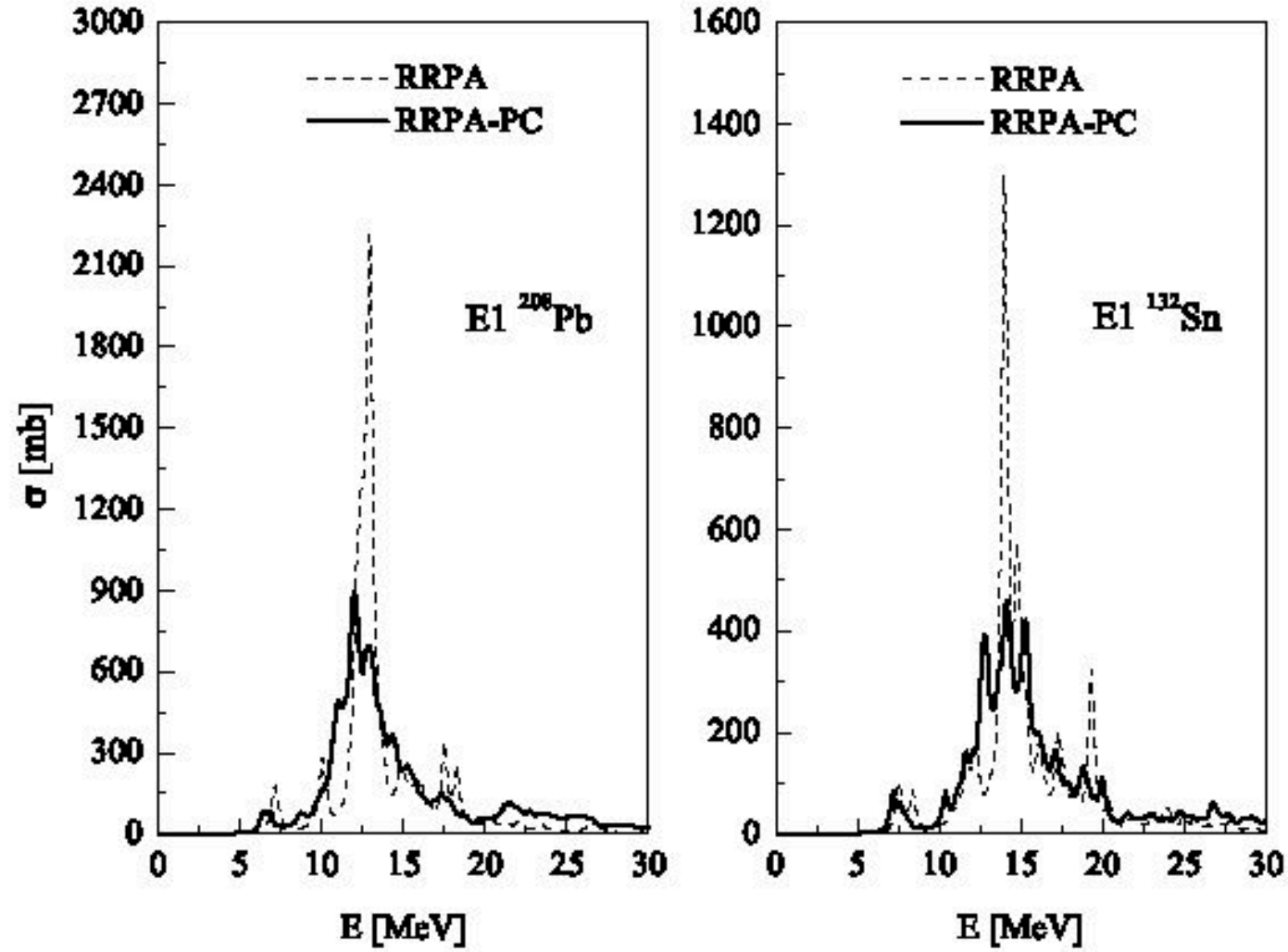


Fig. 1. E1 photoabsorption cross section for  $^{208}\text{Pb}$  and  $^{132}\text{Sn}$ , calculated with the relativistic RPA (dashed), and with the RRPA extended by the inclusion of particle-phonon coupling (solid).

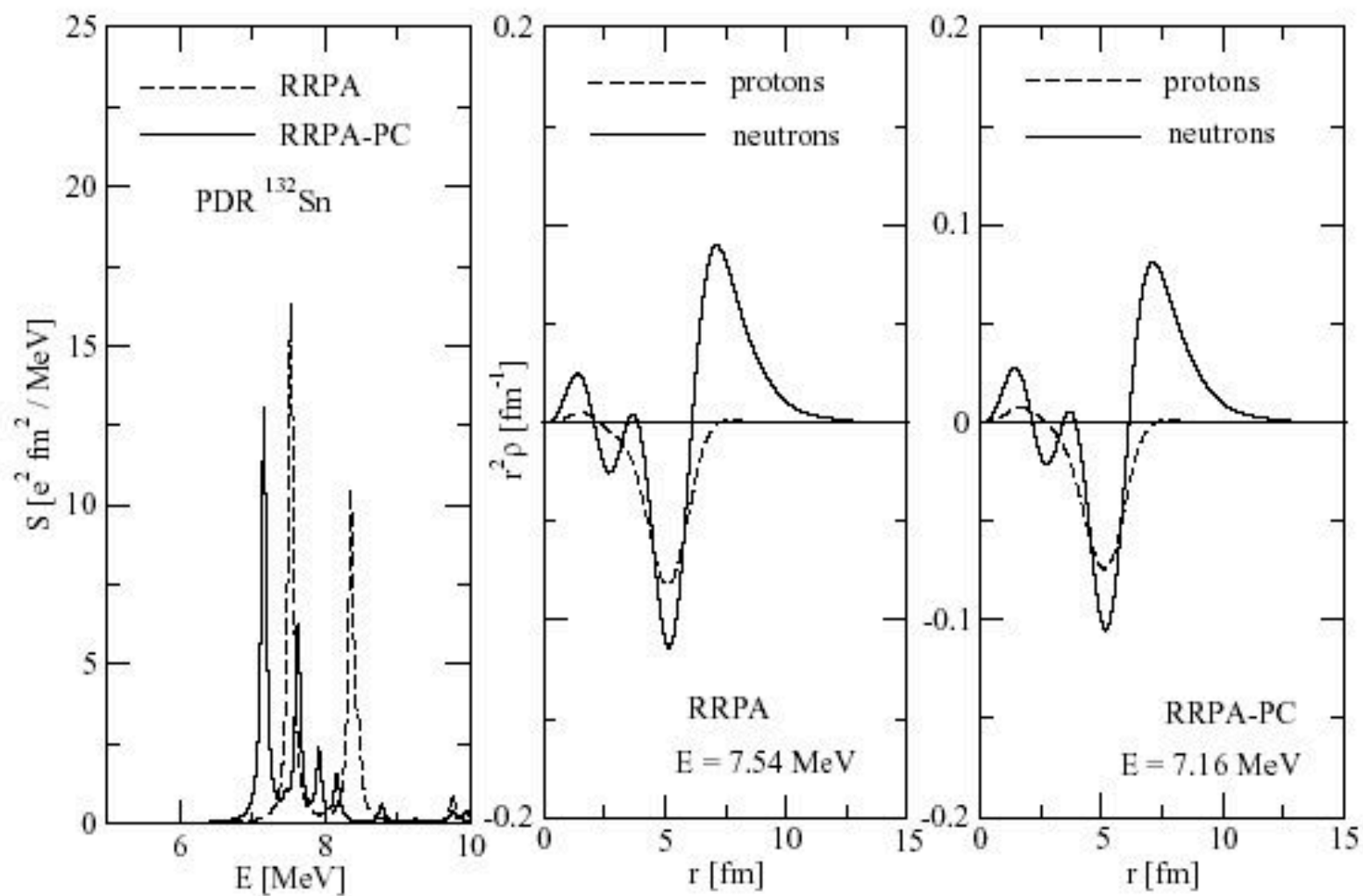


Fig. 3. Same as in Fig. 2, but for  $^{132}\text{Sn}$ . The proton and neutron transition densities correspond to the PDR peaks at 7.54 MeV (RRPA) and 7.16 MeV (RRPA-PC).

Table 3

Same as in Table 2, but for the states at 7.54 MeV (calculated with the RRPA), and at 7.16 MeV (calculated with the RRPA-PC) in  $^{132}\text{Sn}$ .

RRPA, 7.54 MeV	RRPA-PC, 7.16 MeV
53.6 % ( $3s1/2 \rightarrow 3p3/2$ )	49.5 % ( $3s1/2 \rightarrow 3p3/2$ )
16.5 % ( $3s1/2 \rightarrow 3p1/2$ )	21.5 % ( $3s1/2 \rightarrow 3p1/2$ )
9.7 % ( $2d3/2 \rightarrow 3p1/2$ )	6.4 % ( $2d3/2 \rightarrow 3p1/2$ )
7.3 % ( $2d3/2 \rightarrow 3p3/2$ )	4.1 % ( $1h11/2 \rightarrow 1i13/2$ )
4.7 % ( $1h11/2 \rightarrow 1i13/2$ )	3.9 % ( $2d3/2 \rightarrow 3p3/2$ )
0.9 % ( $1g7/2 \rightarrow 1h9/2$ )	0.7 % ( $1g7/2 \rightarrow 1h9/2$ )
0.3 % ( $2d5/2 \rightarrow 3p3/2$ )	0.1 % ( $1g7/2 \rightarrow 2f5/2$ )
0.2 % ( $1g7/2 \rightarrow 2f5/2$ )	0.1 % ( $2d5/2 \rightarrow 3p3/2$ )
0.1 % ( $1g7/2 \rightarrow 2f7/2$ )	0.1 % ( $2d3/2 \rightarrow 4p1/2^*$ )
0.1 % ( $2d3/2 \rightarrow 4p1/2^*$ )	0.1 % ( $1g7/2 \rightarrow 2f7/2$ )
	0.1 % ( $3s1/2 \rightarrow 4p1/2^*$ )
	0.1 % ( $3s1/2 \rightarrow 4p3/2^*$ )
53.4 %	86.7 %

Table 4

Integral photoabsorption cross sections for the PDR and GDR, and their ratios calculated with the RRPA and RRPA-PC, in comparison with the experimental values. See text for description.

		$\sigma_{(PDR)}$ (mb MeV)	$\sigma_{(GDR)}$ (mb MeV)	$\sigma_{(PDR)}/\sigma_{(GDR)}$
$^{208}\text{Pb}$	RRPA	133	3906	0.034
	RRPA-PC	106	3547	0.030
	Exp. [22]		3487	
$^{132}\text{Sn}$	RRPA	115	2162	0.053
	RRPA-PC	91	2087	0.044
	Exp. [5]	75(57)	2330(590)	0.03(2)

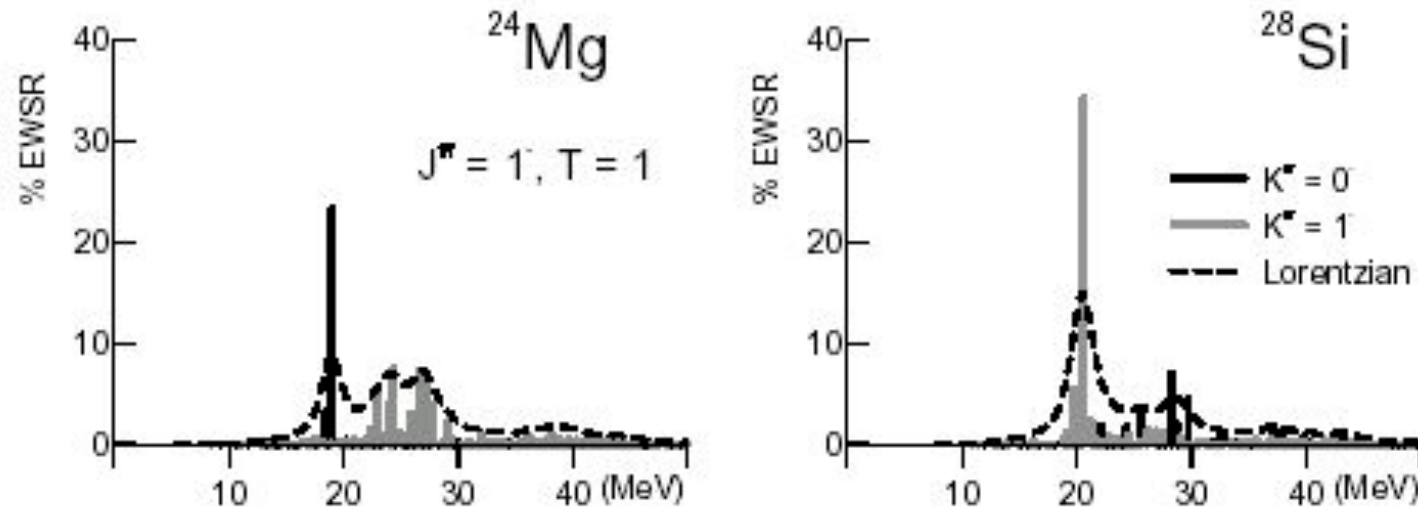


Figure 3. Fraction of the EWSR carried by isovector  $J^\pi = 1^-$  in  $^{24}\text{Mg}$  and  $^{28}\text{Si}$ .  $K^\pi = 0^-$  and  $K^\pi = 1^-$  components are indicated in black and grey respectively.

# Effective mass at finite temperature

- Symmetry energy, stars
- P.Donati, P.M. Pizzochero, PFB, R.A. Broglia, PRL 72 (1994) 2838
- .....and G.E. Brown

# A lot of fun

- Temperature as imaginary time, thank you to Matsubara



## Fermi System at Finite Temperature

The average of any operator  $O$  is given by

$$\langle O \rangle = \sum_i \langle \psi_i | O | \psi_i \rangle p_i = \frac{\text{tr} O \rho}{\text{tr} \rho}$$

being  $\rho$  the *distribution operator*

$$\rho = \exp[-\beta(H - \mu N)]$$

obeing the Bloch's equation

$$\frac{\partial \rho}{\partial \beta} = -(H - \mu N)\rho$$

Imaginary time  $it \leftrightarrow \beta = 1/T!!$

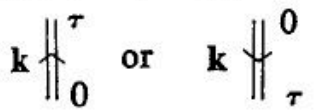
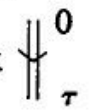
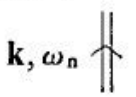

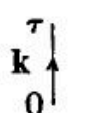
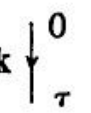
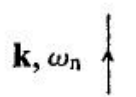





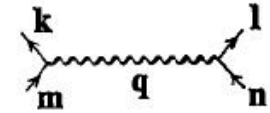
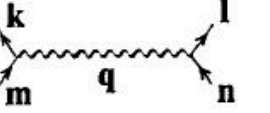


Imaginary Time Green's Function:

$$G(k, \tau_2 - \tau_1) = -i \langle T \{ c_k(\tau_2) c_k^\dagger(\tau_1) \} \rangle$$

where

$$c_{k_1}(\tau) = \exp[(H - \mu N)\tau] c_{k_1} \exp[-(H - \mu N)\tau]$$

Table 14.1 *Diagram dictionary for interacting fermion system at finite temperature (no external potential)*

$(\mathbf{k}, \tau)$ -space		$(\mathbf{k}, \omega_n)$ -space	
Diagram element	Factor	Diagram element	Factor
 or 	$i\mathcal{G}(\mathbf{k}, \tau)$	 or 	$i\mathcal{G}(\mathbf{k}, \omega_n)$
 or 	$i\mathcal{G}_0(\mathbf{k}, \tau) = [\theta_\tau f_k^+ - \theta_{-\tau} f_k^-] \times e^{-(\epsilon_k - \mu)\tau}$	 or 	$i\mathcal{G}_0(\mathbf{k}, \omega_n) = -\frac{1}{i\omega_n - \epsilon_k + \mu},$ $\omega_n = \frac{(2n+1)\pi}{\beta}, \quad \beta = 1/kT$
 or 	$-f_k^- = \frac{-1}{e^{\beta(\epsilon_k - \mu)} + 1}$	 or 	$-f_k^- = \frac{-1}{e^{\beta(\epsilon_k - \mu)} + 1}$
	$-V_{klmn}$		$-V_{klmn}$
fermion loop Ex: 	-1	fermion loop Ex: 	-1
Intermediate $\mathbf{k}, \tau$	$\sum_{\mathbf{k}}, \int_0^\beta d\tau$	Intermediate $\mathbf{k}, \omega_n$	$\sum_{\mathbf{k}}, \frac{1}{\beta} \sum_{n=-\infty}^{+\infty}$

Dyson's equation has the same graphical form as in (10.7), so that

$$\mathcal{G}(\mathbf{k}, \omega_n) = \frac{i}{i\omega_n - \epsilon_k + \mu - \Sigma(\mathbf{k}, \omega_n)}. \quad (14.33)$$

A simple example of this is the finite temperature Hartree-Fock approximation in which the irreducible self-energy,  $\Sigma$ , is given by (10.11). Evaluating this with the aid of Table 14.1 produces

$$\begin{aligned} -\Sigma(\mathbf{k}, \omega_n) &= \text{---}\bigcirc\text{---} \text{P} + \text{---}\bigcirc\text{---} \text{P} \\ &= -\sum_p (V_{kpkp} - V_{pkkp}) f_p^-. \end{aligned} \quad (14.34)$$

Substituting this in (14.33) shows that we have the finite temperature analogue of the Hartree-Fock quasi particle, with energy

$$\epsilon'_k = \epsilon_k + \sum_{\text{all } p} (V_{kpkp} - V_{pkkp}) (e^{\beta(\epsilon_p - \mu)} + 1)^{-1}. \quad (14.35)$$

The effective field seen by the particle in  $\mathbf{k}$  is modified by the fact that some of the particles causing this field are now above the Fermi surface on account of the finite temperature. This is reflected in the statistical factor on the right. Thus the quasi-particle energies have acquired a dependence on temperature through the  $\beta=1/kT$ -factor—a good example of the rather bizarre-sounding concept of 'temperature-dependent energy levels' in quantum mechanics. (The true levels are not temperature dependent, of course.)

The above energy expression may be made 'self-consistent' by replacing  $\epsilon_p$  by  $\epsilon'_p$  on the right of (14.35), giving us a messy equation to be solved for  $\epsilon'_p$ . Graphically, this means that for the irreducible self-energy we are using the first two terms of (11.3), i.e.:

$$\Sigma \approx \text{---}\bigcirc\text{---} + \text{---}\bigcirc\text{---} \quad (14.36)$$

#### 14.4 The finite temperature vacuum amplitude

The zero temperature vacuum amplitude was defined by

$$R(t) = \langle \Phi_0 | U(t) | \Phi_0 \rangle e^{iW_0 t}. \quad (14.37)$$

For our present purposes we need the explicit expression for this in terms of the operator,  $\tilde{U}$ , as it appears in appendix (E.13), with  $t_0=0$ :

$$\begin{aligned} R(t) &= \langle \Phi_0 | \tilde{U}(t) | \Phi_0 \rangle \\ &= \langle \Phi_0 | e^{iH_0 t} e^{-iHt} | \Phi_0 \rangle \end{aligned} \quad (14.38)$$

where appendix (D.1) has been used.

$$\Sigma_{(2)}(1,\omega+il,T)$$

$$=\sum_{2,\lambda}V^2(1,2;\lambda)\left(\frac{1+n_B(\lambda)-n_F(2)}{\omega+il-\epsilon_2-\omega_\lambda}+\frac{n_B(\lambda)+n_F(2)}{\omega+il-\epsilon_2+\omega_\lambda}\right).$$

TABLE I. Values of the ratio  $m_\omega(T)/m$  as a function of the temperature for three different nuclei. The last column gives the best value of the parameter  $T_0$  for the exponential fit  $m_\omega(T) = m + [m_\omega(0) - m]\exp(-T/T_0)$ .

	$T=0$ MeV	$T=1$ MeV	$T=2$ MeV	$T_0$ (MeV)
$^{98}\text{Mo}$	1.7	1.36	1.26	1.89
$^{64}\text{Zn}$	1.8	1.45	1.3	1.97
$^{64}\text{Ni}$	1.45	1.2	1.2	2.05

# Effects on stars

- Smaller effective mass, larger Symmetry Energy (the kinetic part of it), smaller neutronization.....

# DAMPING OF COLLECTIVE MODES

Hierarchy of couplings for damping of giant resonances :  
from mean field states to Compound Nucleus

$$\Gamma_{CN}^{\downarrow} \approx 2\pi \langle v^2 \rangle \rho$$

$$\rho \sim N$$

In the chaotic regime

$$\langle v^2 \rangle \sim u^2/N$$

